

Dr. Rolf M. Schwiete Center for Limbal Stem Cell
and Congenital Aniridia Research,
Saarland University, Homburg/Saar
Chair: Prof. Dr. Nóra Szentmáry

**Gene Expression and the Effect of Ritanserin and Duloxetine on
Primary Congenital Aniridia Limbal Stromal Cells, *In Vitro***

**Cumulative Dissertation for the Degree of
Doctor of Medicine and Natural Sciences (MD/PhD)
Faculty of Medicine**

SAARLAND UNIVERSITY
2025

Submitted by Zhen Li
Born on February 12, 1987, in Hefei, P. R. China

Aus der Dr. Rolf M. Schwiete Zentrum für Limbusstammzellforschung
und kongenitale Aniridie
Universität des Saarlandes, Homburg/Saar
Direktor: Prof. Dr. Nóra Szentmáry

**Genexpression und die Wirkung von Ritanserin und Duloxetin auf
primäre kongenitale Aniridie Limbus-Stromazellen, *In-vitro***

**Kumulative Dissertation zur Erlangung des Grades eines
Doktor der Medizin und der Naturwissenschaften (MD/PhD)
Der Medizinischen Fakultät**

Universität des Saarlandes
2025

Vorgelegt von: Zhen Li
Geb.am: February 12, 1987, in Hefei, P. R. China

Tag der mündlichen Prüfung: 19. 09. 2025

Dekan: Univ.-Prof. Dr. Matthias Hannig

1. Berichtstatter: Prof. Dr. Nóra Szentmáry

2. Berichtstatter: Prof. Dr. Frank Schmitz

1. Table of contents

1. Table of contents	3
2. Zusammenfassung	4
2.1 Summary	7
3. List of abbreviations	9
4. Introduction and motivation	11
4.1 <i>Culturing Limbal Epithelial Cells of Long-term Stored Corneal Donors (Organ Culture) In Vitro – A Stepwise Linear Regression Algorithm (Publication 1)[45]</i>	16
4.2 <i>Expression of PAX6 and keratocyte-characteristic markers in human limbal stromal cells of congenital aniridia and healthy subjects, in vitro (Publication 2)[46]</i>	17
4.3 <i>Effect of the anti-psychotropic drugs ritanserin and duloxetine on gene expression of primary aniridia and healthy human limbal stromal cells, in vitro (Publication 3)[47]</i>	19
Publication 1	21
Publication 2	29
Publication 3	40
8. References	60
9. Publication list	64
10. Presentations	66
11. Acknowledgements	68
12. Curriculum Vitae	70

2. Zusammenfassung

Kongenitales Aniridie ist eine panokuläre Erkrankung, die durch Iris-Hypoplasie und aniridieassoziierte Keratopathie (AAK) gekennzeichnet ist, mit einer Prävalenz von 1:40.000 bis 1:100.000. AAK führt zu fortschreitender Hornhauttrübung und anschließendem Sehverlust. Die Stammzellnische der Limbusregion, bestehend aus verschiedenen Zelltypen und Strukturen, spielt eine entscheidende Rolle bei der Aufrechterhaltung des Mikroumfelds und der Funktion der Stammzellen des limbalen Epithels. Basale limbale Epithelzellen, limbale Stromazellen, Nervenenden, Blutgefäße, extrazelluläre Matrix (ECM) und mikroumwelt Signale tragen zur Integrität und Funktion der Nische bei. Keratozyten produzieren hauptsächlich ECM-Komponenten wie Kollagene. In AAK-Korneas sind veränderte ECM-Komponenten und die Expression fibrotischer Marker (z. B. α -SMA) an der Entwicklung und Progression von AAK beteiligt.

In der ersten Studie haben wir die potenziellen Auswirkungen des Spenderalters, der postmortalen Zeit, der Mediumzeit, der Größe des verwendeten Corneoskleralrings, der Endothelzellendichte (ECD), des Geschlechts, der Anzahl der Kulturmediumwechsel während der Organinkultur und des Spenderursprungs auf das Wachstum limbaler Epithelzellen (LECs) analysiert. Mit einem schrittweisen linearen Regressionsalgorithmus haben wir festgestellt, dass erfolgreiches LEC-Wachstum mit niedrigerem Spenderalter, weniger Kulturmediumwechseln während der Lagerung, kürzerer Mediumzeit in der Organinkultur und kleinerer Größe des Corneoskleralrings zunimmt.

In der zweiten Studie haben wir die Expression von PAX6 und keratzytenspezifischen Markern, einschließlich Kollagen I (COL1A1), Kollagen III (COL3A1), Kollagen V (COL5A1), α -glatter Muskelaktin (ACTA2), Aldehyddehydrogenase

3-Familienmitglied A1 (ALDH3A1), Keratokan (KER), Lumikan (LUM) und CD34, in limbalen Stromazellen von AAK-Subjekten bewertet. Wir haben auch die Auswirkungen von normalem Glukose-Serum-haltigem Zellkulturmedium (NGSC-Medium) und serumfreiem Zellkulturmedium mit niedrigem Glukosegehalt (LGSF-Medium) auf die Markerexpression in Kontroll-Limbalstromazellen (LSCs) und Aniridie-Limbalstromazellen (AN-LSCs) untersucht. Es gab eine veränderte Expression von PAX6 und keratzytenspezifischen Markern in AN-LSCs im Vergleich zu denen in gesunden Kontrollen. Untersuchungen zeigten unterschiedliche Auswirkungen sowohl auf LSCs als auch auf AN-LSCs durch NGSC- und LGSF-Medium. Die festgestellten Unterschiede in der Expression von PAX6 und keratzytenspezifischen Markern innerhalb von AN-LSCs könnten potenziell als entscheidende Faktoren dienen, die den Beginn und Fortschritt von AAK beeinflussen.

In der dritten Studie haben wir die Auswirkungen der Antipsychotika Ritanserin und Duloxetin auf die Genexpression in LSCs und AN-LSCs unter Verwendung von NGSC- und LGSF-Medium in vitro untersucht. Die Ergebnisse ergaben folgende Schlüsselpunkte:

LGSF-Medium und NGSC-Medium haben unterschiedliche Auswirkungen auf die Genexpression in AN-LSCs und LSCs nach Behandlung mit Ritanserin und Duloxetin.

Die Behandlung mit den Antipsychotika Ritanserin und Duloxetin verändert die PAX6- und TGF- β 1-Genexpression in AN-LSCs, die in LGSF-Medium kultiviert wurden.

Die Behandlung mit Ritanserin und Duloxetin beeinflusst die retinoische Säure-Signalgebung und die Expression keratzytenspezifischer Marker in AN-LSCs und LSCs. Diese Behandlungen können die Heilung von Hornhautstroma bei gesunden und angeborenen Aniridie-Korneas beeinflussen.

Um ein umfassendes Verständnis der Auswirkungen von Antipsychotika auf angeborene Aniridie-Korneas zu erlangen, ist eine weitere Untersuchung unerlässlich. Beispielsweise sollten die Auswirkungen unterschiedlicher Glukosekonzentrationen in zwei konditionierten Medien auf LSCs und AN-LSCs untersucht werden, sowie die Leistung von Antipsychotika in einem Tiermodell der PAX6-Haploinsuffizienz-Kornea evaluiert werden. Zusätzlich könnte eine multizentrische, randomisierte klinische Studie weitere Aufschlüsse über Vor- und Nachteile der Verwendung von Antipsychotika bei der Behandlung von AAK liefern.

2.1 Summary

Congenital aniridia is a panocular disorder characterized by iris hypoplasia and aniridia-associated keratopathy (AAK), with a prevalence ranging from 1:40,000 to 1:100,000. AAK leads to progressive corneal opacity and subsequent vision loss. The limbal stem cell niche, comprised of various cell types and structures, plays a crucial role in maintaining the microenvironment and function of limbal epithelial stem cells. Basal limbal epithelial cells, limbal stromal cells, nerve endings, blood vessels, extracellular matrix (ECM), and microenvironmental signals contribute to niche integrity and function. Keratocytes primarily produce ECM components such as collagens. In AAK corneas, altered ECM components and expression of fibrotic markers (e.g., α -SMA) may contribute to the development and progression of AAK.

In the first study, we analyzed the potential effects of donor age, postmortem time, medium time, size of the corneoscleral ring used, endothelial cell density (ECD), gender, number of culture medium changes during organ culture, and donor origin on the outgrowth of limbal epithelial cells (LECs). Using a stepwise linear regression algorithm, we found that successful LEC outgrowth increases with lower donor age, fewer organ culture medium changes during storage, shorter medium time in organ culture, and smaller corneoscleral ring size.

In the second study, we evaluated the expression of PAX6 and keratocyte-specific markers, including Collagen I (COL1A1), Collagen III (COL3A1), Collagen V (COL5A1), α -smooth muscle actin (ACTA2), aldehyde dehydrogenase 3 family member A1 (ALDH3A1), keratocan (KER), lumican (LUM), and CD34, in limbal stromal cells of AAK subjects. We also examined the effects of normal-glucose serum-containing cell culture medium (NGSC-medium) and low-glucose serum-free cell culture medium (LGSF-medium) on marker expression in control limbal stromal cells (LSCs) and aniridia limbal stromal cells (AN-LSCs). There was altered expression of PAX6 and keratocyte-specific markers in AN-LSCs compared to those

in healthy controls. Investigations revealed distinct impacts on both LSCs and AN-LSCs by both NGSC- and LGSF-medium. The identified differences in PAX6 and keratocyte-specific marker expression within AN-LSCs could potentially serve as crucial factors influencing the onset and advancement of AAK.

In the third study, we investigated the effects of the anti-psychotropic drugs ritanserin and duloxetine on gene expression in LSCs and AN-LSCs using NGSC- and LGSF-medium *in vitro*.

The results revealed the following key points:

1. LGSF-medium and NGSC-medium have differing effects on gene expression in AN-LSCs and LSCs following ritanserin and duloxetine treatment.
2. Treatment with the anti-psychotropic drugs ritanserin and duloxetine alters PAX6 and TGF- β 1 gene expression in AN-LSCs cultured in LGSF-medium.
3. Ritanserin and duloxetine treatment affects retinoic acid signaling and the expression of keratocyte characteristic markers in AN-LSCs and LSCs. These treatments may impact corneal stromal wound healing in both healthy and congenital aniridia corneas.

To gain a comprehensive understanding of the effects of anti-psychotropic drugs on congenital aniridia corneas, further investigation is imperative. For example, examining the impact of different glucose concentrations in two conditioned mediums on LSCs and AN-LSCs, as well as evaluating the performance of anti-psychotropic drugs in a PAX6 haploinsufficiency animal cornea model, should be explored in future studies. Additionally, a multicenter, randomized clinical trial could further clarify the advantages and disadvantages of using anti-psychotropic drugs in the treatment of AAK.

3. List of abbreviations

AAK	Aniridia-associated keratopathy
ACTA2A1	Actin Alpha 2A1
ALDH3A1	Aldehyde Dehydrogenase 3 Family Member A1
AN-LSCs	Aniridia Limbal Stromal Cells
α -SMA	alpha smooth muscle actin
ADH7	Alcohol dehydrogenase 7
ABCG2	ATP-binding cassette sub-family G member 2
COL1A1	Collagen Type I Alpha 1 Chain
COL3A1	Collagen Type 3 Alpha 1 Chain
COL5A1	Collagen Type 5Alpha 1 Chain
DMEM	Dulbecco's Modified Eagle's Medium
DSG1	Desmoglein-1
ECD	endothelial cell density
ECM	extracellular matrix
FABP5	Fatty Acid Binding Protein 5
FOSL2	FOS-like antigen 2
KER	Keratocan
LECs	limbal epithelial cells
LESCs	Limbal Epithelial Stem Cells
LGSF-medium	Low Glucose Serum-Free medium
LSCD	Limbal Stem Cell Deficiency
LSCs	Limbal Stromal Cells
LUM	Lumican
MEK	Mitogen-Activated Protein Kinase Kinase
NE	Norepinephrine
NGSC-medium	Normal-Glucose Serum-Containing medium
PAX6	Paired Box 6

PKC	protein kinase C
ROS	Reactive Oxygen Species
SMAD	Mothers against decapentaplegic homolog
TGF- β 1	transforming growth factor-beta 1
5-HT	5-Hydroxytryptamin

4. Introduction and motivation

With a prevalence ranging from 1:40,000 to 1:100,000, congenital aniridia, often associated with Paired Box 6 (PAX6) syndrome, is a rare disease that affects multiple parts of the eye including the cornea, anterior chamber, iris, lens, retina, macula, and optic nerve head [1]. Aniridia-associated keratopathy (AAK) represents a progressive opacification and vascularization in the cornea, mainly due to limbal stem cell deficiency (LSCD). This condition poses a significant risk to vision and is commonly observed in individuals with congenital aniridia. AAK typically initiates in the first decade of life and advances in early adulthood. Its severity is classified using the Lagali grading, with the progression rate often linked to distinct PAX6 mutations [2]. Understanding the pathogenesis of aniridia is imperative for treatments and interventions for those affected by this condition.

The cornea is the window to the eye, responsible for two-thirds of its refractive power. It comprises three distinct layers of cells: a non-keratinized stratified squamous epithelium, a keratocyte-containing collagen-rich stroma, and a posterior monolayer of specialized endothelial cells, separated by Bowman's layer and Descemet's membrane, respectively.

In cases of limbal stem cell deficiency (LSCD), the population of Limbal Epithelial Stem Cells (LESCs) becomes depleted, dysfunctional, or their supportive microenvironment undergoes damage. Consequently, this condition manifests as a distinctive keratopathy with epithelial erosions, persistent epithelial defects, or more severe complications. The breakdown in limbal barrier function precipitates the compensatory ingrowth of an inflamed, opaque pannus, accompanied by the infiltration of conjunctival cells [3, 4]. The application of ex-vivo cultured limbal epithelial cells (LECs) in addressing LSCD has been thoroughly delineated, elevating ophthalmology to a leading position in the realm of regenerative medicine [5, 6]. Numerous methodologies for ex-vivo expansion of LESCs have emerged in recent

years [7-9]. The culture protocols can be categorized into two primary groups: those employing the explant culture system and those utilizing single-cell suspensions obtained through alternative enzymatic isolation methods. The techniques utilized in cultivating LEC exhibit diversity across several dimensions, including the preparation techniques applied to the harvested tissue, selection of appropriate culture medium, duration of culture, types of substrates employed, and the incorporation of supplementary methodologies such as feeder layer utilization, manipulation of oxygen levels (hypoxia), and the application of airlifting techniques. A better understanding of the potential factors affecting human LEC outgrowth *in vitro* may help optimize LEC culture *in vitro*.

Limbal stromal cells, situated in close proximity to the limbal epithelial stem cells, wield significant influence within the limbal stem cell microenvironment [10-12]. *In vivo*, stromal cells contribute to the synthesis of extracellular matrix (ECM) like collagens [13-15]. Previous research has indicated dysregulated expression of ECM constituents and fibrotic indicators, such as alpha smooth muscle actin (α -SMA), in AAK corneas [16].

Limbal keratocytes exhibit distinct characteristics compared to limbal fibroblasts, including differences in appearance, gene expression patterns, transparency, ECM remodeling, and neuroregulatory capabilities [17-19]. In common commercial media solutions like Dulbecco's Modified Eagle's Medium (DMEM), the glucose concentration of 4.5 g/L-1 is notably elevated, surpassing physiological levels observed in the human cornea by 5 to 9 times [20, 21]. Glucose plays a vital dual function as both a primary nutrient and energy provider for cells, while also serving as a foundational regulator of cell phenotype *in vitro*. Its impact extends across various signaling pathways, orchestrating key cellular responses [22-24]. Consequently, when grown *in vitro* using common media compositions such as DMEM supplemented with 1000 mg/L glucose, limbal keratocytes demonstrate an inability to maintain their typical phenotype as seen in the uninjured cornea or upon initial isolation. Instead,

they undergo a transformation process resembling differentiation into fibroblasts. Under normal circumstances, the primary cell type found in the limbal corneal stroma is the keratocyte, which typically exhibits a dendritic shape [25, 26]. However, in response to corneal injury or inflammation, these normally inactive keratocytes transform into myofibroblasts and fibroblasts to aid in the healing process [14, 27, 28]. Previous studies have identified distinctive markers associated with keratocytes, such as Collagen Type I Alpha 1 Chain (COL1A1), Collagen Type 3 Alpha 1 Chain (COL3A1), Collagen Type 5 Alpha 1 Chain (COL5A1), Actin Alpha 2A1 (ACTA2A1), Aldehyde Dehydrogenase 3 Family Member A1 (ALDH3A1), Keratocan (KER), Lumican (LUM), and CD34, which demonstrate positivity when the keratocyte phenotype is present [29]. Moreover, it has been demonstrated that the exclusion of serum from the culture medium leads to a partial reversion of corneal fibroblasts to their native keratocyte phenotype *in vitro* [30, 31]. CD34 serves as an alternative marker for keratocytes [32] and has been observed to undergo downregulation following exposure to conventional tissue culture conditions [33]. Throughout the process of keratocyte phenotype restoration, there is an upsurge in the expression of markers characteristic of keratocytes.

Vicente et al. showed that corneal stromal sections exhibited an anomalous arrangement of collagen lamellae in AAK [16]. Their research also revealed a modified expression pattern of extracellular matrix constituents such as COL1A1 and COL5A1, alongside an increased expression of ACTA2A in untreated AAK corneas as well as in transplanted corneas. Marta Słoniecka et al. developed an *in vitro* AAK model by inducing a mutation in the PAX6 gene via CRISPR/Cas9 technology. Subsequently, their experimentation revealed a notable reduction in the expression levels of ALDH3A1 and KER within their model [34].

Ritanserin and duloxetine are both medications used to treat depression. Ritanserin functions as a potent and targeted antagonist of the 5-Hydroxytryptamin (5-HT) receptor, also known as the serotonin receptor, helping to alleviate symptoms

associated with depression [35]. Duloxetine functions as a dual-action antidepressant, working by impeding the reuptake of both serotonin (5-HT) and norepinephrine (NE) neurotransmitters within neuronal synapses [36]. Recent studies have discovered that ritanserin and duloxetine exhibit significant efficacy in restoring endogenous PAX6 expression in mutant limbal epithelial stem cells [37, 38]. While the precise connection between PAX6 and ritanserin or duloxetine remains uncertain, it is plausible that these compounds may influence PAX6 expression.

Grewal et al. elucidated that 5-HT possesses the capability to stimulate the proliferation of renal mesangial cells by directly activating extracellular signal-regulated kinase (ERK) and triggering a persistent fibrotic response through the upregulation of transforming growth factor-beta 1 (TGF- β 1) expression [39]. They suggested the following signaling cascade: 5-HT 2A receptor – protein kinase C (PKC) – NAD(P)H – Oxidase/ Reactive Oxygen Species (ROS) – MEK – ERK – TGF- β 1 mRNA. Kim et al. elucidated the pivotal involvement of the 5-HT 2A receptor in the activation pathway of hepatic stellate cells, triggering their transformation into myofibroblasts via the activation of TGF- β 1. This cascade instigates a series of deleterious events including lipid peroxidation, mitochondrial impairment, cellular damage, sustained inflammation, and eventual fibrosis [40]. Numerous prior investigations have highlighted a correlation between the expression of PAX6 and TGF- β 1. For example, PAX6, acting as a transcriptional regulator, is observed within the nucleus of both the outer and inner nuclear layers of the mouse retina, where it co-localizes and engages in interactions with TGF- β 1 [41]. Additionally, Yenan Feng et al. illustrated that utilizing siRNA transfection to suppress PAX6 expression effectively fosters an increase in both mRNA and protein expression of TGF- β 1 within cardiac fibroblasts [42].

In a study by Gao et al., it was observed that in instances of vascular injury, there was a notable rise in NE levels. This surge in NE was linked to the activation and proliferation of vascular adventitial fibroblasts, leading to their differentiation into

myofibroblasts. This differentiation process was accompanied by an increase in levels of ACTA2A1, TGF β 1, and SMAD3 [43]. In a prior investigation, it was revealed that the activation of NE prompts the transition of lung cancer cells into a more invasive and metastatic state by triggering epithelial-mesenchymal transition. This process is facilitated through the modulation of the TGF β 1 signaling cascade [44]. All these studies strongly suggest that ritanserin and duloxetine, through their antagonism of the 5-HT₂ receptor and inhibition or antagonism of NE reuptake, may hold promise in facilitating the reinstatement of PAX6 expression, potentially linked to the TGF β 1 signaling pathway.

However, as far as we know, there hasn't been any analysis conducted on the impact of ritanserin and duloxetine on the expression of PAX6, TGF- β 1, retinoic acid signaling components, and keratocyte-characteristic markers in limbal stromal cells of individuals with congenital aniridia. Investigating the effect of ritanserin and duloxetine on the expression of PAX6, TGF- β 1, retinoic acid signaling components, and keratocyte-characteristic markers of primary human aniridia limbal stromal cells (AN-LSCs) and limbal stromal cells (LSCs), *in vitro*, using low glucose serum-free (LGSF) and normal-glucose serum-containing (NGSC) culture medium, could provide a comprehensive understanding of the pathogenesis and development of AAK, and the effect of anti-psychotropic drugs on congenital aniridia limbal stromal cells.

4.1 Culturing Limbal Epithelial Cells of Long-term Stored Corneal Donors (Organ Culture) In Vitro – A Stepwise Linear Regression Algorithm (Publication 1)[45]

In the study, researchers initially analyzed the potential effects of various factors on LEC outgrowth using a stepwise linear regression algorithm. These factors included donor age, postmortem time, medium time, size of the corneoscleral ring, endothelial cell density (ECD), gender, number of culture medium changes during organ culture, and the origin of the donor. The analysis involved 304 donor tissues sourced from 29 distinct donating entities, processed and stored at the Klaus Faber Center for Corneal Diseases. These specimens, obtained from LIONS Cornea Bank Saar-Lor-Lux, Trier/Westpfalz in Homburg, were utilized for corneal transplantation procedures at the Department of Ophthalmology of Saarland University and for LEC culturing at the Dr. Rolf M. Schwiete Center for Limbal Stem Cell and Aniridia Research.

The findings revealed that factors such as donor age, frequency of culture medium changes during organ culture, duration of medium exposure in organ culture, and the dimensions of the corneoscleral rim utilized significantly impacted the proliferation of LEC cultures.

This foundational research provides essential insights for optimizing LEC cultures *in vitro*, thereby laying the groundwork for further investigations..

4.2 Expression of PAX6 and keratocyte-characteristic markers in human limbal stromal cells of congenital aniridia and healthy subjects, in vitro (Publication 2)[46]

In vivo, keratocytes primarily produce extracellular matrix (ECM) components such as collagens [13-15]. Previous studies have indicated altered expression of ECM components and fibrotic markers, such as α -smooth muscle actin (α -SMA), in corneas affected by aniridia-associated keratopathy (AAK) [16]. However, gene expression analysis of limbal stromal cells in individuals with congenital aniridia has not yet been conducted. Therefore, the aim of this study was to investigate the expression of PAX6 and keratocyte-specific markers, including Collagen I (COL1A1), Collagen III (COL3A1), Collagen V (COL5A1), α -SMA (ACTA2), aldehyde dehydrogenase 3 family member A1 (ALDH3A1), keratocan (KER), lumican (LUM), and CD34, in limbal stromal cells of AAK subjects. Additionally, we evaluated the impact of NGSC-medium and LGSF-medium on the expression of these markers in both LSCs and AN-LSCs.

In this study, primary human LSCs were isolated from individuals with aniridia (AN-LSCs) (n=8) and healthy corneas (LSCs) (n=8). We found that *PAX6* mRNA expression significantly decreased in AN-LSCs compared to LSCs in both NGSC- and LGSF-medium. Furthermore, AN-LSCs exhibited a marked reduction in *COL5A1* mRNA expression and notably higher *KER* and *ALDH3A1* mRNA levels compared to LSCs when cultured in NGSC-medium. Conversely, in LGSF-medium, AN-LSCs showed a significant increase in *COL1A1* and *COL5A1* mRNA expression compared to LSCs. Moreover, COL1A1 and α -SMA protein expression were significantly elevated in AN-LSCs compared to LSCs in LGSF-medium. Additionally, in LGSF-medium, the COL5A1 protein level in AN-LSCs was significantly higher than in NGSC-medium.

These findings suggest that variations in PAX6 and keratocyte-specific marker expression in AN-LSCs may play a pivotal role in the development and progression of AAK. Furthermore, both NGSC- and LGSF-medium exerted distinct effects on both LSCs and AN-LSCs. Further investigations are warranted to explore the pathogenesis and potential therapeutic strategies for rescuing PAX6 gene expression and altering keratocyte characteristic markers in AN-LSCs.

4.3 Effect of the anti-psychotropic drugs ritanserin and duloxetine on gene expression of primary aniridia and healthy human limbal stromal cells, in vitro (Publication 3)[47]

Based on the previous study, we know that altered PAX6 and keratocyte-specific marker expression exist in AN-LSCs, and both NGSC- and LGSF-medium exert distinct effects on both LSCs and AN-LSCs. In this study, we investigated the effect of the anti-psychotropic drugs ritanserin and duloxetine on gene expression of primary human limbal stromal cells from congenital aniridia and healthy subjects, *in vitro*.

Ritanserin and duloxetine, both with significant efficacy in restoring endogenous PAX6 expression in mutant limbal epithelial stem cells, are medications used to treat depression [37, 38]. Ritanserin acts as a potent antagonist of the 5-HT₂ receptor, also known as the serotonin receptor, alleviating symptoms associated with depression [35]. Duloxetine, a dual-action antidepressant, inhibits the reuptake of serotonin (5-HT) and norepinephrine (NE) neurotransmitters within neuronal synapses [36].

Previous studies have shown that serotonin (5-HT) can stimulate the proliferation of renal mesangial cells by directly activating extracellular signal-regulated kinase (ERK) and triggering a persistent fibrotic response through the upregulation of TGF- β 1 expression [39]. Additionally, elevated NE levels in vascular injury instances are associated with the activation and proliferation of vascular adventitial fibroblasts, leading to their differentiation into myofibroblasts, accompanied by increased levels of ACTA2A1, TGF β 1, and SMAD3 [43]. Numerous research endeavors have elucidated the correlation between PAX6 and TGF- β 1 expression [41, 42].

In this study, primary human limbal stromal cells from aniridia (AN-LSCs) (n=8) and

healthy corneas (LSCs) (n=8) were cultured in either LGSF-medium or NGSC-medium. The expression of PAX6, FOS-like antigen 2 (FOSL2), TGF- β 1, ACTA2A1, LUM, COL1A1, COL5A1, Desmoglein-1 (DSG1), Fatty Acid Binding Protein 5 (FABP5), Alcohol dehydrogenase 7 (ADH7), and ATP-binding cassette sub-family G member 2 (ABCG2) was determined by qPCR and Western blot.

The results revealed that in AN-LSCs cultured in LGSF-medium, ritanserin treatment significantly increased *PAX6* mRNA expression while significantly decreasing *TGF- β 1* and *FOSL2* mRNA expression. Additionally, ritanserin treatment downregulated TGF- β 1 protein level and upregulated FABP5 protein level. In LSCs cultured in LGSF-medium, both ritanserin and duloxetine treatments significantly downregulated *ACTA2A1* mRNA expression, while ritanserin treatment significantly upregulated *FABP5* mRNA expression. Duloxetine treatment downregulated α -SMA protein and upregulated FABP5 protein. In LSCs cultured in NGSC-medium, ritanserin treatment significantly increased *LUM*, *FABP5*, and *ADH7* mRNA and protein expression.

These findings demonstrate that the anti-psychotropic drugs ritanserin and duloxetine alter PAX6 and TGF- β 1 gene expression in AN-LSCs cultured in LGSF-medium and impact retinoic acid signaling pathways and keratocyte characteristic markers in both LSCs and AN-LSCs, depending on the culture media used.

Publication 1

Experimentelle Studie

Thieme

Culturing Limbal Epithelial Cells of Long-term Stored Corneal Donors (Organ Culture) *In Vitro* – A Stepwise Linear Regression Algorithm

Kultivierung von limbalen Epithelzellen von langzeitgelagerten Hornhautspenden (Organkultur) *in vitro* – ein schrittweiser linearer Regressionsalgorithmus

Authors

Zhen Li¹, Daniel Böhringer², Tanja Stachon¹, Mahsa Nastaranpour¹, Fabian Norbert Fries^{1,3}, Berthold Seitz³, Myriam Ulrich¹, Cristian Munteanu³, Achim Langenbacher⁴, Nóra Szentmáry¹

Affiliations

- 1 Dr. Rolf M. Schwiete Center for Limbal Stem Cell and Congenital Aniridia Research, Saarland University, Homburg, Germany
- 2 Department of Ophthalmology, University of Freiburg, Freiburg im Breisgau, Germany
- 3 Department of Ophthalmology, Saarland University, Homburg, Germany
- 4 Experimental Ophthalmology, Saarland University, Homburg, Germany

Key words

limbal epithelial cell culture, organ culture, stepwise linear regression algorithm

Schlüsselwörter

limbale Epithelzellkultur, Organkultur, schrittweiser linearer Regressionsalgorithmus

received 17.11.2022
 accepted 2.5.2023
 published online

Bibliography

Klin Monatsbl Augenheilkd 2023
 DOI 10.1055/a-2084-7168
 ISSN 0023-2165
 © 2023, Thieme. All rights reserved.
 Georg Thieme Verlag KG, Rüdigerstraße 14,
 70469 Stuttgart, Germany

Correspondence

Zhen Li
 Dr. Rolf M. Schwiete Center for Limbal Stem Cell and Congenital Aniridia Research, Saarland University
 Kirrberger Straße 100, Geb. 22, 66424 Homburg, Germany
 Phone: +49(0)68411621217, Fax: +49(0)68411612310
 Zhen.Li@uks.eu

ABSTRACT

Purpose To assess various potential factors on human limbal epithelial cell (LEC) outgrowth *in vitro* using corneal donor tissue following long-term storage (organ culture) and a stepwise linear regression algorithm.

Methods Of 215 donors, 304 corneoscleral rings were used for our experiments. For digestion of the limbal tissue and isolation of the limbal epithelial cells, the tissue pieces were incubated with 4.0 mg/mL collagenase A at 37°C with 95% relative humidity and a 5% CO₂ atmosphere overnight. Thereafter, limbal epithelial cells were separated from limbal keratocytes using a 20-µm CellTricks filter. The separated human LECs were cultured in keratinocyte serum-free medium medium, 1% penicillin/streptomycin (P/S), 0.02% epidermal growth factor (EGF), and 0.3% bovine pituitary extract (BPE). The potential effect of donor age (covariate), postmortem time (covariate), medium time (covariate), size of the used corneoscleral ring (360°, 270°/180°, 120°, 90°, less than 90°) (covariate), endothelial cell density (ECD) (covariate), gender (factor), number of culture medium changes during organ culture (factor), and origin of the donor (donating institution and storing institution, factor) on the limbal epithelial cell outgrowth was analyzed with a stepwise linear regression algorithm.

Results The rate of successful human LEC outgrowth was 37.5%. From the stepwise linear regression algorithm, we found out that the relevant influencing parameters on the LEC growth were intercept ($p < 0.001$), donor age ($p = 0.002$), number of culture medium changes during organ culture ($p < 0.001$), total medium time ($p = 0.181$), and size of the used corneoscleral ring ($p = 0.007$), as well as medium time × size of the corneoscleral ring ($p = 0.007$).

Conclusions The success of LEC outgrowth increases with lower donor age, lower number of organ culture medium changes during storage, shorter medium time in organ culture, and smaller corneoscleral ring size. Our stepwise linear regression algorithm may help us in optimizing LEC cultures *in vitro*.

ZUSAMMENFASSUNG

Hintergrund Um verschiedene potenzielle Faktoren auf das Wachstum humaner limbalen Epithelzellen (LEC) aus Hornhautspendergewebe nach Langzeitlagerung (Organkultur) *in vitro* zu untersuchen, wurde ein schrittweiser linearer Regressionsalgorithmus verwendet.

Methoden Für unsere Experimente wurden 304 Hornhautrinne von 215 Spendern verwendet. Zunächst wurden die Gewebestücke mit 4,0 mg/mL Kollagenase A bei 37°C mit 95% relativer Luftfeuchtigkeit und 5% CO₂-Atmosphäre über Nacht inkubiert. Danach wurden die limbalen Epithelzellen mithilfe eines 20 µm CellTricks-Filters von den limbalen Keratozyten getrennt. Die humanen LECs wurden in KSFM-Medium, 1% Penicillin/Streptomycin (P/S), 0,02% epidermalem Wachstumsfaktor (EGF) und 0,3% Rinderhypophysenextrakt (BPE) kultiviert. Der potenzielle Einfluss des Spenderalters (Kovariate), der postmortalen Zeit (Kovariate), des Mediums (Kovariate), der Größe des verwendeten korneoskleralen Rings (360°, 270°/180°, 120°, 90°, weniger als 90°; Kovariate), der Endothelzelldichte (ECD; Kovariate), Geschlecht (Faktor), Anzahl der Kulturmediumwechsel während der Organkultur (Faktor)

und Herkunft des Spenders (spendende Institution und aufbewahrende Institution, Faktor) auf das Wachstum der LEC wurde mit einem schrittweisen linearen Regressionsalgorithmus analysiert.

Ergebnisse Die Rate der erfolgreichen Kultivierung humaner LEC betrug 37,5%. Die mit dem schrittweisen linearen Regressionsalgorithmus berechneten relevanten Einflussparameter auf das LEC-Wachstum waren: Intercept ($p < 0,001$), Spenderalter ($p = 0,002$), Anzahl der Kulturmediumwechsel während der Organkultur ($p < 0,001$), Gesamtmediumzeit ($p = 0,181$), Größe des verwendeten korneoskleralen Rings ($p = 0,007$) sowie Mediumzeit und Größe des korneoskleralen Rings ($p = 0,007$).

Schlussfolgerungen Der Erfolg der LEC-Kultivierung steigt mit abnehmendem Alter des Spenders, der geringeren Anzahl von Wechseln des Organkulturmediums während der Lagerung, der kürzeren Mediendauer in der Organkultur und der kleineren Größe des korneoskleralen Rings. Dieser von uns berechneter schrittweiser linearer Regressionsalgorithmus kann uns bei der Optimierung der LEC-Kultur *in vitro* helfen.

Introduction

The cornea is the window to the eye, responsible for two-thirds of its refractive power. It consists of three cellular layers: a non-keratinized stratified squamous epithelium, a keratocyte containing collagen-rich stroma, and a posterior monolayer of specialized endothelial cells, separated by Bowman's layer and Descemet's membrane, respectively [1, 2]. Corneal epithelial cells are continuously lost through aging, environmentally induced dryness, and by the simple act of blinking [3, 4]. The putative location of corneal epithelial stem cells (SCs) is the limbus; a 1–2 mm wide transition zone that separates the cornea from the conjunctiva. The epithelial SCs of the cornea are located almost exclusively in the basal layer of the limbus, hence termed limbal epithelial stem cells (LESCs) [5–8]. Only a small proportion (<10%) of basal limbal epithelial cells (LECs) are considered to be SCs [4]. The epithelial SC's function is to replenish and maintain an intact corneal surface, which is essential for clear vision.

In limbal stem cell deficiency (LSCD), LESCs are depleted, become dysfunctional, and/or their niche microenvironment is damaged. This leads to the development of a whorl-like keratopathy, epithelial erosions, persistent epithelial defects, or worse, with a breakdown in limbal barrier function and subsequent compensatory ingrowth of an inflamed, opaque pannus with conjunctival cells [9, 10].

The treatment of limbal SC failure using *ex vivo* expanded or *in situ* transplants of LESCs has been an important therapeutic advancement. The use of *ex vivo* cultured LECs in the treatment of LSCD is well characterized, and this procedure has placed ophthalmology at the forefront of regenerative medicine [11, 12]. Many protocols of *ex vivo* LESCs expansion have been developed in the past years [13–15]. These culture protocols could be divided into two main groups: the ones using the explant culture system or,

alternatively, the ones in which single-cell suspensions obtained by a different kind of enzymatic isolation are used. Additionally, these two main culture systems have some variants.

Thus, explants or cell suspensions could be cultured on different surfaces. Culture methods for LEC vary with respect to preparation of the harvested tissue, choice of culture medium, culture time, substrates, and supplementary techniques, including the use of a feeder layer, hypoxia, and airlifting. *Ex vivo* expansion of LECs involves the culture of LECs harvested either from the patient [11], a living relative [16], or a cadaver [17]. It has been suggested that limbal tissue that is taken from a cadaver donor should be placed onto the recipient's eye within 72 hours of the donor's death in order to maintain cell viability [18, 19]. However, it is a common practice in the United Kingdom and Europe to store corneoscleral discs intended for corneal transplantation for up to 4 weeks in an organ culture medium at 28–37°C [20]. Other storage methods are common in other countries; for example, hypothermic storage at 4°C is used widely in the United States and Asia. Due to the limited availability of fresh ocular tissue and the logistic advantages of stored tissue, corneoscleral rings have been used to generate limbal epithelial cultures for transplantation [21–23], usually as explant cultures. The methods used for storing corneas, however, have been designed to maintain endothelial cell health. Several studies have shown that the epithelium is harmed in organ culture and hypothermic storage media, resulting in a loss these cells [20, 24] and changes in protein expression in the limbal epithelium [25]. In addition, there is *in vitro* a reduced proliferative potential of LECs following storage, in organ culture medium [26–28].

The objective of our present work was to assess various potential factors on human LEC outgrowth *in vitro* using corneal donor tissue following long-term storage (organ culture) and a stepwise linear regression algorithm.

Materials and Methods

Ethical approval

This study was performed in accordance with the Declaration of Helsinki and followed international ethic requirements for human tissues. The study was approved by the Ethics Committee of Saarland/Germany (No. 41/18).

Donor corneal tissues

Three-hundred and four donor tissues of 215 donors [age: 74.3 ± 26.7 (7–101) years; 80.8% males] were obtained from 29 different donating institutions and were transferred to the Klaus Faber Center for Corneal Diseases, including LIONS Cornea Bank Saar-Lor-Lux, Trier/Westpfalz in Homburg for storage. All donor tissues had long-term storage before culture.

Donor corneoscleral rings, which had not been used during corneal transplantation (remnant tissues, which would have otherwise been thrown away), have been used for our experiments. Donor postmortem time was 11.6 ± 12.4 (0.03–24) hours, medium time was 22.4 ± 15.6 (13.3–38) days, and endothelial cell density (ECD) before transplantation was 2476 ± 2255 (1024–4731)/mm² (► **Table 1**). We also collected data on the cause of death of donors and subgrouped these data as follows: (1) heart disease, (2) lung disease, (3) tumor, (4) sepsis, and (5) other.

Cell culture

The donor corneoscleral rims were first rinsed in phosphate-buffered saline (PBS) (Sigma-Aldrich, St. Louis, MO, USA). Then, round limbal excisions were performed using a 1.5-mm diameter disposable biopsy punch (Kai Europe GmbH, Solingen, Germany). Removal of the small, punched, limbal tissue pieces were completed using surgical microscissors. These tissue pieces reached approximately half of the corneal/scleral thickness.

For digestion of the limbal tissue and isolation of the LECs, the tissue pieces were incubated with 4.0 mg/mL collagenase A (Hoffmann-La Roche, Basel, Switzerland) at 37 °C with 95% relative humidity and 5% CO₂ atmosphere overnight. Thereafter, LECs were separated from limbal fibroblasts using a 20-µm CellTricks filter (Sysmex Partec, Görlitz, Germany). The separated human LECs were cultured in a medium containing keratinocyte serum-free medium (KSFM; Life Technologies, Paisley, UK), 1% penicillin/streptomycin (P/S; Sigma-Aldrich, St. Louis, MO, USA), 0.02% epidermal growth factor (EGF; Life Technologies, Grand Island, NY, USA), and 0.3% bovine pituitary extract (BPE; Life Technologies, Grand Island, NY, USA). The cells were seeded into a 24-well culture plate containing 0.5 mL of cell culture medium for each well. Medium was changed first after 4–5 days, then every 2–3 days until the primary cells attached to the bottom of the plate. When the cells with LEC morphology reached about 90–95% confluence, within 7–14 days, these were detached by trypsin digestion (Sigma-Aldrich, St. Louis, MO, USA) using 0.5 g trypsin and 0.2 g EDTA. The detached cells were divided into 6-well plates for passaging. We defined these LEC cultures as cultures with successful LEC growth (LEC1 group). Some LEC cultures only reached 50–90% confluence after 7–14 days. In case of epithelial cell morphology, we also included those in the LEC1 group.

► **Table 1** Baseline characteristics of the 304 donor tissues.

N	304
Age (years)	74.3 ± 26.7 (7–101)
Gender	
Male	246 (80.9)
Female	58 (19.1)
Size of the corneoscleral rings	
▪ <90°	7 (2.3%)
▪ 90°	2 (0.6%)
▪ 120°	3 (0.9%)
▪ 180°	115 (37.8%)
▪ 270°	49 (16.1%)
▪ 360°	128 (42.1%)
The cause of death of donors	
▪ Heart disease	103 (33.9%)
▪ Lung disease	29 (9.5%)
– Tumor	45 (14.8%)
– Sepsis	28 (9.2%)
– Other	99 (32.6%)
Number of culture medium changes during organ culture	
▪ 3	19 (6.2%)
▪ 4	158 (52.1%)
▪ 5	121 (39.5%)
▪ 6	6 (2.3%)
Postmortem time (hours)	11.6 ± 12.4 (0.03–24)
Medium time (days)	22.4 ± 15.6 (13.3–38)
ECD (/mm ²)	2476 ± 2255 (1024–4731)
Number of donating institutions	29
ECD: endothelial cell density	

However, we could not always observe successful LEC growth in these primary cultures. Some of the cultures did not show outgrowth at all and some others stopped growing at less than about 50% confluence. In some cultures, the epithelial cell morphology seemed to be destroyed within approximately 14–21 days, as the growth of fibroblasts LEC outgrowth. These unsuccessful cultures without sufficient epithelial cell growth or with more than 30% fibroblasts were discarded (LEC2 group).

Statistical analysis

There are several competing options to generate prediction models [29]. The most commonly used setup in this context is a linear prediction model, which is trained with a set of predictor variables to mimic the output variables. With large datasets, we could use,

e.g., machine learning tools for built-up prediction models, which could – dependent on the complexity of the neural network structure – tend to overfitting. In machine learning applications, the (typically very large) dataset is split into training, validation, and test set, and with comparing the performance in the training and test set, the prediction model is evaluated for potential overfitting [29].

In contrast, with (linear) regression prediction models – especially in medical applications – such a split into training and test set is not performed, and the entire dataset is used to define the prediction model and later on to evaluate the performance. If based on a larger dataset, strategies such as hold-out or k-fold subsampling could be used [29].

In the present paper, the predictor variables were not known a priori. Therefore, we decided to implement a stepwise linear regression approach, which balances the complexity of the model with the predictability (the amount of variance that is described by the model). Such a stepwise linear approach starts with a constant model, and stepwise adds and removes potential predictor variables based on the statistical significance. In a first step, we defined all the potential predictors, and the algorithm successively identified the predictors that have the most impact on the output variable. This stepwise linear regression approach could deal with metric as well as categorical variables, and after a couple of iteration steps, the final model is documented together with the metrics for the performance. To our understanding, this approach is suitable for such tasks where a priori, the model predictors are unknown. Beside linear effects of the predictors, we also included interactions of predictors to consider potential correlations.

The effect of donor age (covariate), postmortem time (covariate), medium time (covariate), size of the used corneoscleral ring (360°, 270°/180°, 120°, 90°, less than 90°; covariate), ECD (covariate), gender (factor), number of culture medium changes during organ culture (factor), and origin of the donor (donating institution and storing institution, factor) on the LEC outgrowth was analyzed with a stepwise linear regression algorithm. Initialized with a constant model, we stepwise included potential parameters, as outlined above, based on a significance level of $p < 0.05$, and we excluded parameters if the effect in the linear model was no longer statistically significant ($p \geq 0.05$). With the relevant influencing parameters derived from the stepwise linear regression algorithm, a linear estimation equation was set up, which describes the effect of the above listed covariates and factors (effect sizes) on the LEC growth (LEC1 or LEC2 groups; target).

Results

The rate of successful human LEC outgrowth was 37.5% [114 tissues grew well (LEC1 group)], 190 tissues were discarded (LEC2 group). Results of the stepwise multiple linear regression algorithm method are summarized at ► **Table 2**.

Donor age ($p < 0.001$) and the number of culture medium changes during organ culture ($p < 0.0001$) had a significant negative effect on successful human LEC outgrowth. However, gender ($p = 0.468$), postmortem time ($p = 0.409$), medium time ($p = 0.662$), size of the used corneoscleral ring (360°, 270°, 180°,

► **Table 2** Multivariable linear regression with stepwise variable selection for the outgrowth of LEC culture. Included variables for stepwise selection were age, gender, donating institution, post-mortem time, medium time, number of culture medium changes during organ culture, the cause of death of donors, and the size of the used corneoscleral ring. Donor age, number of culture medium changes during organ culture, and the size of the used corneoscleral ring were highly correlated ($p < 0.05$).

	β	p value
Donor age	-0.006	0.003
Number of culture medium changes during organ culture	-0.282	<0.001
Medium time	0.024	0.181
Size of the used corneoscleral ring	-0.361	0.007
Medium time * size of the used corneoscleral ring	0.013	0.015

90°, less than 90°) ($p = 0.160$), ECD ($p = 0.534$), donating institution ($p = 0.323$), and cause of death of donors ($p = 0.496$) did not have a significant effect on successful human LEC outgrowth.

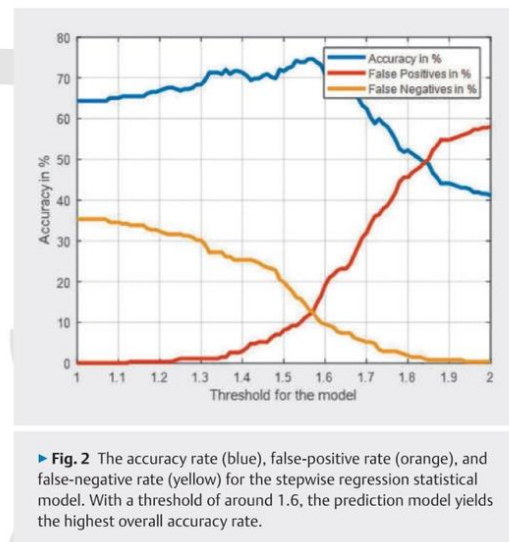
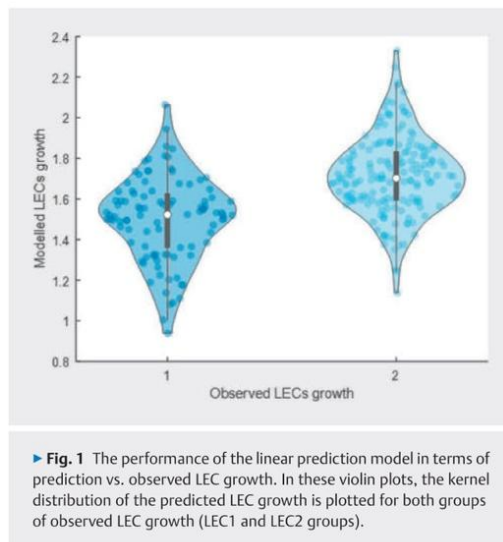
From the stepwise linear regression algorithm, we found out that the relevant influencing parameters on the LEC growth were intercept ($p < 0.001$), donor age ($p = 0.002$), number of culture medium changes during organ culture ($p < 0.001$), total medium time ($p = 0.181$), and size of the used corneoscleral ring ($p = 0.007$), as well as medium time \times size of the corneoscleral ring ($p = 0.007$). The stepwise linear regression algorithm required, in total, 3 iterations for convergence.

The resulting linear estimation equation reads:

$$\begin{aligned} \text{LEC growth} = & 2.859 \text{ (intercept)} \\ & - 0.006147 \times \text{donor age} \\ & - 0.28238 \times \text{number of culture medium changes during organ culture} \\ & + 0.024394 \times \text{medium time} \\ & - 0.36067 \times \text{size of the used corneoscleral ring} \\ & + 0.013123 \times \text{medium time} \times \text{size of the used corneoscleral ring} \end{aligned}$$

The root-mean squared prediction error was 0.431, and the R^2 was 0.215. The prediction model significantly outperformed the constant model [$p = 1.5e-12$ ($F = 14.5$)].

The performance of the linear prediction model in terms of prediction vs. observed LEC growth is shown in the violin plot in ► **Fig. 1**. In this plot, the kernel distribution of the predicted LEC growth is plotted for both groups of observed LEC growth (LEC1 and LEC2 groups). The accuracy rate, false-positive rate, and false-negative rate for the stepwise regression statistical model are shown in ► **Fig. 2**. With a threshold of around 1.6, the prediction model yields the highest overall accuracy rate.



Discussion

The present study analyzed various potential factors effecting human LEC outgrowth *in vitro* using donor corneal tissue following long-term storage (organ culture). Three-hundred and four donor tissues of 29 different donating institutions have been included, which have been processed/stored at the Klaus Faber Center for Corneal Diseases, including LIONS Cornea Bank Saar-Lor-Lux, Trier/Westpfalz in Homburg, used for corneal transplantation at the Department of Ophthalmology of Saarland University and for LEC culturing at the Dr. Rolf M. Schwiete Center for Limbal Stem Cell and Aniridia Research. The number of studies analyzing LEC outgrowth in culture following long-term storage is limited.

Our results showed the influence of donor age, number of culture medium changes during organ culture, medium time in organ culture, and the size of the corneoscleral rim used on the outgrowth of LEC culture as main factors.

The first important influencing factor was donor age. It has previously been suggested that there may be a poorer limbal epithelial culture outcome in older donors [27]. This age-related decline may be explained by the age-related decrease in the amount of stem cell populations at the corneoscleral limbus [30]. Clinical studies have shown similar results in elderly patients, where epithelial healing may be delayed, in contrast to younger subjects [31–33]. Notara et al. examined the limbal niche changes with age using scanning electron microscopy. She described that limbal epithelial crypts and their focal stromal projections appear to deteriorate with age [30] and this may have a critical effect on limbal stem cell density, phenotype, and regenerative capacity.

Interestingly, exposure of stem cells from older individuals to a “younger” stem cell niche can rejuvenate stem cell function [34]. In our own experience, rather younger donors should be considered whenever possible. Nevertheless, age-related changes of

the corneoscleral limbus still should be studied more in detail in the future.

In the Klaus Faber Center for Corneal Diseases, including LIONS Cornea Bank Saar-Lor-Lux, Trier/Westpfalz in Homburg, the corneoscleral buttons were stored for up to 28 days. First, medium I was used, which is an isotonic medium (307 mOsmol/kg) containing 10% minimum essential medium, antibiotics (1% P/S and 1% amphotericin B), 1% L-Glutamin, 1.25% HEPES puffer, 3% NaHCO₃, and 2% fetal calf serum) and this was changed every 7–10 days. Thereafter, as a second step, before corneal transplantation and before initiation of the LEC cultures, corneoscleral buttons were stored up to 4 days in medium II (with the same ingredients as medium I but with the addition of dextran T500 6%). With dextran T500 6%, the osmolarity of the organ culture medium changed from 307 to 353 mOsmol/kg, turning the medium to a hyperosmotic solution that allows deswelling of the donor corneal tissue [35–39]. Along our results, the number of culture medium changes during organ culture should be as low as possible for a successful *in vitro* limbal stem cell culture. To date, most studies only deal with improving corneal organ culture conditions, focusing on endothelial cells [40–42]. Nevertheless, previous studies did not describe the possible LEC damage through medium I, or changes of the medium (with its osmotic stress) [43]. Logically, frequent medium change, with repeat cell stress, may also result in the loss of LECs [44]. Interestingly, Valtink et al. observed that corneal epithelial cells may be more susceptible to culture medium composition than corneal endothelial cells [45]. In addition, potential pH changes may also play an important role in corneal LEC loss in culture, which could also be studied in the future.

In contrast to number of culture medium changes in organ culture, medium time alone did not have a significant effect on human LEC outgrowth. It has been proven that high molecular

weight dextran is intracellularly absorbed by the epithelial cells, but extracellular dextran will also remain in the cornea in organ culture [38,40,46,47]. Damage to basal epithelial cells has been observed from the third day in organ culture medium containing dextran [40]. Nevertheless, during corneal banking, not more than 4 days before use for transplantation, corneal transplants will not be stored in organ culture medium containing dextran [40,46,47]. The exact role of dextran and medium time has to be clarified in the future, increasing the sample size.

In our study, we also observed that the size of the used corneoscleral ring was inversely correlated with the LEC culture outcome, which contradicted our expectations. Nevertheless, previous research has found an inverse relationship between the corneal button size and the swelling tendency in culture, which may also influence the peripheral diffusion of culture medium [43]. In addition, Molvaer et al. described that the limbal epithelial crypts were predominantly located in the superior limbal region [48]. Therefore, the success of LEC outgrowth could also be correlated with the origin of the limbal tissue piece (superior vs. inferior region, etc.), which has to be further analyzed in detail.

Although we expected better LEC outgrowth properties in donors with a sudden death (i.e., cerebrovascular causes or cardiovascular disease with a shorter morbidity period), similar to the previous results of Robert et al. [49] and Spelsberg et al. [51], we also did not find a relationship between the cause of death of donors and successful LEC outgrowth. There was also no significant effect of donor gender [50] or postmortem time [31] on LEC outgrowth, similar to previous reports.

ECD decreases at an average rate of 0.6% per year, with a gradual increase in endothelial polymegethism and pleomorphism [20]. Numerous studies have demonstrated the potential toxicity of dextran on endothelial cells in medium II during organ culture [49,51,52]. Although we analyzed the effect of ECD on LEC outgrowth, our results did not indicate ECD as an influencing factor.

Numerous studies have shown that LSCD can be treated and healed by transplantation of cultured LECs [53–56]. Thus, we investigated factors influencing LEC outgrowth in culture using donors from long-term storage organ culture. The success of LEC outgrowth increased with lower donor age, lower number of organ culture medium changes during storage, greater medium time in organ culture, and with the use of smaller corneoscleral ring sizes for LEC culture. We could develop a stepwise linear regression algorithm, which may help us in optimizing LEC culture *in vitro*. Nevertheless, besides these laboratory findings, the success in clinical use of these cultures has to be evaluated in order to improve limbal stem cell therapy in the future.

In summary, the success of LEC outgrowth increases with lower donor age, lower number of organ culture medium changes during storage, shorter medium time in organ culture, and smaller corneoscleral ring size. Our stepwise linear regression algorithm may help us in optimizing LEC culture *in vitro*.

CONCLUSION BOX

Already known:

- Due to the limited availability of fresh ocular tissue and the logistic advantages of stored tissue, corneoscleral rings have been used to generate limbal epithelial cell (LEC) cultures for transplantation, usually as explant cultures. Nevertheless, the effect of potential factors on LEC outgrowth *in vitro* has not been previously analyzed using a stepwise linear regression algorithm.
- Our present work assessed various potential factors on human LEC outgrowth *in vitro* using corneal donor tissue following long-term storage (organ culture) and a stepwise linear regression algorithm.

Newly described:

- The success of LEC outgrowth increases with lower donor age, lower number of organ culture medium changes during storage, shorter medium time in organ culture, and smaller corneoscleral ring size.
- Our stepwise linear regression algorithm may help us in optimizing LEC culture *in vitro*.

Conflict of Interest

The authors declare that they have no conflict of interest.

References

- [1] Bobba S, Di Girolamo N. Contact Lenses: A Delivery Device for Stem Cells to Treat Corneal Blindness. *Optom Vis Sci* 2016; 93: 412–418. doi:10.1097/OPX.0000000000000699.
- [2] Echevarria TJ, Di Girolamo N. Tissue-regenerating, vision-restoring corneal epithelial stem cells. *Stem Cell Rev Rep* 2011; 7: 256–268. doi:10.1007/s12015-010-9199-1.
- [3] Li W, Hayashida Y, Chen YT et al. Niche regulation of corneal epithelial stem cells at the limbus. *Cell Res* 2007; 17: 26–36. doi:10.1038/sj.cr.7310137
- [4] Schlötzer-Schrehardt U, Kruse FE. Identification and characterization of limbal stem cells. *Exp Eye Res* 2005; 81: 247–264. doi:10.1016/j.exer.2005.02.016.
- [5] Cotsarelis G, Cheng SZ, Dong G et al. Existence of slow-cycling limbal epithelial basal cells that can be preferentially stimulated to proliferate: implications on epithelial stem cells. *Cell* 1989; 57: 201–209. doi:10.1016/0092-8674(89)90958-6
- [6] Lavker RM, Tseng SC, Sun TT. Corneal epithelial stem cells at the limbus: looking at some old problems from a new angle. *Exp Eye Res* 2004; 78: 433–446. doi:10.1016/j.exer.2003.09.008
- [7] Schermer A, Galvin S, Sun TT. Differentiation-related expression of a major 64 K corneal keratin *in vivo* and in culture suggests limbal location of corneal epithelial stem cells. *J Cell Biol* 1986; 103: 49–62. doi:10.1083/jcb.103.1.49
- [8] Pellegrini G, Colisano O, Paterna P et al. Location and clonal analysis of stem cells and their differentiated progeny in the human ocular surface. *J Cell Biol* 1999; 145: 769–782. doi:10.1083/jcb.145.4.769
- [9] Dua HS, Saini JS, Azuara-Blanco A et al. Limbal stem cell deficiency: concept, aetiology, clinical presentation, diagnosis and management. *Indian J Ophthalmol* 2000; 48: 83–92

- [10] Puangsrichareon V, Tseng SC. Cytologic evidence of corneal diseases with limbal stem cell deficiency. *Ophthalmology* 1995; 102: 1476–1485. doi:10.1016/s0161-6420(95)30842-1
- [11] Pellegrini G, Traverso CE, Franzl AT et al. Long-term restoration of damaged corneal surfaces with autologous cultivated corneal epithelium. *Lancet* 1997; 349: 990–993. doi:10.1016/S0140-6736(96)11188-0
- [12] Basu S, Ali H, Sangwan VS. Clinical outcomes of repeat autologous cultivated limbal epithelial transplantation for ocular surface burns. *Am J Ophthalmol* 2012; 153: 643–650. doi:10.1016/j.ajo.2011.09.016
- [13] Shortt AJ, Secker GA, Notara MD et al. Transplantation of *ex vivo* cultured limbal epithelial stem cells: a review of techniques and clinical results. *Surv Ophthalmol* 2007; 52: 483–502. doi:10.1016/j.survophthal.2007.06.013
- [14] Shahdadfar A, Haug K, Pathak M et al. *Ex vivo* expanded autologous limbal epithelial cells on amniotic membrane using a culture medium with human serum as single supplement. *Exp Eye Res* 2012; 97: 1–9. doi:10.1016/j.exer.2012.01.013
- [15] Menzel-Severing J, Kruse FE, Schlötzer-Schrehardt U. Stem cell-based therapy for corneal epithelial reconstruction: present and future. *Can J Ophthalmol* 2013; 48: 13–21. doi:10.1016/j.cjoo.2012.11.009
- [16] Schwab IR. Cultured corneal epithelia for ocular surface disease. *Trans Am Ophthalmol Soc* 1999; 97: 891–986
- [17] Koizumi N, Inatomi T, Suzuki T et al. Cultivated corneal epithelial stem cell transplantation in ocular surface disorders. *Ophthalmology* 2001; 108: 1569–1574. doi:10.1016/s0161-6420(01)00694-7
- [18] Brzeszczynska J, Ramaesh K, Dhillon B et al. Molecular profile of organ culture-stored corneal epithelium: LGR5 is a potential new phenotypic marker of residual human corneal limbal epithelial stem cells. *Int J Mol Med* 2012; 29: 871–876. doi:10.3892/ijmm.2012.904
- [19] James SE, Rowe A, Ilari L et al. The potential for eye bank limbal rings to generate cultured corneal epithelial allografts. *Cornea* 2001; 20: 488–494. doi:10.1097/00003226-200107000-00010
- [20] Armitage WJ. Preservation of Human Cornea. *Transfus Med Hemother* 2011; 38: 143–147. doi:10.1159/000326632
- [21] Kim HS, Jun Song X, de Paiva CS et al. Phenotypic characterization of human corneal epithelial cells expanded *ex vivo* from limbal explant and single cell cultures. *Exp Eye Res* 2004; 79: 41–49. doi:10.1016/j.exer.2004.02.015
- [22] Vemuganti GK, Kashyap S, Sangwan VS et al. *Ex-vivo* potential of cadaveric and fresh limbal tissues to regenerate cultured epithelium. *Indian J Ophthalmol* 2004; 52: 113–120
- [23] Zito-Abbad E, Borderie VM, Baudrimont M et al. Corneal epithelial cultures generated from organ-cultured limbal tissue: factors influencing epithelial cell growth. *Curr Eye Res* 2006; 31: 391–399. doi:10.1080/02713680600681228
- [24] Baylis O, Figueiredo F, Henein C et al. 13 years of cultured limbal epithelial cell therapy: a review of the outcomes. *J Cell Biochem* 2011; 112: 993–1002. doi:10.1002/jcb.23028
- [25] Gavrilov JC, Borderie VM, Laroche L et al. Influencing factors on the suitability of organ-cultured corneas. *Eye (Lond)* 2010; 24: 1227–1233. doi:10.1038/eye.2009.312
- [26] Armitage WJ, Easty DL. Factors influencing the suitability of organ-cultured corneas for transplantation. *Invest Ophthalmol Vis Sci* 1997; 38: 16–24
- [27] Armitage WJ, Jones MN, Zambrano I et al. The suitability of corneas stored by organ culture for penetrating keratoplasty and influence of donor and recipient factors on 5-year graft survival. *Invest Ophthalmol Vis Sci* 2014; 55: 784–791. doi:10.1167/iovs.13-13386
- [28] Bourne WM, Nelson LR, Hodge DO. Central corneal endothelial cell changes over a ten-year period. *Invest Ophthalmol Vis Sci* 1997; 38: 779–782
- [29] Norman RD, Smith H. *Applied Regression Analysis*. Hoboken, NJ: Wiley-Interscience; 1998: 307–312
- [30] Notara M, Shortt AJ, O'Callaghan AR et al. The impact of age on the physical and cellular properties of the human limbal stem cell niche. *Age (Dordr)* 2013; 35: 289–300. doi:10.1007/s11357-011-9359-5
- [31] Constantinou M, Jhanji V, Tao LW et al. Clinical review of corneal ulcers resulting in evisceration and enucleation in elderly population. *Graefes Arch Clin Exp Ophthalmol* 2009; 247: 1389–1393. doi:10.1007/s00417-009-1111-9
- [32] Parmar P, Salman A, Kalavathy CM et al. Microbial keratitis at extremes of age. *Cornea* 2006; 25: 153–158. doi:10.1097/01.icc.0000167881.78513.d9
- [33] Ibrahim YW, Boase DL, Cree IA. Epidemiological characteristics, predisposing factors and microbiological profiles of infectious corneal ulcers: the Portsmouth corneal ulcer study. *Br J Ophthalmol* 2009; 93: 1319–1324. doi:10.1136/bjo.2008.151167
- [34] Zheng W, Wang S, Ma D et al. Loss of proliferation and differentiation capacity of aged human periodontal ligament stem cells and rejuvenation by exposure to the young extrinsic environment. *Tissue Eng Part A* 2009; 15: 2363–2371. doi:10.1089/ten.tea.2008.0562
- [35] Pels E, Schuchard Y. Organ-culture preservation of human corneas. *Doc Ophthalmol* 1983; 56: 147–153. doi:10.1007/BF00154722
- [36] Pels L. Organ culture: the method of choice for preservation of human donor corneas. *Br J Ophthalmol* 1997; 81: 523–525. doi:10.1136/bjo.81.7.523
- [37] van der Want HJ, Pels E, Schuchard Y et al. Electron microscopy of cultured human corneas. Osmotic hydration and the use of a dextran fraction (dextran T₅₀₀) in organ culture. *Arch Ophthalmol* 1983; 101: 1920–1926. doi:10.1001/archoph.1983.01040020922019
- [38] Borderie VM, Baudrimont M, Lopez M et al. Evaluation of the deswelling period in dextran-containing medium after corneal organ culture. *Cornea* 1997; 16: 215–223
- [39] Hamon L, Quintin A, Mäurer S et al. Reliability and efficiency of corneal thickness measurements using sterile donor tomography in the eye bank. *Cell Tissue Bank* 2022; 23: 695–706. doi:10.1007/s10561-021-09980-2
- [40] Sharma N, Shaikh F, Nagpal R et al. Evaluation of various preservation media for storage of donor corneas. *Indian J Ophthalmol* 2021; 69: 2452–2456. doi:10.4103/ijjo.IJO_258_21
- [41] Shehab A, Gram N, Ivarsen A et al. The importance of donor characteristics, post-mortem time and preservation time for use and efficacy of donated corneas for posterior lamellar keratoplasty. *Acta Ophthalmol* 2022; 100: 269–276. doi:10.1111/aos.14943
- [42] Mistò R, Giurgola L, Pateri F et al. A new storage medium containing amphotericin B versus Optisol-GS for preservation of human donor corneas. *Br J Ophthalmol* 2022; 106: 184–189. doi:10.1136/bjophthalmol-2020-317136
- [43] Medin W, Davanger M. Swelling tendency of rabbit cornea in organ culture medium. Influence of button size. *Acta Ophthalmol (Copenh)* 1988; 66: 369–375. doi:10.1111/j.1755-3768.1988.tb04025.x
- [44] Crewe JM, Armitage WJ. Integrity of epithelium and endothelium in organ-cultured human corneas. *Invest Ophthalmol Vis Sci* 2001; 42: 1757–1761
- [45] Valtink M, Donath P, Engelmann K et al. Effect of different culture media and deswelling agents on survival of human corneal endothelial and epithelial cells *in vitro*. *Graefes Arch Clin Exp Ophthalmol* 2016; 254: 285–295. doi:10.1007/s00417-016-3306-1
- [46] Redbrake C, Salla S, Nilius R et al. A histochemical study of the distribution of dextran 500 in human corneas during organ culture. *Curr Eye Res* 1997; 16: 405–411. doi:10.1076/ceyr.16.5.405.7044
- [47] Salla S, Redbrake C, Becker J, Reim M. Remarks on the vitality of the human cornea after organ culture. *Cornea* 1995; 14: 502–508

- [48] Molvaer RK, Andreassen A, Heegaard S et al. Interactive 3D computer model of the human corneolimbal region: crypts, projections and stem cells. *Acta Ophthalmol* 2013; 91: 457–462. doi:10.1111/j.1755-3768.2012.02446.x
- [49] Robert PY, Camezind P, Drouet M et al. Internal and external contamination of donor corneas before *in situ* excision: bacterial risk factors in 93 donors. *Graefes Arch Clin Exp Ophthalmol* 2002; 240: 265–270. doi:10.1007/s004170100322
- [50] Samy MM, Shaaban YM, Badran TAF. Age- and sex-related differences in corneal epithelial thickness measured with spectral domain anterior segment optical coherence tomography among Egyptians. *Medicine (Baltimore)* 2017; 96: e8314. doi:10.1097/MD.00000000000008314
- [51] Spelsberg H, Reinhard T, Sundmacher R. [Epithelial damage of corneal grafts after prolonged storage in dextran-containing organ culture medium – a prospective study]. *Klin Monatsbl Augenheilkd* 2002; 219: 417–421. doi:10.1055/s-2002-32877
- [52] Abdin A, Daas L, Pattmüller M et al. Negative impact of dextran in organ culture media for pre-stripped tissue preservation on DMEK (Descemet membrane endothelial keratoplasty) outcome. *Graefes Arch Clin Exp Ophthalmol* 2018; 256: 2135–2142. doi:10.1007/s00417-018-4088-4
- [53] Lim P, Fuchsluger TA, Jurkunas UV. Limbal stem cell deficiency and corneal neovascularization. *Semin Ophthalmol* 2009; 24: 139–148. doi:10.1080/08820530902801478
- [54] Cauchi PA, Ang GS, Azuara-Blanco A et al. A systematic literature review of surgical interventions for limbal stem cell deficiency in humans. *Am J Ophthalmol* 2008; 146: 251–259. doi:10.1016/j.ajo.2008.03.018
- [55] Kim JY, Djalilian AR, Schwartz GS et al. Ocular surface reconstruction: limbal stem cell transplantation. *Ophthalmol Clin North Am* 2003; 16: 67–77. doi:10.1016/s0896-1549(02)00107-4
- [56] Cheung AY, Eslani M, Kurji KH et al. Long-term Outcomes of Living-Related Conjunctival Limbal Allograft Compared With Keratolimbal Allograft in Patients With Limbal Stem Cell Deficiency. *Cornea* 2020; 39: 980–985. doi:10.1097/ICO.0000000000002329

Publication 2

CURRENT EYE RESEARCH
<https://doi.org/10.1080/02713683.2025.2449915>



Expression of PAX6 and Keratocyte-Characteristic Markers in Human Limbal Stromal Cells of Congenital Aniridia and Healthy Subjects, *In Vitro*

Zhen Li^a, Tanja Stachon^a, Julia Zimmermann^a, Simon Trusen^a, Fabian N. Fries^{a,b}, Maximilian Berger^a, Shweta Suiwal^a, Ning Chai^a, Berthold Seitz^b, Lei Shi^c, Maryam Amini^a and Nóra Szentmáry^a

^aDr. Rolf M. Schwiete Center for Limbal Stem Cell and Congenital Aniridia Research, Saarland University, Saar, Germany; ^bDepartment of Ophthalmology, Saarland University Medical Center, Saar, Germany; ^cDepartment of Ophthalmology, Anhui No.2 Provincial People's Hospital, Hefei, Anhui, China

ABSTRACT

Purpose: Our aim was to examine the expression of PAX6 and keratocyte-specific markers in human limbal stromal cells (LSCs) in congenital aniridia (AN) and in healthy corneas, *in vitro*.

Methods: Primary human LSCs were extracted from individuals with aniridia (AN-LSCs) ($n=8$) and from healthy corneas (LSCs) ($n=8$). The cells were cultured in either normal-glucose serum-containing cell culture medium (NGSC-medium) or low-glucose serum-free cell culture medium (LGSF-medium). Analysis of PAX6 and keratocyte-specific markers was conducted using qPCR and Western blotting. The keratocyte-specific markers included Collagen I (COL1A1), Collagen III (COL3A1), Collagen V (COL5A1), α -smooth muscle actin (ACTA2), Aldehyde Dehydrogenase 3 Family, Member A1 (ALDH3A1), Keratocan (KER), Lumican (LUM), and CD34.

Results: PAX6 mRNA expression exhibited a significant decrease in AN-LSCs compared to LSCs in both NGSC- and LGSF-medium ($p=0.04$; $p=0.014$). There was a marked reduction in COL5A1 mRNA expression ($p=0.011$), accompanied by notably higher ALDH3A1 and KER mRNA levels ($p=0.007$; $p=0.013$) in AN-LSCs compared to LSCs when using NGSC-medium. In LGSF-medium, AN-LSCs showed a significant increase in COL1A1 and COL5A1 mRNA expression compared to LSCs ($p=0.048$; $p=0.002$). Moreover, COL1A1 and α -SMA protein expression were significantly elevated in AN-LSCs compared to LSCs in LGSF-medium ($p=0.048$, $p=0.008$).

Conclusions: Our investigation affirms the altered expression of PAX6 and keratocyte-specific markers in AN-LSCs relative to healthy controls. Both NGSC- and LGSF-medium exerted distinct effects on both LSCs and AN-LSCs. The observed variations in PAX6 and keratocyte-specific marker expression in AN-LSCs may play a pivotal role in the development and progression of aniridia-associated keratopathy.

ARTICLE HISTORY

Received 19 March 2024
 Accepted 24 December 2024

KEYWORDS

Limbal stromal cells; limbal fibroblasts; limbal keratocytes; aniridia-associated keratopathy; PAX6

Introduction

With an incidence of 1:40,000 to 1:100,000, congenital aniridia caused by PAX6 mutations is a rare panocular disorder impacting the cornea, anterior chamber, iris, lens, retina, macula, and optic nerve head.¹⁻³ PAX6, a DNA-binding transcription factor, directly regulates various upstream and downstream transduction pathways.^{4,5} In congenital aniridia, PAX6 haploinsufficiency in most cases leads to pre- and postnatally altered PAX6 gene expression, resulting in structural changes in different eye components.

Probably the most significant clinical sign, affecting visual acuity of congenital aniridia patients is aniridia associated keratopathy (AAK). PAX6 plays a crucial role in guiding the migration and differentiation of corneal epithelial cells, influencing the process of corneal wound healing.^{4,5} In AAK, there is progressive limbal epithelial stem cell deficiency, with impaired corneal epithelial cell differentiation,

migration and adhesion, corneal conjunctivalization and development of a vision-threatening, thick, corneal vascularized pannus.⁶⁻⁸ This is accompanied by recurrent corneal erosions and chronic irritation.^{9,10}

The limbal stem cell niche, consisting of several types of cells and structures plays a decisive role in maintaining limbal epithelial stem cell microenvironment and function. Basal limbal epithelial cells, limbal stromal cells, nerve endings, blood vessels, extracellular matrix and microenvironmental signals play an important role in niche integrity and function.¹¹⁻¹⁶

Limbal stromal cells, in close proximity to the limbal epithelial stem cells, have an important role to play in the limbal stem cell niche.^{11-14,17} There are limbal fibroblasts and keratocytes, which produce cornea-specific extracellular matrix (ECM),^{17,18} and have unique properties of self-renewal, plasticity and a role in modulation of immune responses.¹⁹⁻²³ Nevertheless, only a few studies analyzed gene expression of

CONTACT Zhen Li zhen.li@uks.eu Dr. Rolf M. Schwiete Center for Limbal Stem Cell and Congenital Aniridia Research, Saarland University, Kirrberger Str. 100, Homburg, Saar, 66424, Germany

Supplemental data for this article can be accessed online at <https://doi.org/10.1080/02713683.2025.2449915>.

© 2025 Taylor & Francis Group, LLC

limbal keratocytes and fibroblasts in the past.^{24–26} *In vivo*, the main role of keratocytes is production of ECM components such as collagens.^{27–29} Previous studies have shown that there is an altered expression of ECM components and fibrotic markers (e.g. α -SMA) in AAK corneas.³⁰ Nevertheless, to the best of our knowledge, gene expression of limbal stromal cells in congenital aniridia subjects has not been analyzed, yet.

In our current study, we aimed to examine the expression of PAX6 and keratocyte-specific markers, including Collagen I (COL1A1), Collagen III (COL3A1), Collagen V (COL5A1), α -smooth muscle actin (ACTA2), aldehyde dehydrogenase 3 family member A1 (ALDH3A1), keratocan (KER), lumican (LUM), and CD34, in both control limbal stromal cells (LSCs) and aniridia limbal stromal cells (AN-LSCs).

Materials and methods

Ethical approval and consent to participate

Our study was approved by the Ethics Committee of Saarland, Germany (No. 172/20). We performed our work according to the Principles of the Declaration of Helsinki. All aniridia subjects signed an informed consent before surgery.

Cell culture

Limbal stromal cell culture

1.5 mm limbal biopsies of eight healthy normal control eyes (age: 73.5 ± 15.5 (58–89) years; 3 (37.5%) males) and 1.5 mm limbal biopsies of 8 aniridia eyes (age: 34.5 ± 29.5 (5–64) years; 3 (37.5%) males) have been used for our experiments. Aniridia samples have been obtained from patients of the Department of Ophthalmology, Saarland University Medical

Center, Homburg/Saar, Germany. Control limbal biopsies were obtained from corneal donor eyes of the LIONS Cornea Bank Saar-Lor-Lux, Trier/Westpfalz, Homburg/Saar, Germany.

Before surgery, all aniridia patients underwent slitlamp examination bilaterally, in order to Grade AAK, according to Lagali et al.^{31,32} Descriptive data of healthy and aniridia samples are summarized in Tables 1 and 2.

Limbal stromal cells were isolated as described by Chai et al.³³ Both healthy and aniridia human limbal biopsies were first incubated in 0.5 mg/ml collagenase A (Hoffmann-La Roche, Basel, Switzerland) overnight at 37 °C. Then, the suspensions were filtered through 40 μ m Flowmi cell strainers (Cat-No.: H13680-0040, Bel-Art, Wayne, USA) into one 24 well plate, to remove limbal epithelial cells and incompletely dissociated cells. To obtain the limbal stromal cells, the strainer was washed with 500 μ l PBS and 500 μ l 0.05% trypsin-EDTA, which was followed by an incubation for 5 min to separate cell clusters. Thereafter, the enzyme reaction was stopped using DMEM supplemented by 5% FCS. The filtrate was subsequently centrifuged at 1500 g for 5 min to sediment stromal cells and the supernatant was removed afterwards. The stromal cells were seeded into one 6 well using DMEM supplemented by 5% FCS. Cells were incubated at 37 °C with 95% relative humidity and 5% CO₂, and the medium was changed every 2 to 3 days until stromal cells reached confluence. Thereafter, the cells were cultured in 75 cm² culture flasks following dispersal with 0.05% trypsin-EDTA for 5 min.

The first two days, cell cultivation was performed using DMEM/F12, 5% FCS and 1% P/S (standard procedure for fibroblast cultures) to obtain typical fibroblast cell morphology. This culture medium will be later on referred as normal-glucose serum-containing cell culture medium (NGSC-medium) in the text. NGSC medium has been proven to be effective for culturing corneal fibroblasts, as described by Foster et al.^{34,35} As limbal epithelial cells are extremely sensitive to specific components of the culture medium and hardly grow in culture medium for stromal cells, this step further assured us (beside the use of 40 μ m Flowmi cell strainers for filtering the cells according to their size) to grow purely fibroblast cultures.^{35–37}

To induce the keratocyte-specific phenotype, NGSC-medium was replaced with low-glucose serum-free cell culture medium (LGSF-medium) after 2 days (at approximately 20% cell confluence), as described by Foster et al.³⁵ The LGSF-medium

Table 1. Age and gender of healthy donors.

Healthy Donor No.	Age (years)	Gender
1	89	Male
2	64	Female
3	76	Male
4	82	Female
5	66	Female
6	58	Female
7	72	Male
8	72	Female
Mean \pm SD (min-max)	73.5 \pm 15.5 (58-89)	37.5% Male

Table 2. Age, gender, aniridia associated keratopathy (AAK) stage (according to Lagali et al. [32,33]) and genetic information details of aniridia subjects in our study.

Aniridia Patient No.	Age (years)	Gender	AAK stage	Genetical information details
1	50	F	4	PAX6 missense mutation (c.1268A>T)
2	16	F	4	PAX6 deletion (c. 753_754delGC)
3	2	F	4	PAX6 deletion (21q22.12q22.2(36,472,360-39,889,694) x1)
4	64	F	4	PAX6 deletion (c. 753_754delGC)
5	30	M	3	PAX6 mutation (c. 1191T (q227X))
6	12	M	4	PAX6 missense mutation (c. 607C>T)
7	46	F	5	PAX6 deletion (c. 753_754delGC)
8	11	M	2	PAX6 deletion (c. 753_754delGC)
Total	28.9 \pm 29.5 (2-64)	3 (37.5%) Male	2 (12.5%); 3 (12.5%); 4 (62.5%); 5 (12.5%)	

comprised low-glucose DMEM (Cat-No.: D6046, Sigma Aldrich, St. Louis, MO, USA), supplemented with 1 mM L-ascorbic acid (Cat-No.: A8960, Sigma Aldrich, St. Louis, MO, USA), 2 g/l D-glucose (Cat-No.: X997, Carl ROTH, Karlsruhe, Baden-Württemberg, DE), 2.5 g/l D-mannitol (Cat-No.: 8883.1, Carl ROTH, Karlsruhe, Baden-Württemberg, DE), 1% insulin transferrin selenite (ITS, No. 1884, Sigma-Aldrich, St. Louis, Missouri, USA), and 1% P/S.

Subsequent cell culture procedures involved the use of NGSC-medium for fibroblasts or LGSF-medium for keratocytes, as described by Foster et al.³⁵ Keratocytes were cultivated for a minimum of 14 days with bi-weekly medium changes before harvesting. Cell passages 3 to 8 were utilized for the experiments.

As the growth of corneal stromal cells suppresses corneal epithelial cell growth *in vitro*, the use of cells from passage 3 to 8 for our experiments further supported us with purely fibroblast cultures, as limbal epithelial cells do not survive in direct co-culture with stromal cells using low FCS concentration culture medium for an extended period of time.^{36,37}

Our measurements were conducted using healthy limbal stromal cells (LSCs) and aniridia limbal stromal cells (AN-LSCs) in NGSC-medium and in LGSF-medium. Stable cultured cells in LGSF-medium at approximately the 14th day were included in our experiments. The cell pellet was frozen at -80°C until further use.

Central stromal cell culture

1.5 mm central corneal biopsies of 8 healthy normal donor corneas (age: 30.9 ± 20.2 (2-64) years; 2 (25%) males) underwent the same isolation and culturing procedure, as described above, both in NGSC and LGSF culture media. These corneas were also obtained from the LIONS Cornea Bank Saar-Lor-Lux, Trier/Westpfalz, Homburg/Saar, Germany and their cultures were used as controls for characteristic stromal cells markers.

Morphological analysis

In order to observe limbal stromal cell morphology in NGSC or LGSF culture medium, phase contrast images have been taken at day 7 for NGSC and at day 7 for LGSF culture medium groups, using a Carl Zeiss Microscope with 10x objectives. Images were taken using an AxioCam ERc5s camera.

Cell proliferation and live/dead assay

Cell proliferation was assessed with the Cell Proliferation ELISA BrdU (colorimetric) Kit, following the manufacturer's instructions. All cell types were reseeded in 96-well plates. In the NGSC medium group, LSCs and AN-LSCs were seeded at a density of 1.0×10^3 cells/cm² (100 µl/well) ($n=4$). Cells were cultured for 7 days until reaching 70% confluence, then 10 µl/well of BrdU labeling solution was added, and the cells were incubated at 37°C for 6 h for BrdU incorporation.

In the LGSF medium group, LSCs and AN-LSCs were first seeded at a density of 1.0×10^4 cells/cm² (100 µl/well) ($n=4$) in NGSC medium, for 24 h. Then, the NGSC medium was replaced by LGSF medium (at this time-point, there was about 20% cell confluency) and cells were cultured for 7 days until reaching 70% confluence. Thereafter, 10 µl/well BrdU labeling solution was added, which was followed by 6 h incubation time at 37°C, for BrdU incorporation.

For both NGSC and LGSF culture medium groups, after removing the medium, cells were fixed with FixDenat solution from the test kit and were incubated with an anti-BrdU-POD monoclonal antibody (100 µl/well) for 90 min to bind the incorporated DNA. Subsequently, the solution was removed, and all wells were rinsed three times with washing buffer (200 µl/well for each washing step). Next, 100 µl/well tetramethyl-benzidine substrate solution was added, followed by 50 µl/well of 1-N sulfuric acid to stop the reaction after sufficient color development for photometric detection (10-30 min). Plates were analyzed using a Tecan Infinite Reader (Tecan Group AG, Männedorf, Switzerland) at 450 nm wavelength, with a reference wavelength of 690 nm.

We further used the trypan blue assay to analyze the ratio of live and dead cells in culture. LSCs and AN-LSCs were harvested using trypsin EDTA and were centrifuged at 2000 rpm for 4 min. Thereafter, we removed the supernatant, and added 30 µl NGSC medium or LGSF medium and 30 µl trypan blue solution. Then, 10 µl NGSC medium or LGSF medium was added in order to resuspend the cells, incubated at room temperature for 5 mins, and to calculate the percentage of dead cells in a hemocytometer (WQ-0344, Neolab, Germany).

Evidence on limbal stromal cell culture purity

Limbal stromal cell purity was supported by the use of 40 µm Flowmi cell strainers, to separate limbal epithelial cells from limbal stromal cells. In addition, the use of NGSC medium supported limbal stromal cell growth, enabling only limbal stromal cells to survive in our cultures. As we used limbal stromal cells from passage 3 to 8 for our experiments, potential growth of limbal epithelial cells in our cultures was again made impossible, as limbal epithelial cells do not survive in direct co-culture with stromal cells using low FCS concentration culture medium for an extended period of time.^{36,37}

Nevertheless, to further assure presence of limbal stromal cells in our cultures, ALDH3A1, keratocan, and CD34 mRNA expression has been determined in the used cell cultures, both with NGSC and LGSF culture media.³⁸ These gene expressions were also compared to those in cultures of purely central stromal corneal cells.³⁸ In addition, ABCG2, p63 and keratin 19 (KRT19) mRNA expression has been determined in LSCs, using both culture media.

RNA isolation and cDNA synthesis

RNA isolation followed the manufacturer's protocol using the Total RNA Purification Plus Micro Kit (Norgen Biotek, Ontario, Canada). Eluted RNA was stored at -80°C until cDNA synthesis, which was performed using the One Taq*

RT-PCR Kit (New England Biolabs INC, Frankfurt, Germany). A total of 200 ng of total RNA served as a template for all samples during cDNA synthesis. The resulting cDNA was then stored at -20°C.

Quantitative PCR

Table 3 summarizes the used primers for qPCR. The quantitative Polymerase Chain Reaction (qPCR) mixture (total volume: 9 µl) comprised 1 µl of the specific primer solution, 5 µl SYBR Green Mix (Vazyme, Nanjing, China), and 3 µl nuclease-free water. Following the manufacturer's instructions, samples were processed in a 9 µl volume with 1 µl cDNA. The QuantStudio 5 real-time PCR system (Thermo Fisher Scientific, Waltham, MA, USA) was employed for qPCR, utilizing amplification conditions of 95°C for 10 s, 60°C for 30 s, and 95°C for 15 s (40 cycles). Each sample underwent duplicate measurements, and values were normalized using Tata-binding protein (TBP) and Beta-glucuronidase (GUSB) as endogenous control genes through the $\Delta\Delta CT$ method. For statistical analysis, fold changes ($2^{-\Delta\Delta CT}$ -value) were calculated, with LSCs in NGSC-medium as the reference (fold change = 1).

Protein quantification

Upon reaching confluence, cells from a 75-cm² flask were lysed in 80 µl RIPA buffer (Thermo Fisher Scientific, Waltham, MA, USA), and the protein concentration was assessed using the Pierce™ BCA Protein Assay Kit (Thermo Fisher Scientific, Waltham, MA, USA). The measurement took place with the Tecan Infinite F50 Absorbance Microplate

Reader (Tecan Group AG, Männedorf, Switzerland) at a wavelength of 560 nm. Bovine serum albumin served as the standard, and measurements were conducted in duplicate.

Western blot analysis

For Western blot analysis, 20 µg total protein samples were boiled in 5 µl Laemmli-Buffer for 5 min at 95°C and loaded onto a precast 4-12% NuPage™ Bis-Tris SDS Gel (Invitrogen, Waltham, MA, USA). The first well included 2.5 µl Precision Plus Protein™ Dual Color Standard (Bio-Rad Laboratories, Hercules, USA) for molecular weight determination. NuPAGE™ MOPS SDS Running Buffer (20×) (Thermo Fisher Scientific, Waltham, MA, USA) served as the electrophoresis buffer. After protein separation, semi-dry blotting on a nitrocellulose membrane was conducted using the Trans-Blot Turbo Transfer System (Bio-Rad Laboratories, Hercules, USA) following the pre-installed blotting protocol for high-molecular-weight proteins.

The membrane was incubated with No-Stain™ Protein labeling reagent (ThermoFisher Scientific™ GmbH, Dreieich, Germany) to determine the total protein amount per lane for normalization. The membrane underwent three washes with 10 ml Western Froxx washing solution (BioFroxx GmbH, Einhausen, Germany) for 5 min, followed by overnight primary antibody incubation at 4°C. The utilized antibodies are detailed in Table 4. Primary antibodies were diluted in a combined blocking and secondary antibody solution (WesternFroxx anti-Rabbit HRP; BioFroxx GmbH, Einhausen, Germany). After removing the antibody solution, the membrane was washed three times with 10 ml washing solution.

Protein band detection utilized the Western Lightning Plus Chemiluminescence Reagent (PerkinElmer Inc., Waltham, MA, USA), and the iBright™ CL1500 Imaging System (Cat-No.: A44114, Thermo Fisher Scientific, Waltham, MA, USA) was employed for chemiluminescence detection. Subsequently, membrane stripping was carried out using the Western Froxx stripping solution (BioFroxx GmbH, Einhausen, Germany) for further antibody incubation.

Statistical analysis

Statistical analysis and diagram preparation were performed using GraphPad Prism 9.2.0. Quantitative PCR data were

Table 3. Primer pairs used for qPCR.

Primer	Primer sequence or QIAGEN catalog number	Manufacturer (company, city, country)
PAX6	QT00071169	Qiagen N.V., Venlo, the Netherlands
Collagen 1A1 (COL 1A1)	QT00037793	Qiagen N.V., Venlo, the Netherlands
Collagen 3A1 (COL 3A1)	QT00058233	Qiagen N.V., Venlo, the Netherlands
Collagen 5A1 (COL 5A1)	QT00044527	Qiagen N.V., Venlo, the Netherlands
ACTA 2A1	QT00088102	Qiagen N.V., Venlo, the Netherlands
ALDH 3A1	QT00097636	Qiagen N.V., Venlo, the Netherlands
Keratocan (KER)	QT00021280	Qiagen N.V., Venlo, the Netherlands
Lumican (LUM)	QT00058982	Qiagen N.V., Venlo, the Netherlands
CD34	QT00056497	Qiagen N.V., Venlo, the Netherlands
ABCG2	QT00073206	Qiagen N.V., Venlo, the Netherlands
P63	QT02424251	Qiagen N.V., Venlo, the Netherlands
Keratin (KRT19)	QT00081137	Qiagen N.V., Venlo, the Netherlands
MKi67 (Ki67)	QT00014203	Qiagen N.V., Venlo, the Netherlands
TBP	QT00000721	Qiagen N.V., Venlo, the Netherlands
GUSB	QT00046046	Qiagen N.V., Venlo, the Netherlands

Table 4. Antibodies used for Western blot.

Antibody	Catalog number	Manufacturer (company, city, country)	Dilution
PAX6	AB2237	Millipore, Watford, UK	1:200
Collagen 1A1 (COL1A1)	84336	Cell Signaling Technology, MA, USA	1:1000
Collagen 5A1 (COL5A1)	ab7046	Abcam, Cambridge, UK	1:5000
α-SMA (ACTA 2A1)	19245	Cell Signaling Technology, MA, USA	1:1000
Keratocan (KER)	PA5-79552	Thermo Fisher Scientific, Waltham, MA, USA	1:2000
Lumican (LUM)	MA5-35135	Thermo Fisher Scientific, Waltham, MA, USA	1:1000
CD34	26233	Cell Signaling Technology, MA, USA	1:1000

presented as the geometric mean with geometric standard deviation, while western blot data were expressed as mean \pm standard deviation (SD). The Mann-Whitney U-test was employed for comparing two groups, One-way ANOVA was used to compare three or more groups, with P values <0.05 considered statistically significant.

Results

Limbal stromal cell morphology

Phase-contrast images depicting corneal stromal cells in NGSC- or LGSF-medium are presented in Figure 1(A-D). On the initial day in culture, cell morphology remained consistent in both NGSC- and LGSF-medium. However, thereafter, both

healthy and AN-LSCs exhibited distinct morphologies depending on the culture medium type (NGSC- vs LGSF-medium). In NGSC-medium, fusiform-shaped cells typical of fibroblasts were observed (Figure 1(A,C)). Corneal LSCs in NGSC-medium reached confluence on day 7, maintaining their fusiform shape and subsequently initiating stratification.

Conversely, LGSF-medium displayed dendritic cell morphology indicative of the presence of keratocytes (Figure 1(B,D)). In LGSF-medium, dendritic-shaped corneal LSCs ceased proliferation on the 7th day in culture. Although dendritic-shaped corneal LSCs retained their morphology, a significant cell loss was observed on the 21st day in culture. Morphological differences between corneal LSCs of aniridia and healthy subjects were not evident, regardless of the culture medium used.

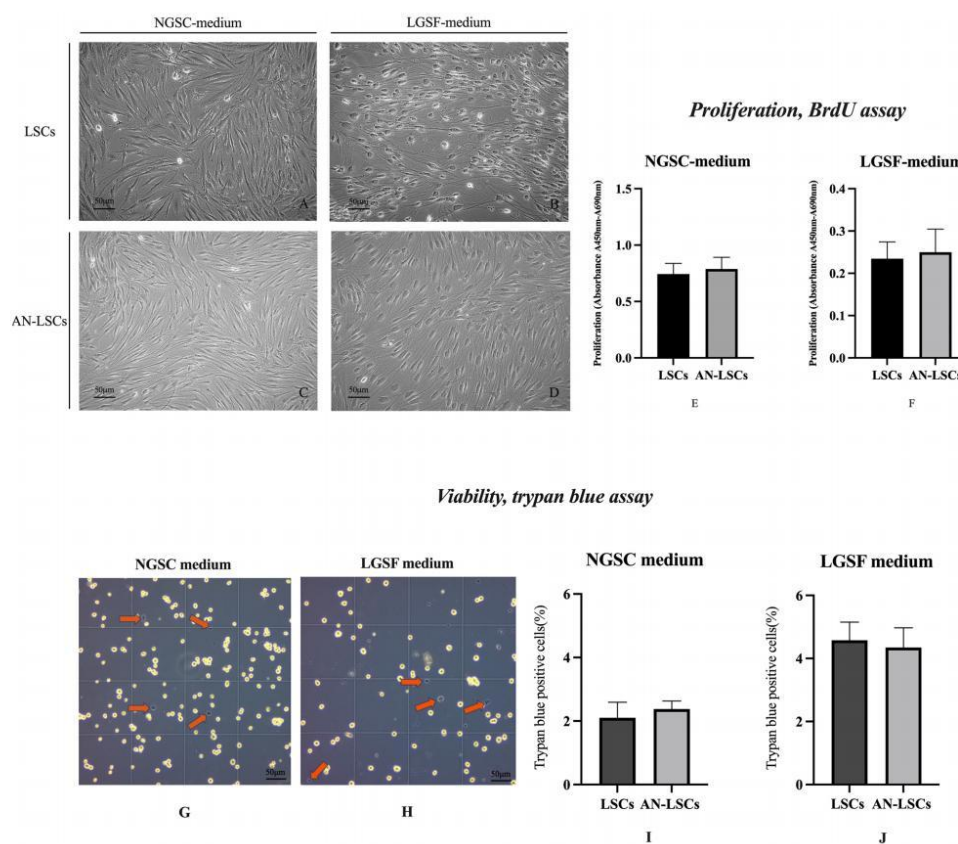


Figure 1. Corneal limbal stromal cell (LSCs) and aniridia limbal stromal cell (AN-LSCs) morphology, proliferation and viability (trypan blue assay) using normal-glucose serum-containing cell culture medium (NGSC-medium) or low glucose serum free medium (LGSF-medium) for 7 days (A-J). E and F show LSCs and aniridia LSCs (AN-LSCs) proliferation using NGSC medium (E) or LGSF medium (F) for 7 days, using the BrdU assay ($n=4$). G-J display results of the trypan blue assay on the 7th day in culture.

At the above time-points, there was a stable LSCs (A, B) and AN-LSCs morphology in culture (C, D), both in NGSC and LGSF culture media. In NGSC-medium, there were fusiform shaped cells characteristic for fibroblasts (A, C). Using LGSF-medium, there was a dendritic cell morphology indicating the presence of keratocytes (B, D). LSCs and AN-LSCs proliferation did not differ significantly using NGSC (E) or LGSF (F) culture medium ($p=0.549$, $p=0.661$). Following 7 days in culture using NGSC medium, there was trypan blue positivity in 2.1% of LSCs and 2.4% of AN-LSCs, without a significant difference in both cell types ($p=0.639$) (G, I). Following 7 days in culture using LGSF medium, there was trypan blue positivity in 4.6% of scale bar: 50 μm .

Limbal stromal cell proliferation and live-dead assay

LSCs and AN-LSCs proliferation in NGSC and LGSF medium is displayed in Figure 1(E,F). LSCs and AN-LSCs proliferation did not differ significantly using NGSC or LGSF culture medium ($p=0.549$, $p=0.661$).

Live-dead assay of LSCs and AN-LSCs using NGSC- and LGSF-medium is displayed at Figure 1(G–J). Following 7 days in culture using NGSC medium, there was trypan blue positivity in 2.1% of LSCs and 2.4% of AN-LSCs, without a significant difference in both cell types ($p=0.639$). Following 7 days in culture using LGSF medium, there was trypan blue positivity in 4.6% of LSCs and 4.4% of AN-LSCs, without a significant difference in both cell types ($p=0.800$).

Limbal stromal cell culture purity - Keratocyte-characteristic marker expression of limbal vs Central stromal cells

In NGSC-medium, there was no significant difference in ALDH3A1 and CD34 mRNA expression between central stromal cells and LSCs ($p=0.517$; $p=0.183$). However, KER mRNA expression was significantly higher in central stromal cells compared to LSCs ($p=0.006$) (Figure 1(A)).

Similarly, in LGSF-medium, ALDH3A1 and CD34 mRNA expression did not show a significant difference between central stromal cells and LSCs ($p=0.517$; $p\geq 0.999$). Nevertheless, KER mRNA expression was significantly higher in central stromal cells compared to LSCs ($p=0.002$) (Figure 1(B)).

ABCG2, p63 and KRT19 mRNA expression in LSCs did not differ significantly, using NGSC or LGSF culture medium ($p\geq 0.158$) (Supplemental Figure 1).

mRNA expression of limbal stromal cells, in vitro

PAX6 mRNA expression of healthy vs aniridia limbal stromal cells

PAX6 mRNA expression exhibited a notable decrease in AN-LSCs compared to LSCs using both NGSC-medium ($p=0.04$) and LGSF-medium ($p=0.014$). While PAX6 mRNA

expression showed no significant difference in LSCs using NGSC or LGSF medium, it was significantly elevated in AN-LSCs using NGSC-medium compared to LGSF-medium ($p=0.007$) (Figure 3(A)).

Keratocyte-characteristic marker expression of healthy vs aniridia limbal stromal cells

Under NGSC-medium conditions, there were no significant differences in COL1A1, COL3A1, LUM, and CD34 mRNA expression between AN-LSCs and LSCs ($p>0.999$; $p=0.209$; $p=0.536$; $p=0.165$) (Figure 3B(C,H,I)). However, AN-LSCs exhibited significantly higher ALDH3A1 and KER mRNA expression compared to LSCs ($p=0.007$; $p=0.013$) (Figure 3(F,G)), while COL5A1 and ACTA2 mRNA expression were significantly lower in AN-LSCs than in LSCs ($p=0.011$; $p=0.041$) (Figure 3(D,E)).

In LGSF-medium, there were no significant differences in COL3A1, ACTA2A1, ALDH3A1, KER, LUM, and CD34 mRNA expression between AN-LSCs and LSCs ($p=0.165$; $p=0.165$; $p=0.902$; $p=0.536$; $p=0.232$; $p=0.620$) (Figure 3(C,E–I)). Nonetheless, COL1A1 ($p=0.048$) and COL5A1 ($p=0.002$) mRNA expression was significantly higher in AN-LSCs than in LSCs (Figure 3(B,D)).

Keratocyte-characteristic marker expression of LSCs and an-LSCs using NGSC- vs LGSF-medium

In LSCs, there were no significant differences in COL1A1, ACTA2, and ALDH3A1 mRNA expression between NGSC- and LGSF-medium ($p=0.343$; $p=0.456$; $p=0.209$) (Figure 3(B,E,F)). However, COL3A1, KER, LUM, and CD34 mRNA expression was markedly lower in NGSC-medium compared to LGSF-medium ($p=0.002$; $p=0.001$; $p=0.003$; $p=0.001$) (Figure 3(C,G,H,I)), while COL5A1 mRNA expression was significantly higher with NGSC-medium than LGSF-medium ($p=0.002$) (Figure 3(D)).

In AN-LSCs, there was no significant difference in ALDH3A1 mRNA expression between NGSC- and LGSF-medium ($p=0.165$) (Figure 3(F)). Nevertheless, LUM mRNA expression was significantly higher with

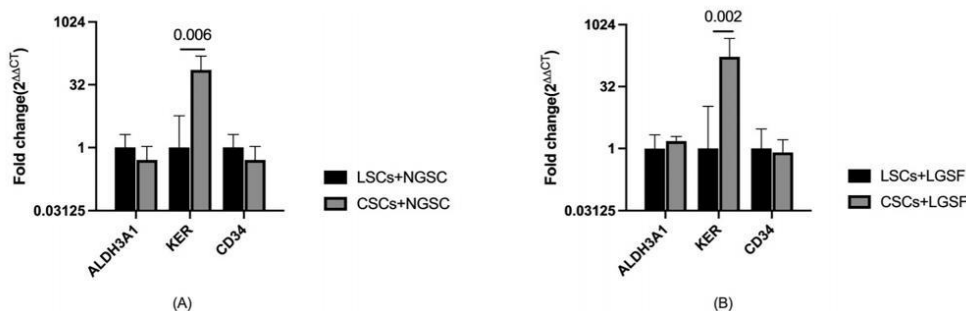


Figure 2. Keratocyte phenotype marker ALDH3A1, KER and CD34 mRNA expression in healthy limbal stromal cells (LSCs) and in healthy central stromal cells (CSCs), using normal-glucose serum-containing (NGSC-) cell culture medium (A) and low-glucose serum-free (LGSF)-medium (B) ($n=8$). Values are shown using a logarithmic scale (Log 2), as geometric mean and SD. Mann-Whitney U test has been used. Significant p values (< 0.05) are highlighted. ALDH3A1 and CD34 mRNA expression did not differ significantly in LSCs and in CSCs, neither in NGSC, nor in LGSF medium. Nevertheless, KER mRNA expression was significantly higher in central stromal cells, than in LSCs, both in NGSC and LGSF medium ($p=0.06$; $p=0.002$).

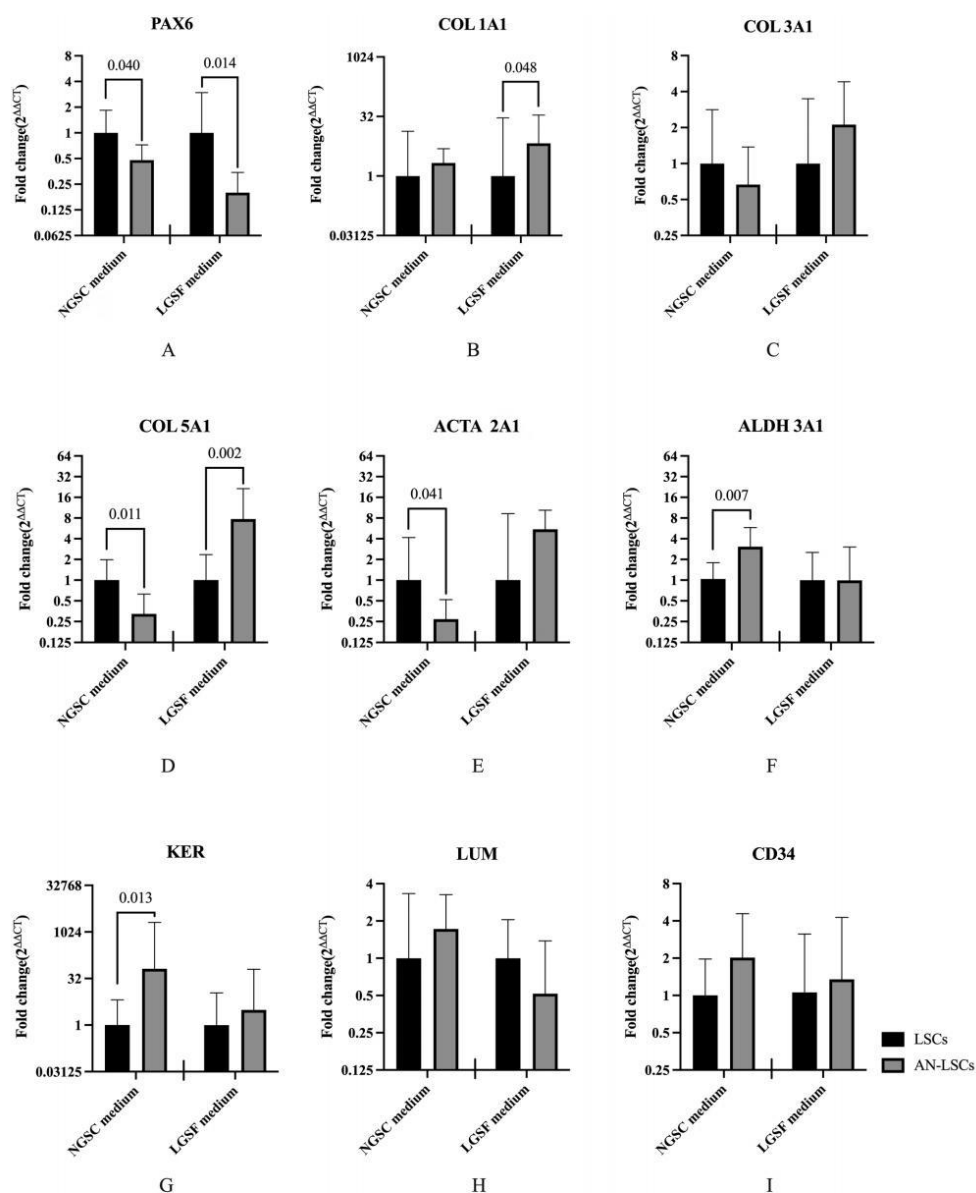


Figure 3. *PAX6*, *COL1A1*, *COL3A1*, *COL5A1*, *ACT2A1*, *ALDH3A1*, *KER*, *LUM* and *CD34* mRNA expression in healthy limbal stromal cells (LSCs) and in aniridia limbal stromal cells (AN-LSCs), using normal-glucose serum-containing (NGSC-) cell culture medium (A) and low-glucose serum-free (LGSF-) medium (B). Expression of the same genes in LSCs (C) and in AN-LSCs (D), using NGSC or LGSF culture medium. Values are shown using a logarithmic scale (Log 2), as geometric mean and SD. A Mann-Whitney U test has been used. Significant p values (< 0.05) were highlighted in the diagrams. In NGSC medium, *PAX6*, *COL5A1* and *ACTA2A1* mRNA expression was significantly lower in AN-LSCs and *ALDH3A1* and *KER* mRNA expression was significantly higher in AN-LSCs, than in LSCs ($p \leq 0.013$). In LGSF medium, *COL1A1* and *COL5A1* mRNA expression was significantly higher in AN-LSCs, than in LSCs ($p \leq 0.048$).

NGSC-medium than LGSF-medium ($p = 0.019$) (Figure 3(H)). Conversely, *COL1A1*, *COL3A1*, *COL5A1*, *ACTA2*, *p = 0.001; $p = 0.026$; $p = 0.001$; $p = 0.038$; $p = 0.001$) (Figure 3(B,C,D,E,G,I)).*

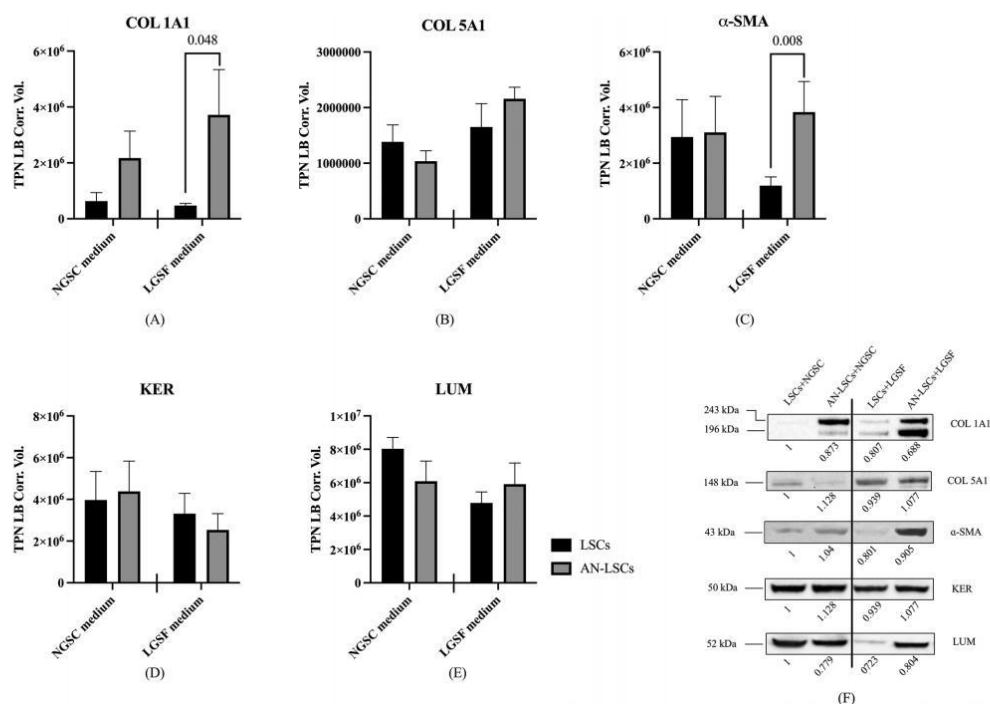


Figure 4. Protein expression of keratocyte-characteristic molecular markers in healthy limbal stromal cells (LSCs) in normal-glucose serum-containing cell culture medium (NGSC)- and low-glucose serum-free (LGSF)-medium, and in aniridia limbal stromal cells (AN-LSCs) in NGSC- and LGSF-medium ($n=8$) (A-E). Values are expressed as mean \pm standard deviation (SD). Representative COL1A1, COL5A1, α -SMA, KER and LUM blots are shown at Figure (F). COL1A1 was detected as double band at 243 and 196 kDa. Total protein normalization (TPN) factors are presented below each lane. Significant p values (< 0.05) were highlighted in the diagrams.

In LGSF medium, COL1A1 and α -SMA protein expression was significantly higher in AN-LSCs, than in LSCs ($p \leq 0.048$). Nevertheless, none of the analyzed protein expressions differed significantly between LSCs and AN-LSCs neither in NGSC medium ($p \geq 0.105$).

mRNA expression levels in passages 4 to 6 in LSCs and an-LSCs, using NGSC-medium

To verify that varying cell passages in LSCs and AN-LSCs do not affect outcomes, we analyzed the mRNA expression levels of *PAX6* and keratocyte-specific markers (*COL1A1*, *COL5A1*, *ACT2A1*, *KER*, and *LUM*) in LSCs and AN-LSCs from passages 4 to 6, using NGSC medium. Our results showed no significant differences in gene expression levels for either LSCs or AN-LSCs ($p \geq 0.157$; $p \geq 0.128$) (Supplemental Figure 2). In addition, Ki67 proliferation marker expression also did not differ significantly between passages 4 to 6 in AN-LSCs and LSCs ($p = 0.156$; $p = 0.555$).

Protein expression of healthy and aniridia limbal stromal cells using NGSC- and LGSF medium, in vitro

Figure 4 illustrates the protein expression patterns of the analyzed genes. Notably, *PAX6* and *CD34* bands were not discernible despite escalating protein amounts to $30 \mu\text{g}$ and extending incubation time up to 72h for gel electrophoresis in all analyzed cell cultures (data not shown).

In NGSC-medium, no significant differences were observed in COL1A1, COL5A1, α -SMA, KER, and LUM protein expression between LSCs and AN-LSCs ($p = 0.485$; $p = 0.505$; $p = 0.852$; $p = 0.853$; $p = 0.336$). Similarly, under LGSF-medium, there were no significant differences in COL5A1, KER, and LUM protein expression between LSCs and AN-LSCs ($p = 0.105$; $p = 0.833$; $p = 0.524$) (Figure 4(A-E)).

For LSCs, protein expression of COL1A1, COL5A1, α -SMA, and KER did not significantly differ between NGSC and LGSF culture medium ($p = 0.548$; $p = 0.798$; $p = 0.699$; $p = 0.662$). In AN-LSCs, no significant differences were observed in COL1A1, α -SMA, KER, and LUM protein expression between the two culture media ($p = 0.589$; $p = 0.336$; $p = 0.442$; $p = 0.645$) (Figure 4(A-E)).

However, LUM protein expression was significantly higher in LSCs using NGSC-medium than with LGSF-medium ($p = 0.018$). COL1A1 and α -SMA protein expression were significantly elevated in AN-LSCs compared to LSCs when utilizing LGSF-medium ($p = 0.048$; $p = 0.008$). Notably, a doublet molecular band at 243 and 196 kDa was detected for COL1A1. Additionally, COL5A1 protein expression was

significantly lower using NGSC-medium than with LGSF-medium ($p=0.003$) (Figure 4(F)).

Discussion

The role of limbal stromal cells in AAK development is poorly understood or analyzed, yet. In our present study, PAX6 and keratocyte-characteristic marker expression of primary limbal stromal cells of AAK subjects has been evaluated, using NGSC- and LGSF-medium. According to Foster et al.,³⁵ NGSC medium promotes fibroblast growth, while LGSF medium is supportive for keratocytes.

Initially, we aimed to clarify, whether there are limbal epithelial cells, limbal fibroblasts/limbal keratocytes in our cultures. Therefore, we assessed gene expression of keratocyte phenotype markers, including ALDH3A1, KER, and CD34, in our limbal stromal cell cultures. In our study, both in LSCs cultured using NGSC- or LGSF-medium, keratocyte phenotype marker ALDH3A1, and CD34 gene expression did not differ from central corneal stromal cells (Figure 2). Therefore, we could demonstrate, that our cultured limbal stromal cells did not belong to epithelial stem cells.³⁸ Additionally, in both LSCs and AN-LSCs, the mRNA expression levels of PAX6, keratocyte-specific markers COL1A1, COL5A1, ACT2A1, KER and LUM and proliferation marker Ki67 remained consistent from passages 4 to 6 (Supplemental Figure 2). Interestingly, we also detected a significantly upregulated KER mRNA expression in central stromal cells, compared to LSCs, with both used culture media. Whether KER plays an important role in central corneal stromal cell differentiation, still needs further research.

We found that both LSCs and AN-LSCs cultured in LGSF medium acquired a flattened, dendritic-shaped morphology, showing pronounced differences from cells cultured in NGSC medium, which had fusiform shape. Regarding cell morphology, there were no differences between AN-LSCs and healthy controls, regardless of the culture medium used (Figure 1(E)). Cell proliferation and live/dead cell ratio did not differ significantly between LSCs and AN-LSCs using NGSC- or LGSF medium (Figure 1), therefore, both stromal cell types were well comparable for our further measurements.

NGSC and LGSF culture media showed different impacts on the phenotype of LSCs and AN-LSCs. It has been established that the omission of serum from the culture medium induces a partial restoration of the native keratocyte phenotype in corneal fibroblasts under *in vitro* conditions.^{39,40} CD34 is regarded as an alternate keratocyte marker⁴¹ and was found to be downregulated upon exposure to standard tissue culture conditions.⁴² During the keratocyte-phenotype-recovery, expression of keratocyte-characteristic markers increases. Our measurement series have shown similar changes, as the expression of two major types of collagens (I and III) and KER and CD34 expression were upregulated in limbal stromal cells cultured in LGSF-medium (Figure 3(B,C,G,I)), both in healthy and aniridia limbal stromal cells.

Nevertheless, there was a reverse COL5A1 and LUM expression using different culture medium for healthy limbal stromal cells and aniridia limbal stromal cells. In healthy

limbal stromal cells, COL5A1 mRNA expression was downregulated (Figure 3(D)), and LUM mRNA expression was upregulated using LGSF medium (Figure 3(H)), instead of NGSF medium. This pattern was reversed in aniridia limbal stromal cells. In aniridia limbal stromal cells, COL5A1 mRNA expression was upregulated (Figure 3(D)), and LUM mRNA expression was downregulated using LGSF medium (Figure 3(H)), instead of NGSF medium. This phenomenon may be related to the interaction of LUM and COL5A1. It has been reported that LUM is able to inhibit TGF- β 1, and TGF- β 1 is able to elicit a 2.5-fold COL5A1 mRNA level increase in bone matrix during osteogenesis.⁴³ Boya Zhou et al. found significantly upregulated TGF- β 1 expression in case of LUM knockdown, which might explain the COL5A1 upregulation in case of LUM knockdown.⁴⁴

In healthy limbal stromal cells, there was no significant PAX6 expression change using the two different culture mediums. Nevertheless, there was a significant PAX6 mRNA expression downregulation using LGSF medium, in aniridia limbal stromal cells (Figure 3(A)). Several previous studies have demonstrated the relationship between PAX6 and TGF- β 1 expression. For instance, PAX6 as a transcriptional regulator, localized in the nucleus of the outer nuclear layer and the inner nuclear layer of the murine retina, is co-localized and interact with TGF- β 1.⁴⁵ Yenan Feng et al. demonstrated that suppression of PAX6 expression by siRNA transfection promoted TGF- β 1 mRNA and protein level.⁴⁶ In our study, a lower PAX6 mRNA expression in AN-LSCs using LGSF-medium may induce upregulation of COL5A1 and downregulation of LUM mRNA expression (Figure 3(D,H)).

We also aimed to investigate the role of PAX6 in aniridia limbal stromal cells and the keratocyte-characteristic markers, by comparing limbal stromal cells of healthy and aniridia corneas. It has been demonstrated that PAX6 controls a numbers of target genes.⁴⁷ Consequently, reduced PAX6 protein amount alters the expression of several genes and influences development of cells and tissues. Recent research demonstrated that there is PAX6 downregulation in fibrotic hearts and that PAX6 downregulation has an inhibitory effect on cardiac fibroblast differentiation and ECM synthesis.⁴⁶ Ming Ying et al. reported that inherited PAX6 gene mutations result in congenital fibrosis of the extraocular muscles,⁴⁸ supporting the hypothesis that PAX6 plays an essential role in preventing fibrosis of several tissues. In our study, we demonstrated a significantly downregulated PAX6 gene expression in aniridia limbal stromal cells, independently from the culturing conditions. We hypothesize that the decreased PAX6 gene expression may also be related to the stromal fibrosis and pannus formation in aniridia patients.

A previous study demonstrated that there is an altered expression of extracellular matrix components COL1A1 and COL5A1 and an increased expression of ACTA2A1 in naive AAK corneas, without any previous treatment, and in transplanted corneas.³⁰ Interestingly, in our research, we also observed a significantly decreased COL5A1 and ACTA2A1 expression (Figure 3(D,E)) and a slightly decreasing trend of COL1A1 gene expression in AN-LSCs, cultured in

NGSC-medium. On the other hand, *COL1A1* and *COL5A1* mRNA levels were significantly increased in AN-LSCs, in LGSF culture medium (Figure 3(B,D)), even though there was no obvious difference in *ACTA2A1* mRNA level (Figure 3(E)), between healthy and AN-LSCs. *ACTA2A1* (α -SMA) protein level was significantly upregulated in AN-LSCs, using LGSF-medium (Figure 4(C)). This suggests a potential differentiation of the cells into myofibroblasts.

Nevertheless, our study used based an *in vitro* analysis, and it is still unclear how PAX6 and keratocyte-characteristic marker expression behave in limbal stromal tissue of aniridia patients. Histological analysis of keratocyte-characteristic markers and PAX6 expression in subjects with congenital aniridia should be performed in the future.

Conclusions

Our study demonstrates altered PAX6 and keratocyte-characteristic marker expression in aniridia limbal stromal cells compared to healthy controls, suggesting a potential role in the development and progression of AAK. These findings shed new light on AAK pathogenesis, highlighting the role of sustained PAX6 expression in preventing the differentiation of aniridia limbal stromal cells and the excessive synthesis of extracellular matrix proteins.

Acknowledgements

The work of Zhen Li, Tanja Stachon, Julia Zimmermann, Simon Trusen, Fabian N. Fries, Maximilian Berger, Shweta Suiwal, Ning Chai, Maryam Amini and Nóra Szentmáry at the Dr. Rolf M. Schwiete Center has been supported by the Dr. Rolf M. Schwiete Foundation. The work of Zhen Li and Ning Chai has been supported by the China Scholarship Council. We thank for the support of the Pitzer Foundation.

Author contributions

Z.L. conducted experiments, analyzed data, and wrote the manuscript. T.S. designed the experiments, analyzed data and reviewed the manuscript. F.N.F., B.S. provided limbal biopsies and reviewed the manuscript. J.Z., S.T., M.B., S.S., N.C., M.A. participated in cell culture work and reviewed the manuscript. L.S. analyzed data and reviewed the manuscript. N.S. designed the experiments, analyzed data and reviewed the manuscript.

Disclosure statement

No potential conflict of interest was reported by the author(s).

Data availability statement

The data presented in this study are available upon reasonable request from the corresponding author.

ORCID

Zhen Li  <http://orcid.org/0000-0001-5491-2169>
 Tanja Stachon  <http://orcid.org/0000-0001-7009-7125>
 Fabian N. Fries  <http://orcid.org/0000-0002-8526-4712>

References

1. Landsend ECS, Lagali N, Utheim TP. Congenital aniridia - A comprehensive review of clinical features and therapeutic approaches. *Surv Ophthalmol.* 2021;66(6):1031–1050. doi: 10.1016/j.survophthal.2021.02.011.
2. Lim HT, Kim DH, Kim H. PAX6 aniridia syndrome: clinics, genetics, and therapeutics. *Curr Opin Ophthalmol.* 2017;28(5):436–447. doi: 10.1097/ICU.0000000000000405.
3. Kasmann-Kellner B, Seitz B. [Congenital aniridia or PAX6 syndrome]. *Ophthalmologe.* 2014;111(12):1144–1144. doi: 10.1007/s00347-014-3058-4.
4. Kucerova R, Ou J, Lawson D, Leiper LJ, Collinson JM. Cell surface glycoconjugate abnormalities and corneal epithelial wound healing in the pax6+/- mouse model of aniridia-related keratopathy. *Invest Ophthalmol Vis Sci.* 2006;47(12):5276–5282. doi: 10.1167/iovs.06-0581.
5. Dorà N, Ou J, Kucerova R, Parisi I, West JD, Collinson JM. PAX6 dosage effects on corneal development, growth, and wound healing. *Dev Dyn.* 2008;237(5):1295–1306. doi: 10.1002/dvdy.21528.
6. Ilnatko R, Eden U, Fagerholm P, Lagali N. Congenital Aniridia and the Ocular Surface. *Ocul Surf.* 2016;14(2):196–206. doi: 10.1016/j.jtos.2015.10.003.
7. Bausili MM, Alvarez de Toledo J, Barraquer RI, Michael R, Tresserra F, de la Paz MF. Histopathology findings of corneal buttons in congenital aniridia patients. *Ophthalmic Res.* 2016;56(4):202–206. doi: 10.1159/00044930.
8. Auw-Haedrich C, Agrawal M, Gabbert HE, Meyer P, Arnold N, Reinhard T. Immunohistochemical expression of epithelial cell markers in corneas with congenital aniridia and ocular cicatrizing pemphigoid. *Acta Ophthalmol.* 2011;89(1):47–53. doi: 10.1111/j.1755-3768.2009.01603.x.
9. Lee H, Khan R, O'Keefe M. Aniridia: current pathology and management. *Acta Ophthalmol.* 2008;86(7):708–715. doi: 10.1111/j.1755-3768.2008.01427.x.
10. Kawashima M, Kawakita T, Higa K, Satake Y, Omoto M, Tsubota K, Shimmura S, Shimazaki J. Subepithelial corneal fibrosis partially due to epithelial-mesenchymal transition of ocular surface epithelium. *Mol Vis.* 2010;16:2727–2732.
11. Pinnamaneni N, Funderburgh JL. Concise review: stem cells in the corneal stroma. *Stem Cells.* 2012;30(6):1059–1063. doi: 10.1002/stem.1100.
12. Polisetty N, Fatima A, Madhira SL, Sangwan VS, Vemuganti GK. Mesenchymal cells from limbal stroma of human eye. *Mol Vis.* 2008;14:431–442.
13. Guo X, Hutcheon AE, Melotti SA, Zieske JD, Trinkaus-Randall V, Ruberti JW. Morphologic characterization of organized extracellular matrix deposition by ascorbic acid-stimulated human corneal fibroblasts. *Invest Ophthalmol Vis Sci.* 2007;48(9):4050–4060. doi: 10.1167/iovs.06-1216.
14. Pei Y, Sherry DM, McDermott AM. Thy-1 distinguishes human corneal fibroblasts and myofibroblasts from keratocytes. *Exp Eye Res.* 2004;79(5):705–712. doi: 10.1016/j.exer.2004.08.002.
15. Latta L, Viestenz A, Stachon T, Colanesi S, Szentmáry N, Seitz B, Kasmann-Kellner B. Human aniridia limbal epithelial cells lack expression of keratins K3 and K12. *Exp Eye Res.* 2018;167:100–109. doi: 10.1016/j.exer.2017.11.005.
16. Schlötzer-Schrehardt U, Latta L, Giefl A, Zenkel M, Fries FN, Kasmann-Kellner B, Kruse FE, Seitz B. Dysfunction of the limbal epithelial stem cell niche in aniridia-associated keratopathy. *Ocul Surf.* 2021;21:160–173. doi: 10.1016/j.jtos.2021.06.002.
17. Wu J, Du Y, Mann MM, Yang E, Funderburgh JL, Wagner WR. Bioengineering organized, multilamellar human corneal stromal tissue by growth factor supplementation on highly aligned synthetic substrates. *Tissue Eng Part A.* 2013;19(17-18):2063–2075. doi: 10.1089/ten.TEA.2012.0545.
18. Wu J, Du Y, Watkins SC, Funderburgh JL, Wagner WR. The engineering of organized human corneal tissue through the spatial guidance of corneal stromal stem cells. *Biomaterials.* 2012;33(5):1343–1352. doi: 10.1016/j.biomaterials.2011.10.055.

19. Motaln H, Schichor C, Lah TT. Human mesenchymal stem cells and their use in cell-based therapies. *Cancer*. 2010;116(11):2519–2530. doi: 10.1002/cncr.25056.
20. Wang J, Liao L, Tan J. Mesenchymal-stem-cell-based experimental and clinical trials: current status and open questions. *Expert Opin Biol Ther*. 2011;11(7):893–909. doi: 10.1517/14712598.2011.574119.
21. Reinshagen H, Auw-Haedrich C, Sorg RV, Boehringer D, Eberwein P, Schwartzkopff J, Sundmacher R, Reinhard T. Corneal surface reconstruction using adult mesenchymal stem cells in experimental limbal stem cell deficiency in rabbits. *Acta Ophthalmol*. 2011;89(8):741–748. doi: 10.1111/j.1755-3768.2009.01812.x.
22. Ma Y, Xu Y, Xiao Z, Yang W, Zhang C, Song E, Du Y, Li L. Reconstruction of chemically burned rat corneal surface by bone marrow-derived human mesenchymal stem cells. *Stem Cells*. 2006;24(2):315–321. doi: 10.1634/stemcells.2005-0046.
23. Zajicova A, Pokorna K, Lencova A, Krulova M, Svobodova E, Kubinova S, Sykova E, Pradny M, Michalek J, Svobodova J, and others, et al. Treatment of ocular surface injuries by limbal and mesenchymal stem cells growing on nanofiber scaffolds. *Cell Transplant*. 2010;19(10):1281–1290. doi: 10.3727/096368910X509040.
24. Yam GH, Williams GP, Setiawan M, Yusoff NZ, Lee XW, Htoon HM, Zhou L, Fuest M, Mehta JS. Nerve regeneration by human corneal stromal keratocytes and stromal fibroblasts. *Sci Rep*. 2017;7(1):45396. doi: 10.1038/srep45396.
25. Yam GH, Teo EP, Setiawan M, Lovatt MJ, Yusoff N, Fuest M, Goh BT, Mehta JS. Postnatal periodontal ligament as a novel adult stem cell source for regenerative corneal cell therapy. *J Cell Mol Med*. 2018;22(6):3119–3132. doi: 10.1111/jcmm.13589.
26. Duarte Campos DF, Rohde M, Ross M, Anvari P, Blaeser A, Vogt M, Panfil C, Yam GH-F, Mehta JS, Fischer H, and others, et al. Corneal bioprinting utilizing collagen-based bioinks and primary human keratocytes. *J Biomed Mater Res A*. 2019;107(9):1945–1953. doi: 10.1002/jbm.a.36702.
27. Chakravarti S, Petroll WM, Hassell JR, Jester JV, Lass JH, Paul J, Birk DE. Corneal opacity in lumican-null mice: defects in collagen fibril structure and packing in the posterior stroma. *Invest Ophthalmol Vis Sci*. 2000;41(11):3365–3373.
28. Funderburgh JL, Mann MM, Funderburgh ML. Keratocyte phenotype mediates proteoglycan structure: a role for fibroblasts in corneal fibrosis. *J Biol Chem*. 2003;278(46):45629–45637. doi: 10.1074/jbc.M303292200.
29. Hassell JR, Birk DE. The molecular basis of corneal transparency. *Exp Eye Res*. 2010;91(3):326–335. doi: 10.1016/j.exer.2010.06.021.
30. Vicente A, Byström B, Lindström M, Stenevi U, Pedrosa Domellöf F. Aniridia-related keratopathy: structural changes in naïve and transplanted corneal buttons. *PLoS One*. 2018;13(6):e0198822. doi: 10.1371/journal.pone.0198822.
31. Edén U, Fagerholm P, Danyali R, Lagali N. Pathologic epithelial and anterior corneal nerve morphology in early-stage congenital aniridic keratopathy. *Ophthalmology*. 2012;119(9):1803–1810. doi: 10.1016/j.ophtha.2012.02.043.
32. Lagali N, Wowra B, Fries FN, Latta L, Moslemani K, Utheim TP, Wylegala E, Seitz B, Kasmann-Kellner B. PAX6 Mutational Status Determines Aniridia-Associated Keratopathy Phenotype. *Ophthalmology*. 2020;127(2):273–275. doi: 10.1016/j.ophtha.2019.09.034.
33. Chai N, Stachon T, Nastaranpour M, Li Z, Seitz B, Ulrich M, Langenbacher A, Szentmáry N. Assessment of Rose Bengal Photodynamic Therapy on Viability and Proliferation of Human Keratolimbic Epithelial and Stromal Cells In Vitro. *Klin Monbl Augenheilkd*. 2024;241(8):972–981. doi: 10.1055/a-2038-8899.
34. Foster J, Wu WH, Scott SG, Bassi M, Mohan D, Daoud Y, Stark WJ, Jun AS, Chakravarti S. Transforming growth factor β and insulin signal changes in stromal fibroblasts of individual keratoconus patients. *PLoS One*. 2014;9(9):e106556. doi: 10.1371/journal.pone.0106556.
35. Foster JW, Gouveia RM, Connon CJ. Low-glucose enhances keratocyte-characteristic phenotype from corneal stromal cells in serum-free conditions. *Sci Rep*. 2015;5(1):10839. doi: 10.1038/srep10839.
36. Loureiro RR, Cristovam PC, Martins CM, Covre JL, Sobrinho JA, Ricardo JR, Hazarbassanov RM, Höfling-Lima AL, Belfort R, Jr., M N, others. Comparison of culture media for ex vivo cultivation of limbal epithelial progenitor cells. *Mol Vis*. 2013;19:69–77.
37. Kawakita T, Shimmura S, Hornia A, Higa K, Tseng SC. Stratified epithelial sheets engineered from a single adult murine corneal/limbal progenitor cell. *J Cell Mol Med*. 2008;12(4):1303–1316. doi: 10.1111/j.1582-4934.2008.00297.x.
38. Sidney LE, Hopkinson A. Corneal keratocyte transition to mesenchymal stem cell phenotype and reversal using serum-free medium supplemented with fibroblast growth factor-2, transforming growth factor- β 3 and retinoic acid. *J Tissue Eng Regen Med*. 2018;12(1):e203–e215. doi: 10.1002/term.2316.
39. Beales MP, Funderburgh JL, Jester JV, Hassell JR. Proteoglycan synthesis by bovine keratocytes and corneal fibroblasts: maintenance of the keratocyte phenotype in culture. *Invest Ophthalmol Vis Sci*. 1999;40(8):1658–1663.
40. Brown CT, Nugent MA, Lau FW, Trinkaus-Randall V. Characterization of proteoglycans synthesized by cultured corneal fibroblasts in response to transforming growth factor beta and fetal calf serum. *J Biol Chem*. 1999;274(11):7111–7119. doi: 10.1074/jbc.274.11.7111.
41. Joseph A, Hossain P, Jham S, Jones RE, Tighe P, McIntosh RS, Dua HS. Expression of CD34 and L-selectin on human corneal keratocytes. *Invest Ophthalmol Vis Sci*. 2003;44(11):4689–4692. doi: 10.1167/iovs.02-0999.
42. Toti P, Tosi GM, Traversi C, Schürfeld K, Cardone C, Caporossi A. CD-34 stromal expression pattern in normal and altered human corneas. *Ophthalmology*. 2002;109(6):1167–1171. doi: 10.1016/s0161-6420(02)01042-4.
43. Moriya K, Bae E, Honda K, Sakai K, Sakaguchi T, Tsujimoto I, Kamisoyama H, Keene DR, Sasaki T, Sakai T. A fibronectin-independent mechanism of collagen fibrillogenesis in adult liver remodeling. *Gastroenterology*. 2011;140(5):1653–1663. doi: 10.1053/j.gastro.2011.02.005.
44. Zhou B, Tu T, Gao Z, Wu X, Wang W, Liu W. Impaired collagen fibril assembly in keloids with enhanced expression of lumican and collagen V. *Arch Biochem Biophys*. 2021;697:108676. doi: 10.1016/j.abb.2020.108676.
45. Shubham K, Mishra R. Pax6 interacts with SPARC and TGF- β in murine eyes. *Mol Vis*. 2012;18:951–956.
46. Feng Y, Li M, Wang S, Cong W, Hu G, Song Y, Xiao H, Dong E, Zhang Y. Paired box 6 inhibits cardiac fibroblast differentiation. *Biochem Biophys Res Commun*. 2020;528(3):561–566. doi: 10.1016/j.bbrc.2020.05.146.
47. Schedl A, Ross A, Lee M, Engelkamp D, Rashbass P, van Heyningen V, Hastie ND. Influence of PAX6 gene dosage on development: overexpression causes severe eye abnormalities. *Cell*. 1996;86(1):71–82. doi: 10.1016/s0092-8674(00)80078-1.
48. Ying M, Han R, Hao P, Wang L, Li N. Inherited KIF21A and PAX6 gene mutations in a boy with congenital fibrosis of extraocular muscles and aniridia. *BMC Med Genet*. 2013;14(1):63. doi: 10.1186/1471-2350-14-63.

Publication 3

Ophthalmol Ther
<https://doi.org/10.1007/s40123-024-01032-8>



ORIGINAL RESEARCH

Effect of Ritanserin and Duloxetine on the Gene Expression of Primary Aniridia and Healthy Human Limbal Stromal Cells, In Vitro

Zhen Li · Nóra Szentmáry · Fabian N. Fries · Shweta Suiwal · Ning Chai ·
 Berthold Seitz · Lei Shi · Maryam Amini · Tanja Stachon

Received: April 11, 2024 / Accepted: August 30, 2024
 © The Author(s) 2024

ABSTRACT

Introduction: In congenital aniridia caused by mutations in paired box 6 (PAX6), PAX6 influences the migration and differentiation of limbal epithelial cells (LECs), thereby playing a pivotal role in aniridia-associated keratopathy.

Prior Presentation: This manuscript is based on work that was previously presented at the Congress of the German Ophthalmological Society (DOG) as a conference poster: Zhen L, Szentmáry N, Fries FN, Suiwal S, Chai N, Seitz B, Shi L, Amini M, Stachon T. Effect of ritanserin and duloxetine on gene expression of primary aniridia and healthy human limbal stromal cells, in vitro; DOG Congress, 30 September 2023, Berlin, Germany, Conference poster.

Supplementary Information The online version contains supplementary material available at <https://doi.org/10.1007/s40123-024-01032-8>.

Z. Li (✉) · N. Szentmáry · F. N. Fries · S. Suiwal ·
 N. Chai · M. Amini · T. Stachon
 Dr. Rolf M. Schwiete Center for Limbal Stem
 Cell and Congenital Aniridia Research, Saarland
 University, Kirrberger Str. 100, Homburg,
 Saarland 66424, Germany
 e-mail: zhen.li@uks.eu

F. N. Fries · B. Seitz
 Department of Ophthalmology, Saarland University
 Medical Center, Homburg, Saarland, Germany

L. Shi
 Department of Ophthalmology, Anhui No.2
 Provincial People's Hospital, Hefei, Anhui, China

The antidepressants ritanserin and duloxetine affect PAX6 expression in LECs. Limbal stromal cells, which support limbal epithelial stem cells, are crucial in the limbal stem cell niche. This study explores how ritanserin and duloxetine influence gene expression in primary human limbal stromal cells from subjects with congenital aniridia and from healthy subjects, in vitro.

Methods: Primary human limbal stromal cells from corneas affected by aniridia (AN-LSCs) ($n=8$) and from healthy corneas (LSCs) ($n=8$) were isolated and cultured in either low-glucose serum-free (LGSF) or normal-glucose serum-containing (NGSC) media. Cells were treated with 4 μ M ritanserin or duloxetine for 24 h. Quantitative PCR (qPCR) and western blot were used to assess the expression of PAX6, FOSL2, TGF- β 1, ACTA2A1, LUM, COL1A1, COL5A1, DSG1, FABP5 and ADH7.

Results: In AN-LSCs with LGSF-medium, ritanserin increased PAX6 messenger RNA (mRNA) ($p=0.007$) and decreased TGF- β 1 and FOSL2 mRNA levels ($P=0.005$, $P=0.038$). In addition, TGF- β 1 protein levels decreased with both treatments ($P=0.02$, $P=0.007$), and FABP5 protein level increased, using ritanserin ($P=0.019$). In LSCs with LGSF-medium, ACTA2A1 mRNA levels decreased using ritanserin and duloxetine ($P=0.028$; $P=0.031$), while FABP5 mRNA levels increased with ritanserin treatment ($P=0.003$). Also, duloxetine use reduced α -SMA protein ($P=0.013$) and increased FABP5 protein levels

($P=0.029$). In LSCs with NGSC-medium, ritanserin elevated LUM, FABP5 and ADH7 mRNA and protein levels ($P=0.025$, $P=0.003$, $P=0.047$, $P=0.024$, $P=0.013$, $P=0.039$).

Conclusions: The results of our study confirmed that the antipsychotropic drugs ritanserin and duloxetine alter *PAX6* and *TGF- β 1* gene expression in AN-LSCs cultured in LGSF-medium. These drugs were found to have an impact on retinoic acid signaling pathways and keratocyte characteristic markers both in LSCs and AN-LSCs, using different culture media.

Keywords: Ritanserin; Duloxetine; *PAX6*; Limbal stromal cells; Limbal fibroblasts; Limbal keratocytes; Aniridia associated keratopathy

Key Summary Points

Why carry out this study?

Our previous research demonstrated altered Paired Box 6 (*PAX6*) expression and changes in keratocyte markers (α -smooth muscle actin [*ACTA2A1*], collagen 5 [*COL5A1*] and collagen 1 [*COL1A1*]) in aniridia limbal stromal cells (AN-LSCs), compared to healthy limbal stromal cells (LSCs).

While ritanserin and duloxetine rescue *PAX6* in mutant limbal epithelial cells via the mitogen-activated protein kinase/extracellular signal-regulated kinase (MAPK/ERK) pathway, their effects on LSCs and the effect on the sight-threatening aniridia-associated keratopathy (AAK) remain unexplored.

We examined how ritanserin and duloxetine affect *PAX6*, transforming growth factor β 1 (*TGF- β 1*), retinoic acid signaling and keratocyte markers in primary AN-LSCs and LSCs, in vitro.

What was learned from the study?

Ritanserin and duloxetine change *PAX6* and *TGF- β 1* gene expression in AN-LSCs, in low glucose serum-free (LGSF)-medium and affects retinoic acid signaling and keratocyte characteristic marker expression of LSCs and AN-LSCs, likely via the ERK pathway.

Ritanserin and duloxetine treatment might impact corneal stromal wound healing in both healthy and congenital aniridia corneas, presumably affecting the MAPK/ERK pathway.

INTRODUCTION

With a prevalence ranging from 1:40,000 to 1:100,000, paired box protein 6 (*PAX6*) haploinsufficiency-related congenital aniridia is a rare panocular disorder affecting the cornea, anterior chamber, iris, lens, retina, macula and optic nerve head [1, 2]. Aniridia-associated keratopathy (AAK) is a progressive opacification and vascularization of the cornea, with limbal stem cell deficiency. It is one of the most sight-threatening manifestations of congenital aniridia, starting in the first decade of life and progressing in early adulthood. AAK is classified using the Lagali grading, and the rate of progression is associated with the specific *PAX6* mutations [3].

PAX6 is a DNA-binding transcription factor that is able to directly regulate several upstream and downstream transduction pathways [4, 5]. In AAK limbal epithelial cells (LECs), the expression of retinoic acid signaling components ADH7 (all-trans-retinol dehydrogenase 7) and FABP5 (fatty acid-binding protein 5) is impaired [6, 7]. DSG1 (Desmoglein-1), which is a cellular junction protein, has also been reported to be downregulated in aniridia LECs [7, 8]. Altogether, reduced *PAX6* expression influences the migration and differentiation of LECs and, therefore, corneal wound healing [4, 5].

It is also known that limbal stromal cells (LSCs), including limbal fibroblasts and keratocytes, in close proximity to the limbal epithelial

stem cells, also have an important role in the limbal stem cell niche [9–12]. Our previous study demonstrated altered *PAX6* messenger RNA (mRNA) expression in aniridia limbal stromal cells (AN-LSCs), compared to healthy LSCs, in vitro (Li Z, Stachon T, Fries FN, et al. Expression of *PAX6* and keratocyte-characteristic markers in human limbal stromal cells of congenital aniridia and healthy subjects, in vitro. *Curr Eye Res.* 2024; under review.). In addition, parallel to lower *PAX6* mRNA expression in AN-LSCs, keratocyte-characteristic marker expression, such as that of α -smooth muscle actin (*ACTA2A1*), collagen 5 (*COL5A1*) and collagen 1 (*COL1A1*), is also altered. In stromal wound healing and in stromal inflammatory processes, in addition to α -smooth muscle actin expression, transforming growth factor β 1 (TGF- β 1) expression plays a pivotal role, with several previous studies demonstrating the relationship between *PAX6* and TGF- β 1 expression [13, 14]. In addition, Fos-related antigen 2 (*FOSL2*), as a novel downstream mediator of TGF- β 1, is also involved in fibrosis pathogenesis of many organs (e.g. cardiac, pulmonary and renal tissues) [15–18].

A previous study screened for small molecules that could rescue *PAX6* protein of mutated limbal epithelial stem cells. In this study, the antipsychotropic compounds ritanserin and duloxetine were able to efficiently rescue endogenous *PAX6* and other target gene expressions in mutated limbal epithelial cells after 24 h, and affected cell migration [19, 20]. Ritanserin and duloxetine are both antidepressant drugs. Ritanserin is a potent and specific 5-hydroxytryptamine (5-HT or serotonin) antagonist [21], and duloxetine is a dual antidepressant drug that inhibits the neuronal reuptake of 5-HT and norepinephrine (NE) [22]. Both have been used in clinical trials as potential treatments of schizophrenia and substance dependence [23].

Ritanserin and duloxetine may rescue endogenous *PAX6* in mutant limbal epithelial stem cells through the non-genomic mitogen-activated protein kinase/extracellular signal-regulated kinase (MAPK/ERK) pathway [19, 20]. It is very important to emphasize that both drugs do not have a direct effect on *PAX6* expression, but

on the MAPK/ERK pathway, and further affect gene expression of the cells, involving several pathways.

To the best of our knowledge, the effect of ritanserin and duloxetine on AN-LSCs, which are in direct proximity of the LECs in the limbal stem cell niche, has not yet been analyzed. Based on our previous work, in which we characterized the expression of *PAX6*, TGF- β 1, retinoic acid signaling components and keratocyte-characteristic markers in AN-LSCs, we aimed to determine the effect of ritanserin and duloxetine on these markers. Expression of all of these markers is directly or indirectly related to the MAPK/ERK pathway, which is affected by ritanserin and duloxetine. To observe the effect of the treatment, we have chosen the timeframe of 24 h, similar to previous studies analyzing the effect of ritanserin and duloxetine on mutated LECs [19, 20].

The purpose of the present study was to investigate the effect of ritanserin and duloxetine on the expression of *PAX6*, TGF- β 1, retinoic acid signaling components and keratocyte-characteristic markers of primary human AN-LSCs and LSCs, in vitro. Keratocytes in the cornea are usually quiescent cells. In the case of keratocyte activation, for example through inflammatory stimuli, keratocytes transform into fibroblast-like cells. In order to evaluate gene expression in both corneal stromal keratocytes and fibroblasts, different culture media can be used, as described by Foster et al. [24]. Therefore, in the present study, we used low glucose serum-free (LGSF)-medium, which supports the keratocyte phenotype, and normal glucose serum-containing (NGSC) culture medium, which supports the fibroblastic phenotype [24].

METHODS

Ethical Approval and Consent to Participate

Our study was approved by the Ethics Committee of Saarland, Germany (No. 172/20). All work was performed according to the Principles of the Declaration of Helsinki. All subjects with

aniridia who participated in the study signed an informed consent before surgery.

Cell Culture

Aniridia samples were collected from patients of the Department of Ophthalmology, Saarland University Medical Center, Homburg, Saarland, Germany. Control limbal biopsies were obtained from corneal donors of the LIONS Cornea Bank Saar-Lor-Lux, Trier/Westpfalz, Homburg/Saar, Germany. Limbal biopsies (1.5 mm) of eight congenital aniridia eyes from donors (mean age [\pm standard deviation] 34.5 ± 29.5 years, range 5–64 years; 3 [37.5%] males) and of eight healthy eyes from donors (age 32.5 ± 17.1 , range 2–50 years; 3 [37.5%] males) were used in our experiments. Before surgery, all patients with aniridia in our study underwent slit lamp examination in order to grade the AAK according to Lagali et al. [25, 26]. The mean age of the eight patients with congenital aniridia in our study was 32.50 ± 17.07 (range 2–50) years. Among these eight patients, three (37.5%) were male, two (25%) had AAK grade 3 and six (75%) had AAK grade 4 (according to Lagali et al. [25, 26]). Four (50%) subjects had a PAX6 missense mutation (c.1268A>T; c. 1226-2A>G; c. 607C>T; c.266A>C), three (37.5%) had a PAX6 deletion

(21q22.12q22.2(36,472,360–39,889,694) × 1; c.959_960delCA; c. 753_754delGC) and one (12.5%) had another type of PAX6 mutation (c. 1191 T (q227X)). Description data of healthy samples are summarized in Table 1.

Isolation of primary LSCs was performed as described by Chai et al. [27]. Both congenital aniridia and healthy human limbal biopsies were first incubated in 0.5 mg/ml collagenase A (Hoffmann-La Roche, Basel, Switzerland) overnight at 37 °C, following which the suspensions were filtered through 40- μ m Flowmi cell strainers (Cat. no.: H13680-0040; Bel-Art, Wayne, NJ, USA) into one 24-well plate, to remove LECs and incompletely dissociated cells. To obtain the LSCs, the strainer was washed with 500 μ l phosphate-buffered saline and 500 μ l 0.05% trypsin-EDTA, followed by incubation for 5 min to separate cell clusters. Thereafter, the enzyme reaction was stopped using Dulbecco's Modified Eagle Medium (DMEM) supplemented with 5% fetal calf serum (FCS). The filtrate was subsequently centrifuged at 1500 g for 5 min to sediment stromal cells and the supernatant was removed afterwards. The stromal cells were seeded into one 6-well plate using DMEM supplemented with 5% FCS. Cells were incubated at 37 °C with 95% relative humidity and 5% CO₂, and the medium was changed every 2–3 days until stromal cells reached confluence. Thereafter, the cells were cultured in 75-cm² culture flasks following dispersal with 0.05% trypsin-EDTA for 5 min. During the first 2 days, cell culturing was performed using DMEM/F12, 5% FCS and 1% penicillin/streptomycin (P/S) (standard procedure for fibroblast cultures) to obtain typical fibroblast cell morphology, as described by Foster et al. [24]. This culture medium is subsequently referred to in the text as normal glucose serum-containing cell culture medium (NGSC-medium).

To obtain the keratocyte-specific phenotype, the NGSC-medium was removed after 2 days (approximately 20% cell confluence) and replaced with a low glucose serum-free cell culture medium (LGSF-medium), as described previously (Li Z, Stachon T, Fries FN, et al. Expression of PAX6 and keratocyte-characteristic markers in human limbal stromal cells of congenital aniridia and healthy subjects, *in vitro*. *Curr Eye Res.* 2024; under review.). LGSF-medium

Table 1 Age and gender of healthy donors

Healthy donor no.	Age (years)	Gender
1	89	Male
2	64	Female
3	76	Male
4	82	Female
5	66	Female
6	58	Female
7	72	Male
8	72	Female
Summary	Mean age (\pm SD) 73.5 \pm 15.5; range 58–89	3 (37.5%) males

consisted of low-glucose DMEM (Cat. no. D6046; Sigma–Aldrich, St. Louis, MO, USA) supplemented with 1 mM L-ascorbic acid (Cat. no. A8960; Sigma–Aldrich), 2 g/l D-glucose (Cat. no. X997; Carl ROTH, Karlsruhe, Baden-Württemberg, Germany), 2.5 g/l D-mannitol (Cat. no. 8883.1; Carl ROTH), 1% insulin transferring selenite (ITS; Cat. no. 1884; Sigma–Aldrich) and 1% P/S. Further cell culture work was performed either using LGSF-medium for keratocytes or with NGSC-medium for fibroblasts [24]. The medium for all corneal stromal cells cultures was changed twice weekly before harvesting, and cell passages 3–8 were used for the experiments.

In our previous study, we characterized AN-LSCs and LSCs in in vitro culture, using either NGSC-medium for 7 days or LGSF-culture medium for 14 days (LGSF cultures reach confluency much slower) (Li Z, Stachon T, Fries FN, et al. Expression of PAX6 and keratocyte-characteristic markers in human limbal stromal cells of congenital aniridia and healthy subjects, in vitro. *Curr Eye Res.* 2024; under review.). LSCs could be isolated without contamination (Li Z, Stachon T, Fries FN, et al. Expression of PAX6 and keratocyte-characteristic markers in human limbal stromal cells of congenital aniridia and healthy subjects, in vitro. *Curr Eye Res.* 2024; under review.). PAX6 mRNA expression was significantly reduced in AN-LSCs compared to LSCs in both NGSC- and LGSF-medium. Additionally, COL5A1 mRNA expression was lower, while ALDH3A1 and KER mRNA levels were elevated in AN-LSCs compared to LSCs in NGSC-medium. In LGSF-medium, AN-LSCs displayed a significant increase in COL1A1 and COL5A1 mRNA expression compared to LSCs. Furthermore, AN-LSCs exhibited significantly higher COL1A1 and alpha-smooth muscle actin (α -SMA) protein levels compared to LSCs in LGSF-medium. Both AN-LSCs and LSCs retained their characteristics across three to eight passages (Li Z, Stachon T, Fries FN, et al. Expression of PAX6 and keratocyte-characteristic markers in human limbal stromal cells of congenital aniridia and healthy subjects, in vitro. *Curr Eye Res.* 2024; under review.).

XTT Assay

Cell viability was assessed by the XTT assay. AN-LSCs and LSCs were plated in 96-well culture plates with NGSC-medium. Once the cells reached approximately 80% confluence, the medium was replaced with fresh medium containing 1, 2, 3, 4 or 5 μ M of either ritanserin or duloxetine, and the cells were incubated for a further 24 h. XTT solution was then added to each well. A well with XTT solution but no cells served as a background control. Absorbance was measured at 550 nm after 30–60 min of incubation using a 96-well microplate reader (Infinite F50 absorbance microplate reader; Tecan Group AG, Männedorf, Switzerland).

Drug Treatment

Ritanserin and duloxetine were first dissolved in dimethylsulfoxid (DMSO) (10.1 mg/ml), and then prior to treatment they were diluted in LGSF- or NGSC-medium to reach the desired concentration treatment. The control cultures were treated using DMSO for the same incubation period.

After reaching approximately 80% confluence in 75-cm² culture flasks with 10 ml LGSF- or NGSC-medium, each individual AN-LSC or LSC culture was treated for 24 h with 4 μ M ritanserin (Cat. no. R103; Sigma–Aldrich) or duloxetine (Cat. no. SML0474; Sigma–Aldrich). Our measurements were conducted using AN-LSCs and healthy LSCs in LGSF- or NGSC-medium. The cell pellet was frozen at -80°C until further use.

RNA Isolation and complementary DNA Synthesis

RNA was isolated following the protocol provided by the manufacturer (Total RNA Purification Plus Micro Kit; Norgen Biotek, Thorold, ON, Canada). The isolated RNA was then stored at -80°C until complementary DNA (cDNA) synthesis was performed (One Taq® RT-PCR Kit; New England Biolabs Inc., Frankfurt, Germany). For the synthesis of cDNA,

Table 2 Primer pairs used for quantitative PCR

Primer	Primer sequence or QIAGEN catalog number	Manufacturer (company, city, country)
PAX6	QT00071169	Qiagen N.V., Venlo, Netherlands
FOSL2	QT01000881	Qiagen N.V., Venlo, Netherlands
TGF- β 1	QT00000728	Qiagen N.V., Venlo, Netherlands
ACTA2A1	QT00088102	Qiagen N.V., Venlo, Netherlands
LUM	QT00058982	Qiagen N.V., Venlo, Netherlands
COL1A1	QT00037793	Qiagen N.V., Venlo, Netherlands
COL5A1	QT00044527	Qiagen N.V., Venlo, Netherlands
DSG1	QT00001617	Qiagen N.V., Venlo, Netherlands
FABP5	QT00225561	Qiagen N.V., Venlo, Netherlands
ADH7	QT00000217	Qiagen N.V., Venlo, Netherlands
ABCG2	QT00073206	Qiagen N.V., Venlo, Netherlands
5-HT2A	QT00054306	Qiagen N.V., Venlo, Netherlands
TBP	QT00000721	Qiagen N.V., Venlo, Netherlands
GUSB	QT00046046	Qiagen N.V., Venlo, Netherlands

PAX6 Paired box 6, *FOSL2* Fos-related antigen 2, *TGF- β 1* transforming growth factor- β 1, *ACTA2A1* α -smooth muscle actin, *LUM* lumican, *COL1A1* collagen 1A1, *COL5A1* collagen 5A1, *DSG1* desmoglein-1, *FABP5* fatty acid binding protein 5, *ADH7* all-trans-retinol dehydrogenase 7, *ABCG2* ATP-binding cassette sub-family G member 2, *5-HT2A* 5-hydroxy-tryptamine 2A, *TBP* TATA-binding protein, *GUSB* beta-glucuronidase

200 ng of total RNA was used as the template for each sample. The resulting cDNA was stored at -20°C .

Quantitative PCR

An overview of the primers used for quantitative PCR (qPCR) is provided in Table 2. The qPCR reaction mix (total volume 9 μl) included 1 μl of the specific primer solution, 5 μl of SYBR Green Mix (Vazyme, Nanjing, China) and 3 μl of nuclease-free water. Following the manufacturer's guidelines, the samples were prepared in a 9- μl volume with 1 μl of cDNA. qPCR was conducted using the QuantStudio 5 real-time PCR system (Thermo Fisher Scientific, Waltham, MA, USA). The amplification protocol involved an initial step at 95°C for 10 s, followed by 30 s at 60°C

and a final step at 95°C for 15 s, repeated for 40 cycles. Each sample was analyzed in duplicate, with data normalized using the TATA-binding protein (TBP) and Beta-glucuronidase (GUSB) as reference genes, employing the $\Delta\Delta\text{CT}$ method. For statistical analysis, fold changes ($2^{-\Delta\Delta\text{CT}}$) were calculated, using AN-LSCs and LSCs in LGSF- or NGSC-medium without any treatment as the baseline (fold change = 1).

Protein Quantification

After the cells reached confluence in 75- cm^2 flasks, eight samples each of AN-LSCs and LSCs were lysed in 80 μl of ice-cold RIPA lysis buffer (Thermo Fisher Scientific). The lysed cell suspension was then centrifuged at 15,000 g for 5 min at 4°C to remove cell debris and unbroken cells. The supernatant, which contains the

soluble proteins, was collected. Protein concentration was measured using the Pierce™ BCA Protein Assay Kit (Thermo Fisher Scientific). In accordance with the kit's instructions, Reagent A and Reagent B were mixed in a 50:1 ratio. Subsequently, 5 µl of the standard protein solutions or samples were added to the wells of a 96-well plate, followed by 40 µl of the working reagent. The plate was then incubated at 37 °C for 2 h. Absorbance was measured at 560 nm using the Infinite F50 absorbance microplate reader (Tecan Group AG). Bovine serum albumin served as the standard, and all measurements were performed in duplicate.

Western Blot Analysis

For Western blot analysis, eight samples from each group, each containing 20 µg of total protein, were boiled in 5 µl of Laemmli sample buffer for 5 min at 95 °C. The samples were then loaded onto a precast 4–12% NuPage™ Bis–Tris sodium dodecyl sulfate gel (Invitrogen, Thermo Fisher Scientific). To determine the molecular weight, the first well was loaded with 2.5 µl

of Precision Plus Protein™ Dual Color Standard (Bio-Rad Laboratories, Hercules, CA, USA). Electrophoresis was performed using NuPAGE™ MOPS SDS Running Buffer (20×) (Thermo Fisher Scientific). Following protein separation, the proteins were transferred onto a nitrocellulose membrane using the Trans-Blot Turbo Transfer System (Bio-Rad Laboratories), following the system's pre-installed protocol for high-molecular-weight proteins.

The membrane was then stained with No-Stain™ Protein labeling reagent (Thermo Fisher Scientific GmbH, Dreieich, Germany) to determine the total protein amount per lane for normalization. The membrane was washed 3 times with 10 ml of Western Froxx washing solution (BioFroxx GmbH, Einhausen, Germany) for 5 min each. It was then incubated with primary antibodies at 4 °C overnight, as summarized in Table 3. The primary antibodies were diluted in a combined blocking and secondary antibody solution (WesternFroxx anti-Rabbit HRP; BioFroxx GmbH). After removing the antibody solution, the membrane was washed 3 times with 10 ml of washing solution. Protein bands were detected using the Western Lightning

Table 3 Antibodies used for Western blot

Antibody	Catalog number	Manufacturer (company, city, country)	Dilution
PAX6	AB2237	Millipore, Watford, UK	1:200
FOSL2	15832-1-AP	Proteintech, Chicago, Rosemont, IL USA	1:200
TGF-β1	21898-1-AP	Proteintech, Chicago, Rosemont, IL, USA	1:1000
α-SMA (ACTA 2A1)	19245	Cell Signaling Technology, MA, USA	1:1000
LUM	MA5-35135	Thermo Fisher Scientific, Waltham, MA, USA	1:1000
COL1A1	84336	Cell Signaling Technology, Danvers, MA, USA	1:1000
COL5A1	ab7046	Abcam, Cambridge, UK	1:1000
DSG1	SC-59904	Santa Cruz Biotechnology, Dallas, TX, USA	1:1000
FABP5	12348-1-AP	Proteintech, Chicago, Rosemont, IL, USA	1:500
ADH7	PA5-98484	Thermo Fisher Scientific, Waltham, MA, USA	1:5000
pERK	4370	Cell Signaling Technology, Danvers, MA, USA	1:1000
ERK	4695	Cell Signaling Technology, Danvers, MA, USA	1:1000

α-SMA (ACTA 2A1) α-smooth muscle actin, pERK phospho-extracellular signal-regulated kinase, ERK extracellular signal-regulated kinase; for other abbreviations, see footnote to Table 2

Plus Chemiluminescence Reagent (PerkinElmer Inc., Waltham, MA, USA) and visualized with the iBright™ CL1500 Imaging System (Cat. no. A44114; Thermo Fisher Scientific). Finally, membrane stripping was carried out using Western Froxx stripping solution (BioFroxx GmbH) for further antibody incubation.

In additions to LSCs, we used different cells as positive controls of western blot analysis: LECs as positive controls for PAX6 protein, mouse cerebellar cells as positive controls for [24] protein and central corneal epithelial cells (CECs) and a human cervical cancer cell line (HeLa cells) as positive controls for DSG1 protein.

Statistical Analysis

GraphPad Prism 9.2.0 (GraphPad Software, San Diego, CA, USA) was used for statistical analysis and for preparation of the diagrams. XTT data were expressed as mean \pm SD, qPCR data were expressed as geometric mean with geometric SD, viability and western blot data were expressed as the mean \pm SD. For all treatment types (ritanserin and duloxetine), viability, mRNA expression values ($2^{\Delta\Delta CT}$ values) and protein level were

compared to the controls using one-way analysis of variance (ANOVA). Baseline gene expression was analyzed using the unpaired *t*-test. *P* values < 0.05 were considered to indicate statistical significance.

RESULTS

Cell Viability Assay After Ritanserin or Duloxetine Treatment, In Vitro

Although cell viability slightly decreased with increasing ritanserin and duloxetine concentrations, treatments with ritanserin concentrations (1–5 μ M) and duloxetine concentrations (1–4 μ M) did not change the viability of primary LSCs after 24 h (Fig. 1a, b). Nevertheless, cell viability was significantly lower using 5 μ M duloxetine than in the controls ($P=0.001$) (Fig. 1b).

mRNA Expression in AN-LSCs and LSCs, Following Ritanserin or Duloxetine Treatment, In Vitro

PAX6 and *TGF- β 1* mRNA expression in AN-LSCs and LSCs without treatment is shown in Fig. 2a. *PAX6* mRNA expression was significantly lower and *TGF- β 1* mRNA expression was significantly higher in AN-LSCs than in LSCs, using LGSF-medium. Nevertheless, *PAX6* and *TGF- β 1* mRNA expression did not differ between AN-LSCs and LSCs using NGSC-medium.

5-HT2A receptor mRNA expression in LSCs and AN-LSCs, in LGSF- and in NGSC-medium is shown in Fig. 3. *5-HT2A* receptor mRNA expression did not differ significantly between LSCs and AN-LSCs, either using LGSF or using NGSC-medium ($P \geq 0.265$).

mRNA expression in aniridia and control limbal stromal cells after treatment is summarized in Fig. 4a–d. *DSG1* mRNA expression was extremely low in all untreated and treated samples and, therefore, CT values could not be determined during qPCR in any of the analyzed groups.

Using LGSF-medium, *PAX6* mRNA expression was significantly upregulated ($P=0.007$) and *TGF- β 1* and *FOSL2* mRNA expression were

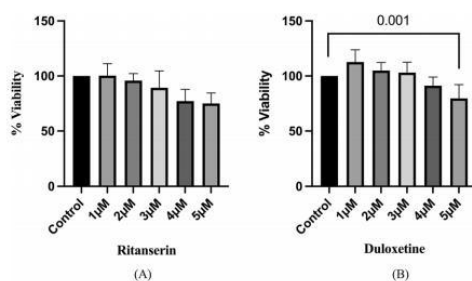


Fig. 1 XTT assay of primary limbal stromal cells (healthy control cultures) 24 h after treatment with different concentrations (1–5 μ M) ritanserin or duloxetine (1–5 μ M). Values are expressed as the mean \pm standard deviation (SD). One-way analysis of variance was used. Treatment with 1–5 μ M ritanserin and 1–4 μ M duloxetine did not change the viability of primary limbal stromal cells after 24 h. However cell viability was significantly lower using 5 μ M duloxetine concentration than in controls ($P=0.001$) ($n=3$)

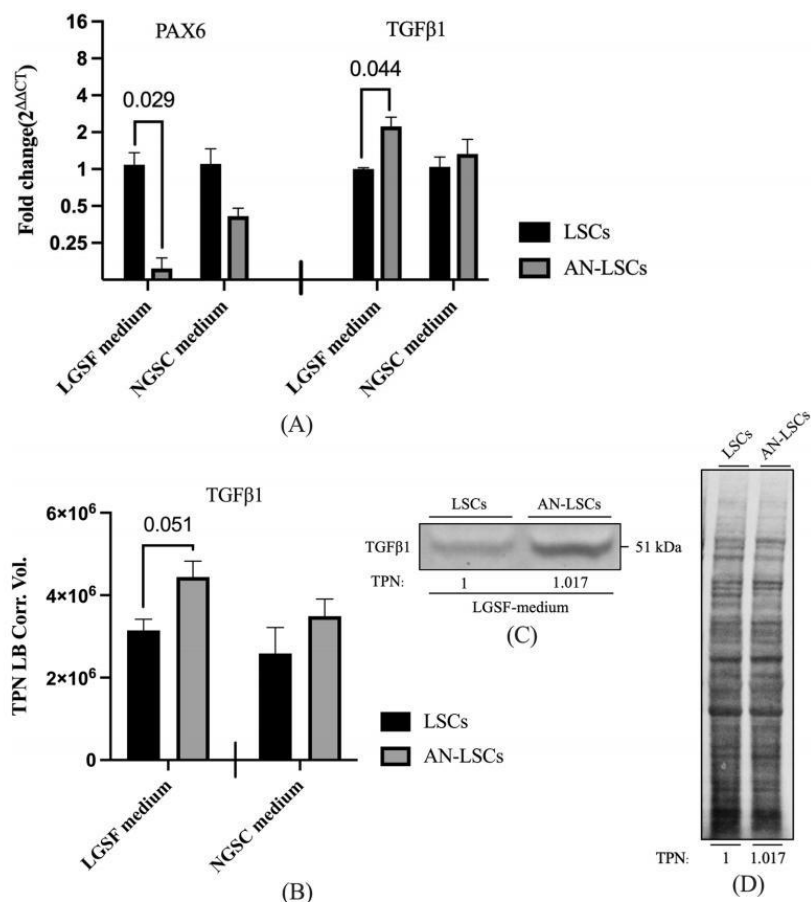


Fig. 2 Paired box 6 (*PAX6*) messenger RNA (mRNA) and transforming growth factor β 1 (*TGF- β 1*) mRNA (a) and *PAX6* and *TGF- β 1* protein (b-d) levels in aniridia limbal stromal cells (*AN-LSCs*) and in healthy limbal stromal cells (*LSCs*). *PAX6* mRNA expression was downregulated and *TGF- β 1* mRNA expression was upregulated in *AN-LSCs* compared to controls, using low-glucose serum-free cell culture medium (*LGSF medium*), but not in normal-

glucose serum-containing cell culture medium (*NGSC medium*). In addition, the *TGF- β 1* protein level tended to be higher in *AN-LSCs* than in *LSCs* ($P=0.051$) in *LGSF medium*. *PAX6* protein level was below the detection level in both *LSCs* and *AN-LSCs* (Electronic Supplementary Material Fig. 1). *TPN LB Corr. Vol.* Total lane protein local background corrected volume at the *Y*-axis

significantly downregulated in *AN-LSCs* after ritanserin treatment ($P=0.005$, $P=0.038$). Using *LGSF-medium*, *TGF- β 1* and *ACTA2A1* mRNA expression tended to decrease in *AN-LSCs*

after duloxetine treatment ($P=0.052$, $P=0.055$) (Fig. 4a).

Using *LGSF-medium*, *FABP5* was significantly upregulated ($P=0.020$) and *ACTA2A1* was significantly downregulated in *LSCs* after duloxetine

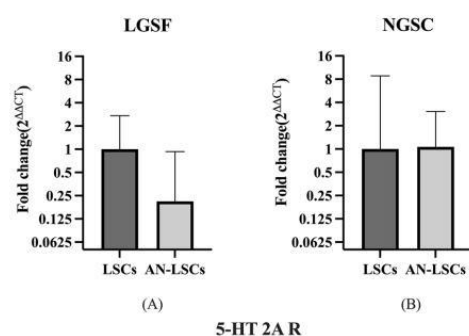


Fig. 3 5-hydroxytryptamine 2A receptor (*5-HT2A R*) mRNA expression in healthy limbal stromal cells (*LSCs*) and in aniridia limbal stromal cells (*AN-LSCs*), cultured in low-glucose serum-free cell culture medium (*LGSF*) (a) and in normal-glucose serum-containing cell culture medium (*NGSC*) (b). Values are shown using a logarithmic scale (Log 2), as geometric mean with geometric standard deviation. There was no significant difference between groups using the unpaired *t*-test ($P \geq 0.265$)

treatment ($P=0.028$). In addition, *ACTA2A1* was also significantly downregulated using ritanserin ($P=0.031$) (Fig. 4c).

Using NGSC-medium, ritanserin and duloxetine did not have an effect on the mRNA expression of AN-LSCs ($P > 0.082$) (Fig. 4b). Using NGSC-medium, *FABP5*, *ADH7* and lumican (*LUM*) mRNA expression were significantly upregulated in LSCs after ritanserin treatment ($P=0.003$, $P=0.047$ and $P=0.025$). Nevertheless, duloxetine did not show an effect on the analyzed mRNA expressions in LSCs ($P > 0.088$) (Fig. 4d).

Protein in AN-LSCs and LSCs, Following Ritanserin or Duloxetine Treatment, In Vitro

PAX6 and TGF- β 1 protein levels in AN-LSCs and LSCs without treatment are shown in Fig. 2b–d. TGF- β 1 protein level tended to be higher in AN-LSCs compared to LSCs using LGSF-medium ($P=0.051$), without any treatment.

Protein of the analyzed markers following ritanserin or duloxetine treatment are shown in Fig. 5. Even increasing the protein amount

to 30 μ g and extending the incubation time of antibodies up to 72 h for gel electrophoresis in all analyzed cell cultures, there were no visible PAX6, FOSL2 and DSG1 bands in primary human LSCs and AN-LSCs, although clearly visible bands were present in the positive control cells (see ESM Fig. 1).

Using LGSF-medium, TGF- β 1 protein level was significantly downregulated ($P=0.007$) and FABP5 protein level was significantly upregulated ($P=0.019$) in AN-LSCs, after ritanserin treatment. The TGF- β 1 protein level was also significantly downregulated after duloxetine treatment ($P=0.020$), in AN-LSCs (Fig. 5a–c).

Using LGSF-medium, α -SMA protein was significantly downregulated ($P=0.013$) and FABP5 protein level was significantly upregulated ($P=0.029$) in LSCs, after duloxetine treatment (Fig. 5e–g). pERK/ERK protein level in LSCs and AN-LSCs in LGSF-medium is shown in ESM Fig. 2. pERK/ERK protein level did not differ significantly in any of the duloxetine and ritanserin treated LSC and AN-LSC groups ($P \geq 0.145$).

Using NGSC-medium, we did not observe protein changes in AN-LSCs following the treatments with ritanserin or duloxetine. Nevertheless, LUM protein level tended to be significantly downregulated using ritanserin ($P=0.061$) (Fig. 5d).

Using NGSC-medium, LUM, FABP5 and ADH7 protein levels were significantly upregulated ($P=0.024$, $P=0.013$ and $P=0.039$) in LSCs after ritanserin treatment (Fig. 5h–j).

DISCUSSION

PAX6 haploinsufficiency-related AAK is known to result in progressive visual loss. Yet, there is to date still no proven clinical treatment option to prevent its progression. In our previous experiments, we demonstrated an altered PAX6 and keratocyte-characteristic marker (*KER*, *COL5A1* and *ALDH3A1* mRNA, COL1A1 and α -SMA protein) expression—in the absence of contamination—in isolated primary aniridia limbal stromal cells, compared to healthy controls, in vitro, with these characteristics maintained

over several passages (Li Z, Stachon T, Fries FN, et al. Expression of PAX6 and keratocyte-characteristic markers in human limbal stromal cells of congenital aniridia and healthy subjects, *in vitro*. *Curr Eye Res.* 2024; under review.). Recent research found that ritanserin and duloxetine, two anti-psychotropic compounds, were able to effectively rescue endogenous PAX6 in mutant limbal epithelial stem cells through the non-genomic MAPK/ERK pathway [19, 20]. ERK may also further affect retinoic acid (RA) signaling components through PAX6 expression and, in addition, ERK affects the TGF- β 1 signaling pathway (Fig. 6). Both pathways may interact in AAK development and progression [6, 7]. In our present work, we aimed to analyze the effect of ritanserin and duloxetine in rescuing PAX6 expression and other related gene expressions in human congenital aniridia and healthy control LSCs cultured in LGSF- and NGSC-medium, *in vitro*. Figure 6 illustrates the pathways involved with ritanserin and duloxetine treatment and the analyzed gene expressions in the current study.

Effect of Ritanserin on AN-LSCs and LSCs, Using LGSF-Medium

Ritanserin, which is characterized as a serotonin (5-HT) receptor (5-HTR) antagonist, has been used in clinical trials treating schizophrenia, alcoholism and insomnia [23, 28, 29]. Grewal et al. reported that 5-HT could lead to proliferation of renal mesangial cells via direct ERK activation and the generation of a sustained fibrotic stimulus by inducing TGF- β 1 expression [30]. These authors suggested the following signaling cascade: 5-HT_{2A} receptor–protein kinase C (PKC)–NAD(P)H–Oxidase/ROS–MEK–ERK–TGF- β 1 mRNA [30] (Fig. 6). Kim et al. demonstrated that the 5-HT_{2A} receptor has a crucial role in activating hepatic stellate cells, leading to transdifferentiation of these into myofibroblasts, through TGF- β 1 activation. This process results in lipid peroxidation, mitochondrial damage, cellular injury, chronic inflammation and, ultimately, fibrosis [31].

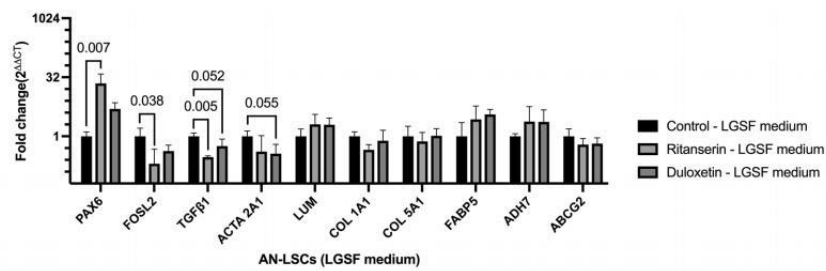
Several previous studies have demonstrated that there is a relationship between PAX6 and

TGF- β 1 expression. For example, PAX6 as a transcriptional regulator, localized in the nucleus of the outer nuclear layer and the inner nuclear layer of the murine retina, is co-localized and interacts with TGF- β 1 [13]. In addition, Yen-an Feng et al. demonstrated that suppression of PAX6 expression by small interfering RNA (siRNA) transfection promotes TGF- β 1 mRNA and protein levels in cardiac fibroblasts [14]. Therefore, ritanserin as 5-HT_{2A} receptor antagonist may play an important role in preventing the transformation of limbal stromal cells into myofibroblasts by regulating PAX6 expression, through the TGF- β 1 signaling pathway. The MAPK/ERK pathway may play here an important role.

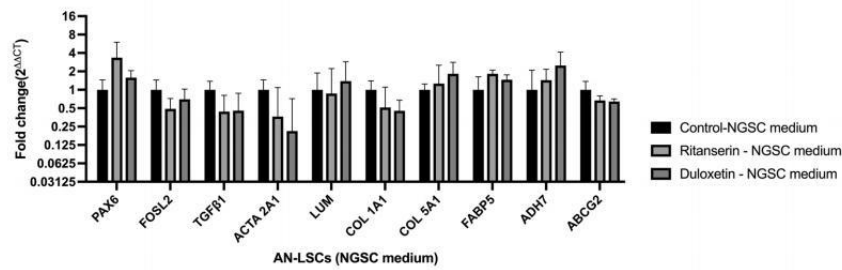
In our present study, using LGSF-medium, PAX6 mRNA expression was lower in AN-LSCs than in LSCs (Fig. 2a), and in parallel, TGF- β 1 mRNA expression was higher and TGF- β 1 protein level tended to be higher in AN-LSCs (Fig. 2a–c).

Our study could also confirm using LGSF-medium that TGF- β 1 mRNA and protein levels were downregulated in AN-LSCs after ritanserin treatment, coinciding with upregulated PAX6 mRNA expression. Nevertheless, we could only observe this phenomenon in AN-LSCs, in LGSF-medium. In parallel, with ritanserin treatment, pERK/ERK protein levels were slightly decreased in AN-LSCs, without reaching statistical significance (ESM Fig. 2). In healthy limbal stromal cells, PAX6 mRNA expression was not upregulated, even though a slight tendency to upregulation could be observed after ritanserin treatment and PAX6 protein level remained unchanged. In our opinion, the basically very low PAX6 mRNA expression in AN-LSCs could result in its significant increase after ritanserin treatment, being more sensitive to treatment, than in LSCs with probably slightly higher PAX6 levels.

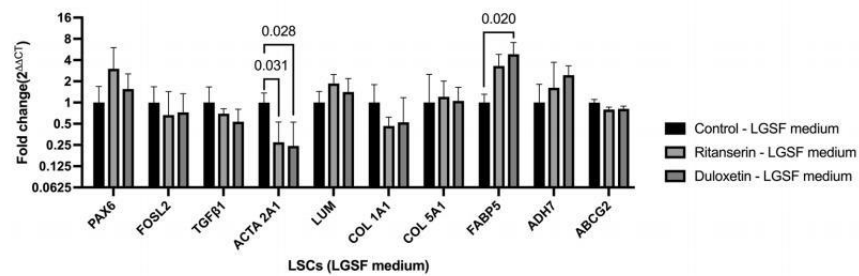
Saurabh et al. observed the antifibrotic effects of 5-HT₂ and 5-HT₂ inhibition on 5-HT/TGF- β 1-stimulated fibroblasts [32], suggesting that 5HT₂ acts directly through the 5HT_{2R}, leading to activation of the guanosine triphosphatase (GTPase) and ERK pathways, which further regulate ACTA2 expression. In this study, we demonstrated that ritanserin decreased ACTA2A1 mRNA expression in LSCs but not in AN-LSCs, a result that is



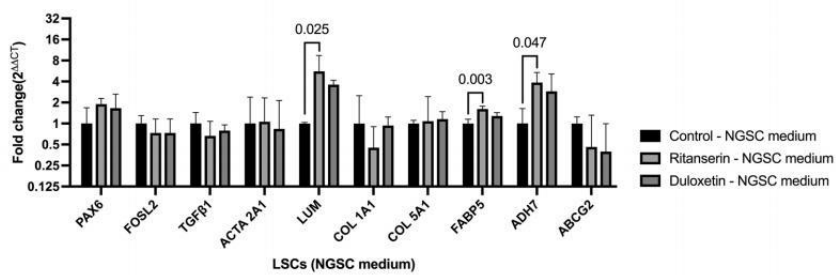
(A)



(B)



(C)



(D)

◀**Fig. 4** Paired box 6 (*PAX6*), Fos-related antigen 2 (*FOSL2*), transforming growth factor- β 1 (*TGF- β 1*), α -smooth muscle actin (*ACTA2A1*), lumican (*LUM*), collagen 1 (*COL1A1*), collagen 5 (*COL5A1*), fatty acid binding protein 5 (*FABP5*), all-trans-retinol dehydrogenase 7 (*ADH7*) and ATP-binding cassette sub-family G member 2 (*ABCG2*) messenger RNA expression in aniridia limbal stromal cells (*AN-LSCs*) (a, b) and in healthy limbal stromal cells (*LSCs*) (c, d), using low-glucose serum-free cell culture medium (*LGSF medium*) (a, c) or normal-glucose serum-containing cell culture medium (*NGSC medium*) (b, d) and 24 h after 4 μ M ritanserin or duloxetine treatment. Values are shown using a logarithmic scale (Log 2), as the geometric mean with geometric standard deviation. One-way analysis of variance was used. Significant *P* values (< 0.05) are highlighted on the diagrams ($n = 8$)

consistent with the findings reported by Saurabh et al. [32]. However, there were highly variant CT values of *ACTA2A1* mRNA expression 24 h after ritanserin treatment, which might indicate a possibly significant decrease using a prolonged ritanserin treatment. This aspect requires further measurements.

FOSL2 has also been shown to play an important role in fibrogenesis [15–18]. Our previous research demonstrated that FOSL2, as a direct PAX6 target gene, is a novel candidate associated with corneal opacity [33]. Minal Jaggari et al. found that a selective serotonin reuptake inhibitor could induce a robust baseline downregulation of FOSL2 gene expression in stress-responsive brain regions [34]. Our results are largely in agreement with those of these authors. In parallel with PAX6 mRNA upregulation after ritanserin treatment, FOSL2 mRNA expression also significantly decreased in AN-LSCs. Nevertheless, this phenomenon could not be observed in healthy LSCs, in which ritanserin treatment did not trigger PAX6 mRNA expression changes. In addition, FOSL2 protein could not be verified neither before or after treatment in LSCs or AN-LSCs in our in vitro measurements, providing evidence against the role of FOSL protein in AAK fibrogenesis.

Effect of Ritanserin on AN-LSCs and LSCs, Using NGSC-Medium

NGSC-medium is the most commonly used culture medium for corneal stromal cells. This medium has a glucose concentration of 4.5 g l⁻¹, which corresponds to a five- to ninefold higher concentration compared to that in the human cornea [35, 36]. The 5-HT₂ antagonist ritanserin decreases TGF- β 1 expression [30]; nevertheless, in the case of a higher glucose concentration, TGF- β 1 expression increases [37]. Therefore, in NGSC-medium, with its higher glucose concentration, we found a relatively higher expression of TGF- β 1 mRNA in AN-LSCs, which was also related to the observed limited upregulation of PAX. Therefore, PAX6 mRNA upregulation and TGF- β 1 and ACTA2A1 downregulation are only significant in AN-LSCs cultured in LGSF-medium, but not in NGSC-medium (Fig. 4). These effects of glucose concentration may also be associated with the behavior of limbal or more central corneal stromal cells, depending on the glucose concentration in their environment. In addition, several studies have described the effect of serum in cell culture, which must also have played a role in our study. Using serum-free culture medium, most cells will express a keratocyte-like phenotype, whereas in culture medium with serum, these cells show a fibroblast-like phenotype (Li Z, Stachon T, Fries FN, et al. Expression of PAX6 and keratocyte-characteristic markers in human limbal stromal cells of congenital aniridia and healthy subjects, in vitro. *Curr Eye Res.* 2024; under review.) [38–40]. The exact effect of serum on AN-LSCs remains to be analyzed more in detail in future studies.

Interestingly, we observed a significant upregulation of FABP5 and ADH7 mRNA and protein in healthy limbal stromal cells treated with ritanserin, which could not be verified in AN-LSCs. pERK/ERK protein levels were slightly decreased in LSCs through ritanserin treatment, but without reaching statistical significance (ESM Fig. 2). We consider that a relative lower PAX6 mRNA expression level in AN-LSCs still did not reach the trigger threshold for FABP5 and ADH7 mRNA upregulation in AN-LSCs. On the other hand, it is still not clear whether there are

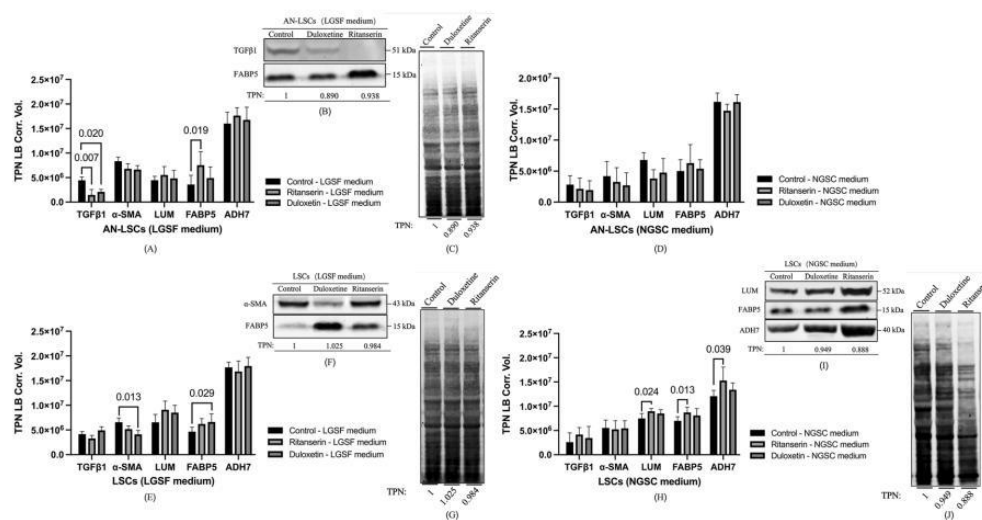


Fig. 5 Protein levels in aniridia limbal stromal cells (*AN-LSCs*) (a–d) and in healthy limbal stromal cells (*LSCs*) (e–j) in low-glucose serum-free (*LGSF medium*) (a–c, e–g) and in normal-glucose serum-containing cell culture medium (*NGSC medium*) (d, h–j). In *AN-LSCs*, transforming growth factor β 1 (*TGF- β 1*) protein level was significantly lower after ritanserin and duloxetine treatment ($P=0.007$, $P=0.02$) and fatty acid-binding protein 5 (*FABP5*) protein level was significantly higher after ritanserin treatment ($P=0.019$), using *LGSF-medium* (a–c). In *LSCs*, *FABP5*, all-trans-retinol dehydrogenase 7 (*ADH7*) and lumican (*LUM*) protein levels were significantly higher after ritanserin treatment ($P\geq 0.013$), using *NGSC*

medium (h–j). In *LSCs*, *FABP5* protein level was significantly higher ($P=0.029$) and α -smooth muscle actin (α -*SMA*) protein level was significantly lower ($P=0.013$) after duloxetine treatment, using *LGSF medium* (e–g). Total protein normalization (*TPN*) was performed using Invitrogen™ No-Stain™ Protein Labeling Reagent (c, g, j). Values are expressed as the mean \pm standard deviation, using one-way analysis of variance. *TPN LB Corr. Vol.* Total lane protein local background corrected volume at the *Y*-axis

any unknown interfering factors between *PAX6* and *RA* signaling that might explain the upregulation of *FABP5* and *ADH7* mRNA expression through ritanserin treatment in healthy *LSCs*, but not in *AN-LSCs*. Using an siRNA-based *PAX6* LEC model with a strong *PAX6* knockdown, both *FABP5* and *ADH7* mRNA expression were significantly downregulated, which also indicates the interaction of the *PAX6* and retinoic acid signaling pathways in human cells [7, 41].

Our previous study demonstrated that *LUM* mRNA expression was significantly lower in *LSCs* using *NGSC-medium*, compared to *LGSF-medium* (Li Z, Stachon T, Fries FN, et al. Expression of *PAX6* and keratocyte-characteristic markers in human limbal stromal cells of congenital

aniridia and healthy subjects, in vitro. *Curr Eye Res.* 2024; under review.). In addition, it has been reported that *LUM* interacts with *TGF- β 1* expression, as *TGF- β 1* is able to suppress *LUM* expression [42–44]. In the present study, there was an increase in *LUM* mRNA and protein levels through ritanserin treatment in *LSCs*, but not in *AN-LSCs*, using *NGSC-medium*. We consider that through the relative lower *TGF- β 1* expression level in healthy *LSCs*, which might be further supported by ritanserin treatment, the suppression effect on *LUM* expression further decreases, resulting in an increased *LUM* level.

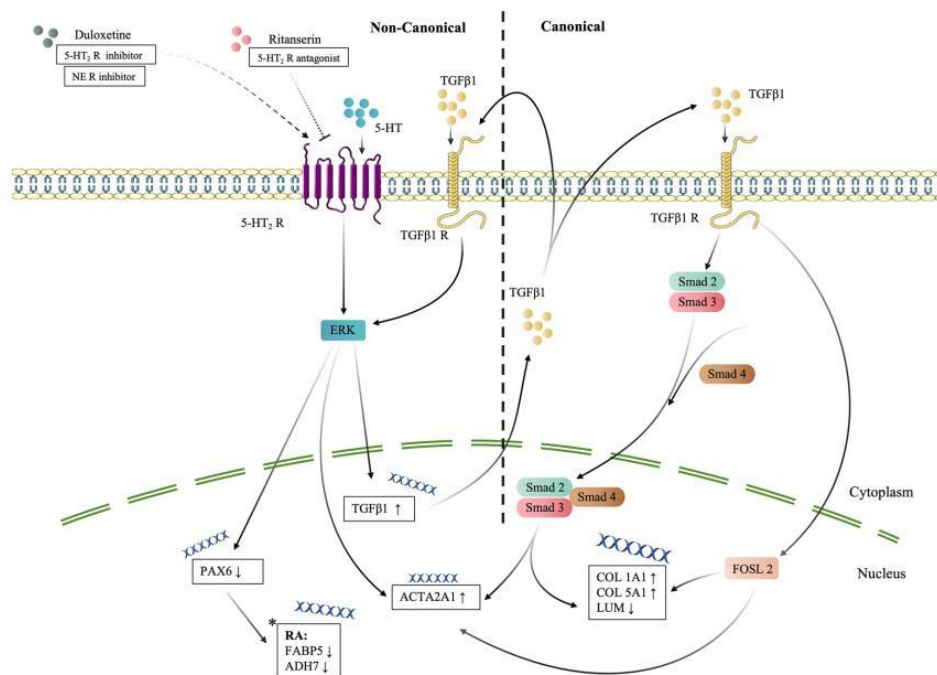


Fig. 6 Hypothetical metabolism of 5-hydroxytryptamine (5-HT or serotonin) in human corneal limbal stromal cells (LSCs) displaying the canonical and non-canonical transforming growth factor β 1 (*TGF- β 1*) signaling pathways. Activation of 5-HT₂-receptors (5-HT₂R) stimulates TGF- β 1 and decreases Paired Box 6 (*PAX6*) transcription in the cell nucleus. α -smooth muscle actin (*ACTA2A1*) transcription can be further activated by extracellular signal-regulated kinase (*ERK*) or the canonical TGF- β 1-dependent pathway. TGF- β 1 also stimulates Fos-related antigen 2 (*FOSL2*) activation [16]. Retinoic acid signaling component (*RA*) fatty acid-binding protein 5 (*FABP5*) and all-trans-retinol dehydrogenase 7 (*ADH7*) transcrip-

tion are reduced parallel to a reduced *PAX6* expression. Through drug treatment, keratocyte-characteristic marker expression, such as *ACTA2A1*, collagen 5 (*COL5A1*) and collagen 1 (*COL1A1*) levels are upregulated and lumican (*LUM*) level is downregulated. In this process, TGF- β 1 and Small mother against decapentaplegic (*Smad*) components play an important role. Ritanserin, as 5-HT₂ receptor antagonist, blocks 5-HT receptors and duloxetine inhibits 5-HT receptors, which can lead to decreased TGF- β 1 and increased *PAX6* expression, as confirmed by our data. All these components play an important role in extracellular matrix formation. *NE R* Norepinephrine receptor

Effect of Duloxetine on AN-LSCs and LSCs, in LGSF and NGSC Culture Medium

Duloxetine is an antidepressant drug inhibiting the neuronal reuptake of 5-HT and norepinephrine (NE) [22]. Dorot et al. generated a *PAX6* haploinsufficient cell line by genome editing of healthy LECs in vitro, inserting a nonsense mutation in one allele of the *PAX6* gene. In

these cells, using 1 μ M duloxetine treatment for 48 h, *PAX6* expression returned to the previously recorded amounts in the original wild-type healthy LECs [20].

Our previous study confirmed a significantly increased α -SMA (*ACTA2A1*) protein level in aniridia limbal stromal cells, compared to healthy controls, using LGSF culture medium (Li Z, Stachon T, Fries FN, et al. Expression of *PAX6* and keratocyte-characteristic markers in human

limbal stromal cells of congenital aniridia and healthy subjects, in vitro. *Curr Eye Res.* 2024; under review.). Therefore, ACTA2A1 may play an important role in AAK development and progression. During vascular injury, Gao et al. found an increased NE level, which induced activation and proliferation of vascular adventitial fibroblast differentiation into myofibroblasts, with parallel increases in ACTA2A1, TGF- β 1 and Smad3 levels [45]. In the present study, using the NE inhibitor duloxetine for 24 h, we observed a tendency for decreased ACTA2A1 mRNA expression in AN-LSCs ($P=0.055$) and significantly decreased ACTA2A1 mRNA and protein levels in healthy LSCs, using LGSF-medium. Using duloxetine, TGF- β 1 mRNA expression also tended to decrease ($P=0.052$) and TGF- β 1 protein significantly decreased in AN-LSCs, but not in LSCs, in LGSF-medium. These slight differences in the response to duloxetine treatment between AN-LSCs and LSCs need further clarification, but are probably regulated by Smads through the canonical TGF- β 1 signaling pathway.

Duloxetine is able to enhance dopamine levels by inhibiting NE transporters. Dopamine increase specifically takes place in the prefrontal cortex, where dopamine transporters are scarce, and dopamine reuptake relies more heavily on NE transporters. Interestingly, dopamine inactivation in the retina also induces keratoconus. In addition, PAX6 expression is decisive in development of the dopaminergic phenotype in the olfactory bulb [26]. A previous study demonstrated that NE induces epithelial-mesenchymal transformation of lung cancer cells and promotes invasion and metastasis of lung cancer through the TGF- β 1 signaling pathway [46]. The results from all of these studies strongly suggest that duloxetine, by inhibiting NE reuptake, could have a potential role in the restoration of PAX6 expression, in relation to the TGF- β 1 signaling pathway. In our present study, even though we did not see significant changes in the levels of PAX6 and TGF- β 1 mRNA expression in any of the duloxetine-treated groups, there was still a slight trend in PAX6 upregulation and TGF- β 1 downregulation after duloxetine treatment in all groups. In addition, TGF- β 1 mRNA expression tended to decrease ($P=0.052$) and

TGF- β 1 protein was significantly downregulated in AN-LSCs, following duloxetine treatment.

Duloxetine treatment also resulted in a significant increase in FABP5 mRNA and protein levels in LSCs using LGSF-medium, after 24 h. Not only PAX6 expression levels, but also other factors may have an important role in the regulation of FABP5 level; for example environmental inflammatory stimuli. In addition, once again the ERK pathway may play a pivotal role.

Differentiation marker DSG1 expression was altered in aniridia mouse models and upon PAX6 knockdown in primary human corneal epithelial cells [8, 47]. Rubelowski et al. described high DSG1 expression levels in central differentiated corneal epithelial cells, but not in LECs [41, 48]. Therefore, we suggest that by increasing PAX6 levels and therefore cell differentiation using ritanserin and duloxetine treatment, DSG1 expression may also increase in LSCs. Although DSG1 expression could be detected in epithelial cells, and skin keratinocytes in previous studies [41, 49], DSG1 mRNA and protein were not detectable either in AN-LSCs or LSCs, using LGSF- or NGSC-medium, even using ritanserin or duloxetine treatment. Most probably, human corneal fibroblasts express extremely low DSG1 levels.

A previous study demonstrated that the expression of extracellular matrix components COL1A1 and COL5A1 is altered in corneas with AAK, without any previous treatment, and also in transplanted corneas [50]. In a previous study, we observed significantly increased COL1A1 and COL5A1 mRNA levels in AN-LSCs, using LGSF -medium, and significantly decreased COL5A1 mRNA expression in AN-LSCs, in NGSC-medium (Li Z, Stachon T, Fries FN, et al. Expression of PAX6 and keratocyte-characteristic markers in human limbal stromal cells of congenital aniridia and healthy subjects, in vitro. *Curr Eye Res.* 2024; under review.). LUM is able to inhibit TGF- β 1, and TGF- β 1 is able to elicit an increase in COL5A1 mRNA level in bone matrix during osteogenesis [42]. Boya Zhou et al. found significantly upregulated TGF- β 1 expression in the case of LUM knockdown [43]. There is a strong relationship between extracellular matrix components and TGF- β 1 expression, which also plays an important role in AAK development and progression. Nevertheless, duloxetin treatment did not change

COL1A1 and *COL5A1* mRNA or protein levels, even though we observed a significant change in TGF- β 1 in AN-LSCs, using LGSF medium.

Limitations

Although significant alterations were observed in *PAX6* and *TGF- β 1* mRNA expression in AN-LSCs after ritanserin treatment, further investigation is necessary to determine the long-term effect of both ritanserin and duloxetine on healthy and aniridia limbal stromal cells. In addition, *in vivo* experiments should be performed to analyze the effect of both drugs on the limbal stem cell niche in both the short and long term.

CONCLUSIONS

In summary, we confirmed that the expressions of both *PAX6* and *TGF- β 1* mRNA are sensitive to ritanserin treatment. Both ritanserin and duloxetine have an impact on retinoic acid signaling and keratocyte characteristic markers in both healthy and aniridia limbal stromal cells. In these changes, the ERK pathway may play an important role. Therefore, ritanserin and duloxetine treatment may affect corneal stromal wound healing both in healthy and in congenital aniridia corneas.

ACKNOWLEDGEMENTS

We thank the participants of the study.

Author Contributions. Zhen Li: conceptualization, investigation, data curation, methodology and writing-original draft. Nóra Szentmáry: conceptualization, data curation, methodology, writing-review and editing. Fabian N Fries: resources, writing-review and editing. Shweta Suiwal: writing-review and editing. Ning Chai: writing-review and editing. Berthold Seitz: resources, writing-review and editing. Lei Shi: data curation, writing-review and editing. Maryam Amini: writing-review and editing. Tanja

Stachon: conceptualization, data curation, methodology, writing-review and editing.

Funding. The work of Zhen Li, Nóra Szentmáry, Fabian N Fries, Shweta Suiwal, Ning Chai, Maryam Amini and Tanja Stachon at the Rolf M. Schwiete Center for Limbal Stem Cell and Congenital Aniridia Research was supported by the Rolf M. Schwiete Foundation. This work was supported by the Pitzer Foundation. The funding organization had no role in the design or conduct of this research. No funding or sponsorship was received for the publication of this article.

Data Availability. The datasets generated during and/or analyzed during the current study are available from the corresponding author on reasonable request.

Declarations

Conflict of Interest. Zhen Li, Nóra Szentmáry, Fabian N Fries, Shweta Suiwal, Ning Chai, Berthold Seitz, Lei Shi, Maryam Amini and Tanja Stachon have no conflict of interests. Nóra Szentmáry is a member of the Editorial Board of *Ophthalmology and Therapy*. Nóra Szentmáry was not involved in the selection of peer reviewers for the manuscript nor of any of the subsequent editorial decisions.

Ethical Approval. Our study was approved by the Ethics Committee of Saarland, Germany (No. 172/20). All work was performed according to the Principles of the Declaration of Helsinki. All subjects with aniridia who participated in the study signed an informed consent before surgery.

Open Access. This article is licensed under a Creative Commons Attribution-NonCommercial 4.0 International License, which permits any non-commercial use, sharing, adaptation, distribution and reproduction in any medium or format, as long as you give appropriate credit to the original author(s) and the source, provide a link to the Creative Commons licence, and indicate if changes were made. The images or other third

party material in this article are included in the article's Creative Commons licence, unless indicated otherwise in a credit line to the material. If material is not included in the article's Creative Commons licence and your intended use is not permitted by statutory regulation or exceeds the permitted use, you will need to obtain permission directly from the copyright holder. To view a copy of this licence, visit <http://creativecommons.org/licenses/by-nc/4.0/>.

REFERENCES

1. Landsend ECS, Lagali N, Utheim TP. Congenital aniridia—a comprehensive review of clinical features and therapeutic approaches. *Surv Ophthalmol*. 2021;66:1031–50.
2. Lim HT, Kim DH, Kim H. PAX6 aniridia syndrome: clinics, genetics, and therapeutics. *Curr Opin Ophthalmol*. 2017;28:436–47.
3. Lagali N, Wowra B, Fries FN, et al. PAX6 mutational status determines aniridia-associated keratopathy phenotype. *Ophthalmology*. 2020;127:273–5.
4. Kucerova R, Ou J, Lawson D, Leiper LJ, Collinson JM. Cell surface glycoconjugate abnormalities and corneal epithelial wound healing in the Pax6^{+/-} mouse model of aniridia-related keratopathy. *Invest Ophthalmol Vis Sci*. 2006;47:5276–82.
5. Dorà N, Ou J, Kucerova R, Parisi I, West JD, Collinson JM. PAX6 dosage effects on corneal development, growth, and wound healing. *Dev Dyn*. 2008;237:1295–306.
6. Latta L, Ludwig N, Krammes L, Stachon T, Fries FN, Mukwaya A, et al. Abnormal neovascular and proliferative conjunctival phenotype in limbal stem cell deficiency is associated with altered microRNA and gene expression modulated by PAX6 mutational status in congenital aniridia. *Ocul Surf*. 2021;19:115–27.
7. Latta L, Nordström K, Stachon T, Langenbacher A, Fries FN, Szentmáry N, et al. Expression of retinoic acid signaling components ADH7 and ALDH1A1 is reduced in aniridia limbal epithelial cells and a siRNA primary cell based aniridia model. *Exp Eye Res*. 2019;179:8–17.
8. Davis J, Duncan MK, Robison WG Jr, Piatigorsky J. Requirement for Pax6 in corneal morphogenesis: a role in adhesion. *J Cell Sci*. 2003;116:2157–67.
9. Pinnamaneni N, Funderburgh JL. Concise review: stem cells in the corneal stroma. *Stem Cells*. 2012;30:1059–63.
10. Polisetty N, Fatima A, Madhira SL, Sangwan VS, Vemuganti GK. Mesenchymal cells from limbal stroma of human eye. *Mol Vis*. 2008;14:431–42.
11. Guo X, Hutcheon AE, Melotti SA, Zieske JD, Trinkaus-Randall V, Ruberti JW. Morphologic characterization of organized extracellular matrix deposition by ascorbic acid-stimulated human corneal fibroblasts. *Invest Ophthalmol Vis Sci*. 2007;48:4050–60.
12. Pei Y, Sherry DM, McDermott AM. Thy-1 distinguishes human corneal fibroblasts and myofibroblasts from keratocytes. *Exp Eye Res*. 2004;79:705–12.
13. Shubham K, Mishra R. Pax6 interacts with SPARC and TGF- β in murine eyes. *Mol Vis*. 2012;18:951–6.
14. Feng Y, Li M, Wang S, Cong W, Hu G, Song Y, et al. Paired box 6 inhibits cardiac fibroblast differentiation. *Biochem Biophys Res Commun*. 2020;528:561–6.
15. Seidenberg J, Stellato M, Hukara A, et al. The AP-1 transcription factor fosl-2 regulates autophagy in cardiac fibroblasts during myocardial fibrogenesis. *Int J Mol Sci*. 2021;22(4):1861.
16. Reich N, Maurer B, Akhmetshina A, et al. The transcription factor Fra-2 regulates the production of extracellular matrix in systemic sclerosis. *Arthritis Rheum*. 2010;62:280–90.
17. Eferl R, Hasselblatt P, Rath M, et al. Development of pulmonary fibrosis through a pathway involving the transcription factor Fra-2/AP-1. *Proc Natl Acad Sci USA*. 2008;105:10525–30.
18. Higashi AY, Aronow BJ, Dressler GR. Expression profiling of fibroblasts in chronic and acute disease models reveals novel pathways in kidney fibrosis. *J Am Soc Nephrol*. 2019;30:80–94.
19. Oved K, Zennaro L, Dorot O, et al. Ritanserin, a potent serotonin 2A receptor antagonist, represses MEK/ERK signalling pathway to restore PAX6 production and function in aniridia-like cellular model. *Biochem Biophys Res Commun*. 2021;582:100–4.
20. Dorot O, Roux LN, Zennaro L, et al. The antipsychotic drug Duloxetine rescues PAX6 haploinsufficiency of mutant limbal stem cells through inhibition of the MEK/ERK signaling pathway. *Ocul Surf*. 2022;23:140–2.

21. Monti JM, Alterwain P. Ritanserin decreases alcohol intake in chronic alcoholics. *Lancet*. 1991;337:60.
22. Wong DT, Bymaster FP, Mayle DA, Reid LR, Krushinski JH, Robertson DW. LY248686, a new inhibitor of serotonin and norepinephrine uptake. *Neuropsychopharmacology*. 1993;8:23–33.
23. Leysen JE, Gommeren W, Van Gompel P, Wynants J, Janssen PF, Laduron PM. Receptor-binding properties in vitro and in vivo of ritanserin: a very potent and long acting serotonin-5₂ antagonist. *Mol Pharmacol*. 1985;27:600–11.
24. Foster JW, Gouveia RM, Connon CJ. Low-glucose enhances keratocyte- characteristic phenotype from corneal stromal cells in serum-free conditions. *Sci Rep*. 2015;5:10839.
25. Lagali N, Wowra B, Dobrowolski D, Utheim TP, Fagerholm P, Wylegala E. Stage-related central corneal epithelial transformation in congenital aniridia-associated keratopathy. *Ocul Surf*. 2018;16:163–72.
26. Edén U, Fagerholm P, Danyali R, Lagali N. Pathologic epithelial and anterior corneal nerve morphology in early-stage congenital aniridic keratopathy. *Ophthalmology*. 2012;119:1803–10.
27. Chai N, Stachon T, Berger T, et al. Human corneal epithelial cell and fibroblast migration and growth factor secretion after rose bengal photodynamic therapy (RB-PDT) and the effect of conditioned medium. *PLoS One*. 2023;18: e0296022.
28. Wiesel FA, Nordström AL, Farde L, Eriksson B. An open clinical and biochemical study of ritanserin in acute patients with schizophrenia. *Psychopharmacology*. 1994;114:31–8.
29. Johnson BA, Jasinski DR, Galloway GP, et al. Ritanserin in the treatment of alcohol dependence—a multi-center clinical trial. Ritanserin Study Group. *Psychopharmacology*. 1996;128:206–15.
30. Grewal JS, Mukhin YV, Garnovskaya MN, Raymond JR, Greene EL. Serotonin 5-HT_{2A} receptor induces TGF- β 1 expression in mesangial cells via ERK: proliferative and fibrotic signals. *Am J Physiol*. 1999;276:F922–30.
31. Kim DC, Jun DW, Kwon YI, Lee KN, Lee HL, Lee OY, et al. 5-HT_{2A} receptor antagonists inhibit hepatic stellate cell activation and facilitate apoptosis. *Liver Int*. 2013;33:535–43.
32. Chaturvedi S, Misra DP, Prasad N, et al. 5-HT(2) and 5-HT(2B) antagonists attenuate pro-fibrotic phenotype in human adult dermal fibroblasts by blocking TGF- β 1 induced non-canonical signaling pathways including STAT3: implications for fibrotic diseases like scleroderma. *Int J Rheum Dis*. 2018;21:2128–38.
33. Smits JGA, Cunha DL, Amini M, et al. Identification of the regulatory circuit governing corneal epithelial fate determination and disease. *PLoS Biol*. 2023;21: e3002336.
34. Jaggar M, Banerjee T, Weisstaub N, Gingrich JA, Vaidya VA. 5-HT(2A) receptor loss does not alter acute fluoxetine-induced anxiety and exhibit sex-dependent regulation of cortical immediate early gene expression. *Neuronal Signal*. 2019;3:Ns20180205.
35. McCarey BE, Schmidt FH. Modeling glucose distribution in the cornea. *Curr Eye Res*. 1990;9:1025–39.
36. Thoft RA, Friend J, Dohlman CH. Corneal glucose concentration. Flux in the presence and absence of epithelium. *Arch Ophthalmol*. 1971;85:467–72.
37. Jansen F, Yang X, Franklin BS, et al. High glucose condition increases NADPH oxidase activity in endothelial microparticles that promote vascular inflammation. *Cardiovasc Res*. 2013;98:94–106.
38. Scott SG, Jun AS, Chakravarti S. Sphere formation from corneal keratocytes and phenotype specific markers. *Exp Eye Res*. 2011;93:898–905.
39. Jester JV, Ho-Chang J. Modulation of cultured corneal keratocyte phenotype by growth factors/cytokines control in vitro contractility and extracellular matrix contraction. *Exp Eye Res*. 2003;77:581–92.
40. Funderburgh ML, Mann MM, Funderburgh JL. Keratocyte phenotype is enhanced in the absence of attachment to the substratum. *Mol Vis*. 2008;14:308–17.
41. Katiyar P, Stachon T, Fries FN, et al. Decreased FABP5 and DSG1 protein expression following PAX6 knockdown of differentiated human limbal epithelial cells. *Exp Eye Res*. 2022;215: 108904.
42. Moriya K, Bae E, Honda K, et al. A fibronectin-independent mechanism of collagen fibrillogenesis in adult liver remodeling. *Gastroenterology*. 2011;140:1653–63.
43. Zhou B, Tu T, Gao Z, Wu X, Wang W, Liu W. Impaired collagen fibril assembly in keloids with enhanced expression of lumican and collagen V. *Arch Biochem Biophys*. 2021;697: 108676.
44. Talpan D, Salla S, Seidelmann N, Walter P, Fuest M. Antifibrotic effects of caffeine, curcumin and

-
- pirfenidone in primary human keratocytes. *Int J Mol Sci.* 2023;24(2):1461.
45. Gao J, Li L, Zhou D, et al. Effects of norepinephrine-induced activation of rat vascular adventitial fibroblasts on proliferation and migration of BMSCs involved in vascular remodeling. *Exp Ther Med.* 2023;25:290.
46. Zhang J, Deng YT, Liu J, et al. Norepinephrine induced epithelial-mesenchymal transition in HT-29 and A549 cells in vitro. *J Cancer Res Clin Oncol.* 2016;142:423–35.
47. Kitazawa K, Hikichi T, Nakamura T, Sotozono C, Kinoshita S, Masui S. PAX6 regulates human corneal epithelium cell identity. *Exp Eye Res.* 2017;154:30–8.
48. Rubelowski AK, Latta L, Katiyar P, et al. HCE-T cell line lacks cornea-specific differentiation markers compared to primary limbal epithelial cells and differentiated corneal epithelium. *Graefes Arch Clin Exp Ophthalmol.* 2020;258:565–75.
49. Burks HE, Pokorny JL, Koetsier JL, et al. Melanoma cells repress Desmoglein 1 in keratinocytes to promote tumor cell migration. *J Cell Biol.* 2023;6:222(11):e202212031. <https://doi.org/10.1083/jcb.202212031>.
50. Vicente A, Byström B, Lindström M, Stenevi U, Pedrosa DF. Aniridia-related keratopathy: structural changes in naïve and transplanted corneal buttons. *PLoS One.* 2018;13:e0198822.

8. References

1. Landsend ECS, Lagali N, Utheim TP. Congenital aniridia - A comprehensive review of clinical features and therapeutic approaches. *Surv Ophthalmol* 2021; 66: 1031-1050. doi:10.1016/j.survophthal.2021.02.011
2. Lagali N, Wowra B, Fries FN, Latta L, Moslemani K, Utheim TP, Wylegala E, Seitz B, Käsmann-Kellner B. PAX6 mutational status determines aniridia-associated keratopathy phenotype. *Ophthalmology* 2020; 127: 273-275. doi:10.1016/j.ophttha.2019.09.034
3. Dua HS, Saini JS, Azuara-Blanco A, Gupta P. Limbal stem cell deficiency: concept, aetiology, clinical presentation, diagnosis and management. *Indian J Ophthalmol* 2000; 48: 83-92
4. Puangsricharern V, Tseng SC. Cytologic evidence of corneal diseases with limbal stem cell deficiency. *Ophthalmology* 1995; 102: 1476-1485. doi:10.1016/s0161-6420(95)30842-1
5. Pellegrini G, Traverso CE, Franzi AT, Zingirian M, Cancedda R, De Luca M. Long-term restoration of damaged corneal surfaces with autologous cultivated corneal epithelium. *Lancet* 1997; 349: 990-993. doi:10.1016/s0140-6736 (96) 11188-0
6. Basu S, Ali H, Sangwan VS. Clinical outcomes of repeat autologous cultivated limbal epithelial transplantation for ocular surface burns. *Am J Ophthalmol* 2012; 153: 643-650, 650.e641-642. doi:10.1016/j.ajo.2011.09.016
7. Shortt AJ, Secker GA, Notara MD, Limb GA, Khaw PT, Tuft SJ, Daniels JT. Transplantation of ex vivo cultured limbal epithelial stem cells: a review of techniques and clinical results. *Surv Ophthalmol* 2007; 52: 483-502. doi:10.1016/j.survophthal.2007.06.013
8. Shahdadfar A, Haug K, Pathak M, Drolsum L, Olstad OK, Johnsen EO, Petrovski G, Moe MC, Nicolaisen B. Ex vivo expanded autologous limbal epithelial cells on amniotic membrane using a culture medium with human serum as single supplement. *Exp Eye Res* 2012; 97: 1-9. doi:10.1016/j.exer.2012.01.013
9. Menzel-Severing J, Kruse FE, Schlötzer-Schrehardt U. Stem cell-based therapy for corneal epithelial reconstruction: present and future. *Can J Ophthalmol* 2013; 48: 13-21. doi:10.1016/j.jcjo.2012.11.009
10. Polisetty N, Fatima A, Madhira SL, Sangwan VS, Vemuganti GK. Mesenchymal cells from limbal stroma of human eye. *Mol Vis* 2008; 14: 431-442
11. Guo X, Hutcheon AE, Melotti SA, Zieske JD, Trinkaus-Randall V, Ruberti JW. Morphologic characterization of organized extracellular matrix deposition by ascorbic acid-stimulated human corneal fibroblasts. *Invest Ophthalmol Vis Sci* 2007; 48: 4050-4060. doi:10.1167/iovs.06-1216
12. Pei Y, Sherry DM, McDermott AM. Thy-1 distinguishes human corneal

- fibroblasts and myofibroblasts from keratocytes. *Exp Eye Res* 2004; 79: 705-712. doi:10.1016/j.exer.2004.08.002
13. Chakravarti S, Petroll WM, Hassell JR, Jester JV, Lass JH, Paul J, Birk DE. Corneal opacity in lumican-null mice: defects in collagen fibril structure and packing in the posterior stroma. *Invest Ophthalmol Vis Sci* 2000; 41: 3365-3373
 14. Funderburgh JL, Mann MM, Funderburgh ML. Keratocyte phenotype mediates proteoglycan structure: a role for fibroblasts in corneal fibrosis. *J Biol Chem* 2003; 278: 45629-45637. doi:10.1074/jbc.M303292200
 15. Hassell JR, Birk DE. The molecular basis of corneal transparency. *Exp Eye Res* 2010; 91: 326-335. doi:10.1016/j.exer.2010.06.021
 16. Vicente A, Byström B, Lindström M, Stenevi U, Pedrosa Domellöf F. Aniridia-related keratopathy: Structural changes in naïve and transplanted corneal buttons. *PLoS One* 2018; 13: e0198822. doi:10.1371/journal.pone.0198822
 17. Yam GH, Williams GP, Setiawan M, Yusoff NZ, Lee XW, Htoon HM, Zhou L, Fuest M, Mehta JS. Nerve regeneration by human corneal stromal keratocytes and stromal fibroblasts. *Sci Rep* 2017; 7: 45396. doi:10.1038/srep45396
 18. Yam GH, Teo EP, Setiawan M, Lovatt MJ, Yusoff N, Fuest M, Goh BT, Mehta JS. Postnatal periodontal ligament as a novel adult stem cell source for regenerative corneal cell therapy. *J Cell Mol Med* 2018; 22: 3119-3132. doi:10.1111/jcmm.13589
 19. Duarte Campos DF, Rohde M, Ross M, Anvari P, Blaeser A, Vogt M, Panfil C, Yam GH, Mehta JS, Fischer H et al. Corneal bioprinting utilizing collagen-based bioinks and primary human keratocytes. *J Biomed Mater Res A* 2019; 107: 1945-1953. doi:10.1002/jbm.a.36702
 20. McCarey BE, Schmidt FH. Modeling glucose distribution in the cornea. *Curr Eye Res* 1990; 9: 1025-1039. doi:10.3109/02713689008997577
 21. Thoft RA, Friend J, Dohlman CH. Corneal glucose concentration. Flux in the presence and absence of epithelium. *Arch Ophthalmol* 1971; 85: 467-472. doi:10.1001/archopht.1971.00990050469013
 22. Towle HC. Glucose as a regulator of eukaryotic gene transcription. *Trends Endocrinol Metab* 2005; 16: 489-494. doi:10.1016/j.tem.2005.10.003
 23. Lee AS. Glucose-regulated proteins in cancer: molecular mechanisms and therapeutic potential. *Nat Rev Cancer* 2014; 14: 263-276. doi:10.1038/nrc3701
 24. Jansson D, Ng AC, Fu A, Depatie C, Al Azzabi M, Sreaton RA. Glucose controls CREB activity in islet cells via regulated phosphorylation of TORC2. *Proc Natl Acad Sci U S A* 2008; 105: 10161-10166. doi:10.1073/pnas.0800796105
 25. Müller LJ, Pels L, Vrensen GF. Novel aspects of the ultrastructural organization of human corneal keratocytes. *Invest Ophthalmol Vis Sci* 1995; 36: 2557-2567
 26. Funderburgh ML, Du Y, Mann MM, SundarRaj N, Funderburgh JL. PAX6

- expression identifies progenitor cells for corneal keratocytes. *Faseb j* 2005; 19: 1371-1373. doi:10.1096/fj.04-2770fje
27. Jester JV, Barry-Lane PA, Cavanagh HD, Petroll WM. Induction of alpha-smooth muscle actin expression and myofibroblast transformation in cultured corneal keratocytes. *Cornea* 1996; 15: 505-516
 28. Berger T, Szentmáry N, Chai N, Flockerzi E, Daas L, Stachon T, Seitz B. In vitro expression analysis of cytokines and ROS-Related genes in human corneal fibroblasts and keratocytes of healthy and keratoconus corneas. *Ocul Immunol Inflamm* 2023. doi:10.1080/09273948.2023.2176325
 29. Foster JW, Gouveia RM, Connon CJ. Low-glucose enhances keratocyte-characteristic phenotype from corneal stromal cells in serum-free conditions. *Sci Rep* 2015; 5: 10839. doi:10.1038/srep10839
 30. Beales MP, Funderburgh JL, Jester JV, Hassell JR. Proteoglycan synthesis by bovine keratocytes and corneal fibroblasts: maintenance of the keratocyte phenotype in culture. *Invest Ophthalmol Vis Sci* 1999; 40: 1658-1663
 31. Brown CT, Nugent MA, Lau FW, Trinkaus-Randall V. Characterization of proteoglycans synthesized by cultured corneal fibroblasts in response to transforming growth factor beta and fetal calf serum. *J Biol Chem* 1999; 274: 7111-7119. doi:10.1074/jbc.274.11.7111
 32. Joseph A, Hossain P, Jham S, Jones RE, Tighe P, McIntosh RS, Dua HS. Expression of CD34 and L-selectin on human corneal keratocytes. *Invest Ophthalmol Vis Sci* 2003; 44: 4689-4692. doi:10.1167/iovs.02-0999
 33. Toti P, Tosi GM, Traversi C, Schürfeld K, Cardone C, Caporossi A. CD-34 stromal expression pattern in normal and altered human corneas. *Ophthalmology* 2002; 109: 1167-1171. doi:10.1016/s0161-6420(02)01042-4
 34. Marta S, André V, Berit B, Fátima Pedrosa D. Cell signaling pathways in human mutant PAX6 corneal cells: an in vitro model for aniridia-related keratopathy. *bioRxiv* 2021. doi:10.1101/2021.03.19.436143.
 35. Monti JM, Alterwain P. Ritanserin decreases alcohol intake in chronic alcoholics. *Lancet* 1991; 337: 60. doi:10.1016/0140-6736(91)93386-n
 36. Wong DT, Bymaster FP, Mayle DA, Reid LR, Krushinski JH, Robertson DW. LY248686, a new inhibitor of serotonin and norepinephrine uptake. *Neuropsychopharmacology* 1993; 8: 23-33. doi:10.1038/npp.1993.4
 37. Oved K, Zennaro L, Dorot O, Zerbib J, Frank E, Roux LN, Bremond-Gignac D, Pichinuk E, Aberdam D. Ritanserin, a potent serotonin 2A receptor antagonist, represses MEK/ERK signalling pathway to restore PAX6 production and function in aniridia-like cellular model. *Biochem Biophys Res Commun* 2021; 582: 100-104. doi:10.1016/j.bbrc.2021.10.036
 38. Dorot O, Roux LN, Zennaro L, Oved K, Bremond-Gignac D, Pichinuk E, Aberdam D. The antipsychotropic drug duloxetine rescues PAX6 haploinsufficiency of mutant limbal stem cells through inhibition of the MEK/ERK signaling pathway. *Ocul Surf* 2022; 23: 140-142. doi:10.1016/j.jtos.2021.12.003
 39. Grewal JS, Mukhin YV, Garnovskaya MN, Raymond JR, Greene EL.

- Serotonin 5-HT_{2A} receptor induces TGF-beta1 expression in mesangial cells via ERK: proliferative and fibrotic signals. *Am J Physiol* 1999; 276: F922-930. doi:10.1152/ajprenal.1999.276.6.F922
40. Kim DC, Jun DW, Kwon YI, Lee KN, Lee HL, Lee OY, Yoon BC, Choi HS, Kim EK. 5-HT_{2A} receptor antagonists inhibit hepatic stellate cell activation and facilitate apoptosis. *Liver Int* 2013; 33: 535-543. doi:10.1111/liv.12110
 41. Shubham K, Mishra R. Pax6 interacts with SPARC and TGF- β in murine eyes. *Mol Vis* 2012; 18: 951-956
 42. Feng Y, Li M, Wang S, Cong W, Hu G, Song Y, Xiao H, Dong E, Zhang Y. Paired box 6 inhibits cardiac fibroblast differentiation. *Biochem Biophys Res Commun* 2020; 528: 561-566. doi:10.1016/j.bbrc.2020.05.146
 43. Gao J, Li L, Zhou D, Sun X, Cui L, Yang D, Wang X, Du P, Yuan W. Effects of norepinephrine-induced activation of rat vascular adventitial fibroblasts on proliferation and migration of BMSCs involved in vascular remodeling. *Exp Ther Med* 2023; 25: 290. doi:10.3892/etm.2023.11989
 44. Zhang J, Deng YT, Liu J, Wang YQ, Yi TW, Huang BY, He SS, Zheng B, Jiang Y. Norepinephrine induced epithelial-mesenchymal transition in HT-29 and A549 cells in vitro. *J Cancer Res Clin Oncol* 2016; 142: 423-435. doi:10.1007/s00432-015-2044-9
 45. Li Z, Böhringer D, Stachon T, Nastaranpour M, Fries FN, Seitz B, Ulrich M, Munteanu C, Langenbacher A, Szentmáry N. Culturing limbal epithelial cells of long-term stored corneal donors (organ culture) in vitro - A stepwise linear regression algorithm. *Klin Monbl Augenheilkd* 2023. doi:10.1055/a-2084-7168.
 46. Li Z, Stachon T, Zimmermann J, Trusen S, Fries FN, Berger M, Suiwal S, Chai N, Seitz B, Shi L et al. Expression of PAX6 and keratocyte-characteristic markers in human limbal stromal cells of congenital aniridia and healthy subjects, in vitro. *Curr Eye Res* 2025. doi:10.1080/02713683.2025.2449915: 1-11.
 47. Li Z, Szentmáry N, Fries FN, Suiwal S, Chai N, Seitz B, Shi L, Amini M, Stachon T. Effect of ritanserin and duloxetine on the gene expression of primary aniridia and healthy human limbal stromal cells, in vitro. *Ophthalmol Ther* 2024; 13: 2931-2950. doi:10.1007/s40123-024-01032-8

9. Publication list

1. Li Z, Stachon T, Zimmermann J, Trusen S, Fries FN, Berger M, Suiwal S, Chai N, Seitz B, Shi L, Amini M, Szentmáry N. Expression of PAX6 and Keratocyte-Characteristic Markers in Human Limbal Stromal Cells of Congenital Aniridia and Healthy Subjects, In Vitro. *Curr Eye Res.* 2025 Jan 10:1-11. doi: 10.1080/02713683.2025.2449915. Epub ahead of print.
2. Li Z, Stachon T, Häcker S, Fries FN, Chai N, Seitz B, Shi L, Hsu SL, Li S, Liu S, Amini M, Suiwal S, Szentmáry N. Increased glucose concentration modifies TGF- β 1 and NF κ B signaling pathways in aniridia limbal fibroblasts, in vitro. *Exp Eye Res.* 2025 Jan;250:110163. doi: 10.1016/j.exer.2024.110163. Epub 2024 Nov 20.
3. Li Z, Szentmáry N, Fries FN, Suiwal S, Chai N, Seitz B, Shi L, Amini M, Stachon T. Effect of Ritanserine and Duloxetine on the Gene Expression of Primary Aniridia and Healthy Human Limbal Stromal Cells, In Vitro. *Ophthalmol Ther.* 2024 Nov;13(11):2931-2950. doi: 10.1007/s40123-024-01032-8. Epub 2024 Sep 21.
4. Li Z, Böhringer D, Stachon T, Nastaranpour M, Fries FN, Seitz B, Ulrich M, Munteanu C, Langenbacher A, Szentmáry N. Culturing Limbal Epithelial Cells of Long-term Stored Corneal Donors (Organ Culture) In Vitro - A Stepwise Linear Regression Algorithm. *Klin Monbl Augenheilkd.* 2024 Aug;241(8):964-971. English. doi: 10.1055/a-2084-7168. Epub 2023 May 2.
5. Trusen S, Zimmermann JSA, Fries FN, Li Z, Chai N, Seitz B, Suiwal S, Amini M, Szentmáry N, Stachon T. Increased susceptibility of human limbal aniridia fibroblasts to oxidative stress. *Exp Eye Res.* 2024 Nov;248:110105. doi: 10.1016/j.exer.2024.110105. Epub 2024 Sep 19.
6. Chai N, Stachon T, Berger T, Li Z, Amini M, Suiwal S, Seitz B, Langenbacher A, Szentmáry N. Rose Bengal Photodynamic Therapy (RB-PDT) Modulates the Inflammatory Response in LPS-Stimulated Human Corneal Fibroblasts By

- Influencing NF- κ B and p38 MAPK Signaling Pathways. *Curr Eye Res.* 2024 Aug;49(8):803-814. doi: 10.1080/02713683.2024.2342600. Epub 2024 Apr 22.
7. Chai N, Stachon T, Berger T, Li Z, Seitz B, Langenbucher A, Szentmáry N. Human corneal epithelial cell and fibroblast migration and growth factor secretion after rose bengal photodynamic therapy (RB-PDT) and the effect of conditioned medium. *PLoS One.* 2023 Dec 27;18(12):e0296022. doi: 10.1371/journal.pone.0296022.
 8. Chai N, Stachon T, Berger T, Li Z, Seitz B, Langenbucher A, Szentmáry N. Short-Term Effect of Rose Bengal Photodynamic Therapy (RB-PDT) on Collagen I, Collagen V, NF- κ B, LOX, TGF- β and IL-6 Expression of Human Corneal Fibroblasts, In Vitro. *Curr Eye Res.* 2024 Feb;49(2):150-157. doi: 10.1080/02713683.2023.2276057. Epub 2024 Jan 18.
 9. Chai N, Stachon T, Nastaranpour M, Li Z, Seitz B, Ulrich M, Langenbucher A, Szentmáry N. Assessment of Rose Bengal Photodynamic Therapy on Viability and Proliferation of Human Keratolimbic Epithelial and Stromal Cells In Vitro. *Klin Monbl Augenheilkd.* 2024 Aug;241(8):972-981. English. doi: 10.1055/a-2038-8899. Epub 2023 Feb 20.

10. Presentations

1. Li Z, Böhringer D, Stachon T, Nastaranpour M, Fries FN, Seitz B, Munteanu C, Ulrich M, Achim Langenbacher A, Szentmáry N. Culturing limbal epithelial cells of long-term stored corneal donors (organ culture) in vitro – a stepwise linear regression algorithm. 2022, Jahrestagung der Deutschen Ophthalmologischen Gesellschaft, Berlin, Deutschland
2. Li Z, Stachon T, Chai N, Seitz B, Amini M, Shi L, Szentmáry N. Expression of PAX6 and keratocyte-characteristic markers in human limbal fibroblasts and keratocytes of congenital aniridia and healthy corneas, in vitro. 2023, Jahrestagung der Deutschen Ophthalmologischen Gesellschaft, Berlin, Deutschland
3. Li Z, Stachon T, Fries FN, Suiwal S, Chai N, Seitz B, Shi L, Amini M, Szentmáry N. PAX6, FABP5 and keratocyte-characteristic marker expression in human limbal fibroblasts and keratocytes of congenital aniridia and healthy subjects, in vitro. October 2023, Jahrestagung der European Society for Vision and Eye Research, Valencia, Spain.
4. Li Z, Stachon T, Fries FN, Suiwal S, Chai N, Seitz B, Shi L, Amini M, Szentmáry N. Increased glucose concentration modifies TGF- β 1 and NF κ B signaling pathways in aniridia limbal fibroblasts, in vitro. 2024, Jahrestagung der Deutschen Ophthalmologischen Gesellschaft, Berlin, Deutschland
5. Li Z, Szentmáry N, Fries FN, Suiwal S, Chai N, Seitz B, Shi L, Amini M, Stachon T. Effect of the anti-psychotropic drugs ritanserin and duloxetine on gene expression of primary aniridia and healthy human limbal stromal cells, in vitro. 2024, Jahrestagung der Deutschen Ophthalmologischen Gesellschaft, Berlin, Deutschland
6. Chai N, Stachon T, Nastaranpour N, Li Z, Seitz B, Ulrich M, Langenbacher A, Szentmáry N. Assessment of Rose Bengal Photodynamic Therapy on viability and proliferation of human limbal epithelial stem cells (T-LSCs), corneal epithelial

- cells (HCE-T), limbal fibroblasts (LCFs), normal and keratoconus fibroblasts (HCFs and KC-HCFs), in vitro. 2022, Jahrestagung der Deutschen Ophthalmologischen Gesellschaft, Berlin, Deutschland
7. Suiwal S, Nastaran Pour M, Fries. N, Li Z, Chai N, Seitz B, Amini M, Stachon T, Szentmáry N. Ritanserin and duloxetine as treatment options for aniridia associated keratopathy (AAK)–gene expression using the siRNA based anidria limbal epithelial cell model. 2023, Jahrestagung der Deutschen Ophthalmologischen Gesellschaft, Berlin, Deutschland
 8. Trusen S, Zimmermann J, Fries FN, Li Z, Chai N, Seitz B, Suiwal S, Amini M., Szentmáry N., Stachon T. Erhöhte Sensibilität limbalen Aniridie-Fibroblasten auf oxidativen Stress. 2023, Jahrestagung der Deutschen Ophthalmologischen Gesellschaft, Berlin, Deutschland
 9. Zimmermann J, Trusen S, Fries FN, Li Z, Chai N, Seitz B, Suiwal S, Amini M., Szentmáry N., Stachon T. LPS-induzierte Infammation bei limbalen Aniridie Fibroblasten. 2023, Jahrestagung der Deutschen Ophthalmologischen Gesellschaft, Berlin, Deutschland
 10. Chai N, Stachon T, Berger T, Li Z, Seitz B, Langenbucher A, Szentmáry N. Human corneal epithelial cell and fbroblast migration and growth factor secretion after rose bengal photodynamic therapy (RB-PDT) and the effect of conditioned medium. 2023, Jahrestagung der Deutschen Ophthalmologischen Gesellschaft, Berlin, Deutschland
 11. Stachon T, Amini M, Nastaranpour M, Suiwal S, Li Z, Chai N, Fries FN, Seitz B, Ludwig N, Szentmáry N. MicroRNAs as markers of congenital aniridia. EVER Kongress, October 2023, Jahrestagung der European Society for Vision and Eye Research, Valencia, Spain.

11. Acknowledgements

First and foremost, I would like to express my deepest appreciation to my "Doktormutter," Professor Nóra Szentmáry, whose insightful feedback and unwavering dedication have been pivotal in shaping all studies belonging to this dissertation. Her mentorship has served as a guiding light, helping me navigate through the challenges with grace and perseverance.

I am also profoundly grateful to Professor Seitz, who introduced me to Saarland University and provided me with the opportunity to fulfill my childhood dreams. His support and encouragement have been invaluable throughout this journey.

A special acknowledgment goes to my dear friend and mentor, Dr. Tanja Stachon, whose encouragement, patience, and willingness to share her expertise have been a source of inspiration. I will always cherish the memories of overcoming experimental challenges with her by my side, offering unwavering support and guidance.

I extend my heartfelt thanks to my friends and colleagues, Dr. Maryam Amini and Dr. Shweta Suiwal, for their wisdom, optimism, and resilience. Whether working together in the laboratory or sharing moments in daily life, your collaboration has enriched my experience, and your friendship has filled my heart with warmth and affection.

I am grateful to my friend and colleague, Ms. Sabrina Häcker, whose sunny disposition and friendly demeanor have brought joy to both my laboratory and daily life.

I extend my appreciation to Professor Langenbacher, whose expertise in statistics has been invaluable in my research endeavors.

I am thankful to Dr. Fries for our enlightening conversations and for imparting valuable knowledge about ophthalmology.

To my Chinese friends, Dr. Ning Chai and Dr. Tianci Tang, I am grateful for making me feel at home in Homburg. Beyond our time in the lab, our shared experiences of exploring Europe together have been truly memorable. It has been a joy to embark on new adventures with friends by my side.

Of course, my deepest gratitude goes to my beloved family and friends in China for their unwavering support, motivation, and belief in my abilities.

The past three years in Homburg have been filled with unforgettable experiences, both personally and professionally. These moments will forever hold a special place in my heart and serve as invaluable treasures. I look forward to the opportunity to reunite with everyone in the future and continue our shared pursuit of advancing ophthalmology.

Lastly, I extend a warm welcome to all of you to visit China in the future.!

12. Curriculum Vitae

The curriculum vitae was removed from the electronic version of the doctoral thesis for reasons of data protection.